Protein quality control in the ER: balancing the ubiquitin chequebook

Coverdesign by: Jasper Claessen

The research described in this thesis was conducted at the Whitehead Institute for Biomedical Research, Massachusetts Institute of Technology, Cambridge, USA, under the supervision of Prof. Dr. H.L. Ploegh.

Printed by Gildeprint B.V., Enschede, the Netherlands

ISBN: 978-94-6108-316-6

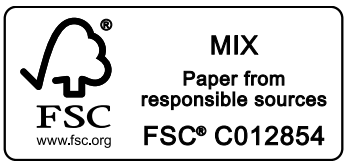

Protein quality control in the ER: balancing the ubiquitin chequebook

Kwaliteits-kontrole voor eiwitten in het ER: het opmaken van de ubiquitine balans

(met een samenvatting in het Nederlands)

Proefschrift

ter verkrijging van de graad van doctor aan de Universiteit Utrecht op gezag van de rector magnificus, prof.dr. G.J. van der Zwaan, ingevolge het besluit van het college voor promoties in het openbaar te verdedigen op donderdag 5 juli des ochtends te 10.30 uur

door

Jasper Henri Laurens Claessen

geboren op 21 mei 1984
te Hardenberg

Promotiecommissie

Promotoren:	Prof. Dr. H.L. Ploegh
	Prof. Dr. E.J.H.J. Wiertz
Overige leden:	Prof. Dr. J. Klumperman
	Prof. Dr. I. Braakman
	Prof. Dr. J. Boonstra
	Prof. Dr. A. Heck
	Dr. M. Maurice
	Dr. F. Reggiori

Table of contents

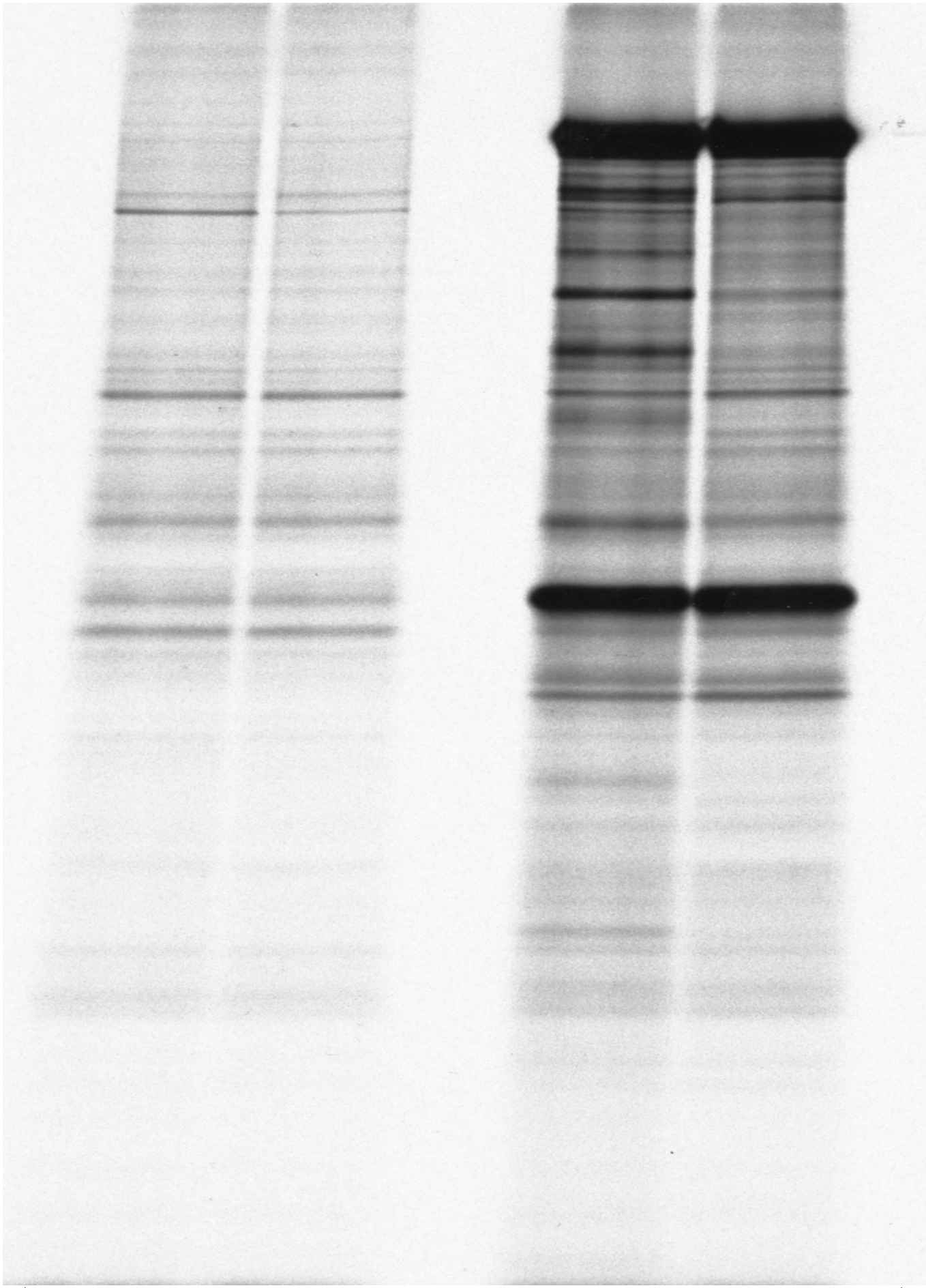

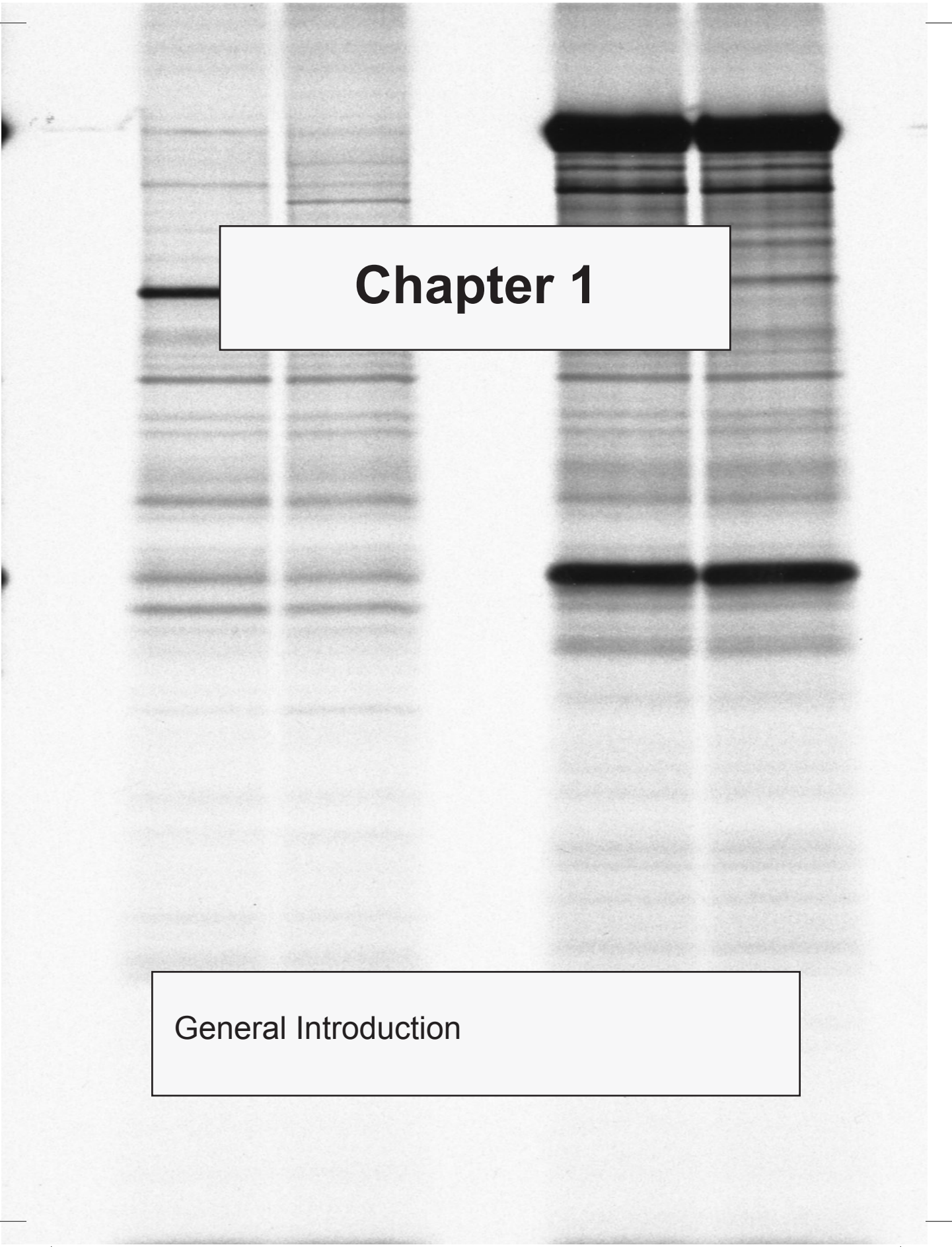

Chapter 1

General Introduction

Where proteins fold

Proteins destined for secretion from the cell or for the endocytic system originate by translation in the cytoplasm, from where they enter the endoplasmic reticulum (ER), typically cotranslationally. The nascent polypeptide enters the ER via the Sec61 translocon and – when the requisite signals are present and can be recognized – engages the glycosylation machinery. Nascent chains encounter chaperones that govern the folding process and allow the introduction of disulfide bonds. For protein complexes composed of multiple subunits, their proper association is an essential criterion for quality control and must not be jeopardized by aggregation. This is all the more remarkable when different subunits of a multi-protein complex are produced from the correspondingly distinct and individually translated mRNAs. Newly synthesized polypeptides thus attain their final conformation – autonomously or in complex with binding partners – while protected from aggregation within the crowded ER environment through transient association with components of the folding machinery (Figure 1, for detailed review see [1]).

Nonetheless, protein folding in the ER is inherently imperfect and errors made at any step *en route* to the final product reduce the fraction of proteins that reach their proper conformation. For some proteins, like the cystic fibrosis chloride conductance regulator (CFTR), more than half of the newly synthesized polypeptide may not reach maturity [2]. Any significant accumulation of misfolded proteins inside the ER entails the risk of aggregation, and is likely to compromise ER function. Polypeptides that fail to meet ER quality control and cannot be rescued must be degraded. Indeed, the build-up of misfolded proteins that can occur in either professional secretory cells or in cells treated with compounds such as tunicamycin or dithiothreitol (DTT) evokes the unfolded protein response (UPR), a stereotypic transcriptional response that ultimately adjusts the composition – both lipid and protein – of the ER [3]. These changes include upregulation of folding chaperones and quality control machinery, a decrease in protein synthesis and, if the damage is deemed beyond repair, induced cell death (apoptosis). We know of no ER-resident proteases that can deal with the onslaught of terminally misfolded proteins inside the ER lumen of cells exposed to tunicamycin or DTT. Instead, the consensus view is that misfolded proteins are ejected into the cytoplasm -a step we shall refer to as dislocation- where they are targeted for ubiquitin-dependent degradation by the proteasome [4]. The steps that contribute to this means of protein elimination are collectively referred to as ER associated degradation (ERAD). Although this

aspect of ER quality control has received the most attention by far, not all misfolded proteins follow this route: proteins with only slight imperfections may still enter the secretory pathway and eventually be targeted to endolysosomal compartments for degradation, just like proteins that sustain damage at other intracellular locations are delivered to lysosomes to be cannibalized for salvaging of their building blocks. We shall discuss the nature of the misfolded polypeptide and the role of the ubiquitylation machinery in its elimination.

Tracking misfolded proteins

What exactly constitutes a misfolded protein? Structural alterations caused by amino acid replacements, truncations of the polypeptide chain, or non-native disulfide bonds, to name a few examples – while evidently causing alterations in covalent structure – are difficult to characterize in conformational terms. Even more problematic are structural changes that result from a failure to engage the necessary folding assistants without alteration to the covalent structure of the newly synthesized protein itself. None of these products can be obtained in quantities that allow an assessment of their conformation by standard physico-chemical means (crystallography, NMR, CD). Instead, surrogate measures are used to diagnose the misfolded state, such as the failure to enter the secretory pathway and lack of terminal carbohydrate modifications [1], the loss or acquisition of epitopes recognized by antibodies, altered susceptibility to protease digestion, and loss of enzymatic or binding activity. There likely exists a continuum of folded and misfolded states, with the tipping point for diagnosis as seriously damaged and terminally misfolded being different for each protein. It has been surprisingly difficult to design mutant versions of endogenous proteins that show drastically altered kinetics of turnover and so serve as substrates to study ER quality control. As a result, relatively few substrates have been analyzed in detail. In addition, such substrates are commonly expressed at high levels in the setting of a transfection experiment. While overexpression allows easy detection of the misfolded product, it has the drawback that such substrates can saturate or even overwhelm the quality control machinery that is the object of study, likely inducing UPR-mediated remodeling of the ER [3].

Dislocation across the ER membrane barrier is proposed to take place through a protein-conducting channel, akin to translocation into the ER. In contrast to the canonical translocon, the composition of which is largely agreed on [5], no singular or definitive complex has been assigned to perform this task in dislocation, but

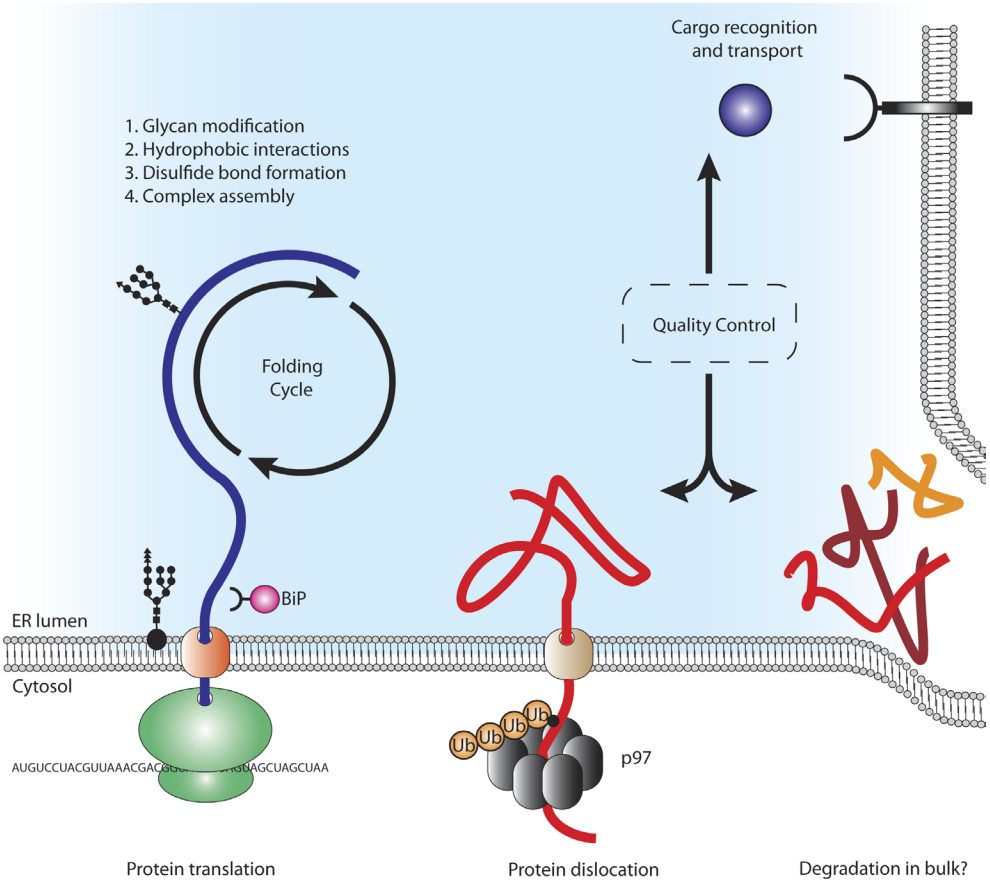

Figure 1: Protein folding in the ER.
Schematic overview of a nascent polypeptide entering the ER lumen co-translationally, where it engages folding machinery to obtain its final conformation (folding cycle). Quality control check-point(s) establish the folding status of the poly-peptide which then either proceeds to its final destination or is selectively degraded, either via the dislocation pathway or via a bulk degradation mechanism (e.g. autophagy or lipid droplet formation).

several promising 'dislocon' candidates have been proposed.

Sec61: The first candidate is the translocon itself. This dual function was proposed on the basis of the rapid dislocation of Class I MHC products by the immuno-evasin US2, and the occurrence of a diagnostic deglycosylated dislocation intermediate in association with Sec61ß [57]. Sec61 has since been found to engage in complex formation with different members of the dislocation machinery [58].

Derlins: In mammals, the family of Derlin proteins (whose name derives from its

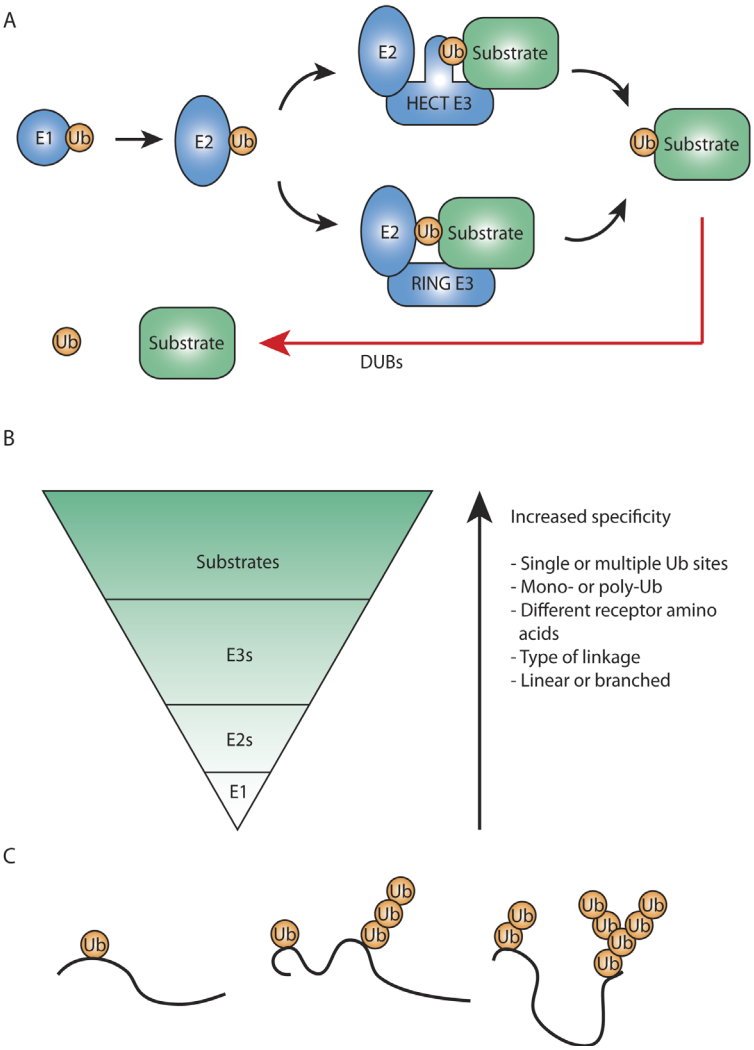

Figure 2: The ubiquitin system.
(A) Substrates are ubiquitylated via an E1-E2-E3 cascade. Ubiquitin is activiated by the E1 enzyme, and transferred to the E2 ubiquitin conjugating enzyme. An E3 ubiquitin ligase from either the RING domain family or the HECT domain family assist in transfer of the ubiquitin from the E2 to the substrate. This process is reversible by the activity of de-ubiquitylating enzymes (DUBs). (B) The increasing number of E2 and E3 enzymes suggest an attractive model to explain substrate specificity in the ubiquitin modification.(C) Schematic examples of mono-, multi- and complex poly-ubiquitylation.

founding member, the yeast Der1p protein involved in degradation of misfolded CPY* [59]) consists of three members (Derlin1-3) that have all been implicated in ER quality control [40]. They bear no obvious functional domains, carry multiple transmembrane domains and form both homo- and heterodimers, giving rise to the hypothesis that they could form (part of) a protein-conducting channel.

Ubiquitin ligases: A sizeable group of E3 ubiquitin ligases is directly anchored to, or associates with, the ER membrane and a growing number are implicated in ER quality control (Table 2). Sizeable proteins, they often include multiple transmembrane domains that do not obviously contribute to their enzymatic function and are more likely important for their intracellular positioning. The strongest case for ubiquitin ligase-mediated transport has been made for Hrd1p in yeast, which forms oligomers with the aid of Usa1 [60], associates with Der1p [60], and has been site-specifically photo-crosslinked to a dislocation substrate at residues in the Hrd1p transmembrane domains [20,21].

Involvement of lipid droplet formation [6] as well as autophagy [7] have been proposed as a possible means to relieve the ER of proteinaceous waste, but so far with little hard evidence in support. At least in yeast, visible lipid droplet formation was dispensable for dislocation of tested substrates [8]. This observation does not formally exclude a role for a mechanism akin to lipid droplet formation in dislocation, and the detection of components of the dislocation machinery (AUP1, UBE2G2) [9,10] on lipid droplets continues to fuel this hypothesis. Autophagy of an ER folding compartment overwhelmed with misfolded proteins (perchance UPR-dependent) remains an attractive means to clear misfolded proteins in bulk and deserves further investigation (Figure 1). The fidelity of the ER membrane as a barrier impermeant to proteins unless facilitated by the appropriate channels is perhaps too easily assumed in light of the dynamic nature of the ER and the abundance of fission and fusion events that take place there [11]: (even temporary) perforations of the ER membrane could allow escape of unwanted products.

Ubiquitylation is a general requirement for the dislocation of individual misfolded proteins. Attachment of a poly-ubiquitin chain triggers two important steps: first is the recruitment of the AAA (ATPase associated with a variety of cellular activities) ATPase p97 (VCP; Cdc48 in yeast), thought to provide the mechanical force to extract the misfolded polypeptide from the ER [12]; and, second, ubiquitylation flags the protein for targeting to the proteasome and thus its final demise [4]. The unity of function of poly-ubiquitylation has led to the proposal that dislocation and degradation are tightly coupled. This view requires modification: involvement of de-ubiquitylation enzymes (DUBs) in the dislocation reaction [13,14,15], demonstrates an uncoupling of dislocation from degradation [16]. The complexity of the mammalian ubiquitylation machinery, the build and type of ubiquitin linkages themselves, and the association of cytosolic chaperones with dislocation substrates [16], indicate

that proteasomal degradation of misfolded ER proteins is more complex than previously considered.

Ubiquitylation drives dislocation

Where examined, the extraction of a misfolded ER glycoprotein requires its ubiquitylation. The poly-ubiquitin chain serves as a recognition handle for p97 through its cofactors UFD1 and NPL4, and recruits it to drive dislocation [12]. Accordingly, obstruction of ubiquitylation causes the misfolded protein to accumulate inside the lumen of the ER. Whether or not the requirement for poly-ubiquitylation applies universally, or whether in select cases even a single ubiquitin (or multiple single ubiquitins) would suffice to engage the dislocation machinery remains to be clarified. Recruitment of substrates to the proteasome is believed to require a minimum of 4 ubiquitin units for a single chain to result in productive engagement of the 19S cap [4], but whether this $(Ub)_4$ rule applies generally is, again, not known. Turnover of at least Pax3 has been reported to rely on only a single ubiquitin moiety [17].

Ubiquitylation of proteins takes place via an E1-E2-E3 cascade [18] (Figure 2A). In mammalian cells, two E1s have been identified, about 40 E2s (ubiquitin conjugating enzymes) and possibly as many as 1000 E3s (ubiquitin ligases), although for the vast majority of E3s their enzymatic activity remains to be verified experimentally. Notwithstanding striking homologies, their function as enzymatically active E3s may not simply be assumed, as proteins with near-identical folds may serve very different functions. Nonetheless, this hierarchy would obviously allow a great deal of specificity (Figure 2B). Variables that control the operation of the ubiquitin system include the identity of the substrate and the E3 ligase that modifies it, the amino acid to which ubiquitin is conjugated, and the type of oligo- or poly-ubiquitin linkage made. The possibility of mono-, multi-, or poly-ubiquitylation adds yet further complexity (Figure 2C). The fact that certain proteins can be ubiquitylated at multiple distinct acceptor residues implies that *different* E3-type activities target these substrates, or that a *single* E3 activity is capable of *sequential and/or processive* engagement of one and the same substrate. The relevance of this point will become clear when we discuss sequential rounds of ubiquitin addition and removal as a requirement for destruction of misfolded ER proteins.

In the case of poly-ubiquitylation, there is the variety in linkage to consider. Ubiquitin offers seven lysine residues to which a following ubiquitin molecule can be

Mammalian ubiquitin conjugating enzymes	Topology/Functional Domains	Interacting mammalian ubiquitin ligases
UBE2J1 (UBC6E, NCUBE1) [65]	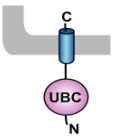	HRD1 [45] RMA1 [22]
UBE2J2 (UBC6, NCUBE2) [65]	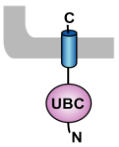	Parkin [66]
UBE2G2 (UBC7) [65]		Gp78 [65] HRD1 [67] Parkin [66]
Yeast ubiquitin conjugating enzymes		**Interacting yeast ubiquitin ligases**
Ubc1 [65]	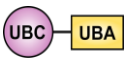	Hrd1p [65]
Ubc6 [65]	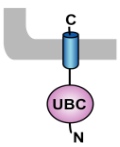	Doa10 [65]
Ubc7 [65]		Hrd1p [65] Doa10 [65]

Table 1: Mammalian and yeast ubiquitin conjugating enzymes and interacting ubiquitin ligases involved in ER dislocation.

UBC (ubiquitin conjugating domain); UBA (ubiquitin-associated domain). The ER membrane is represented by a shaded bar with the ER lumen in the upper right corner.

attached. Individual linkages are named for the position of the accepting lysine residue (e.g. K48 for attachment of ubiquitin to the lysine at position 48). Each type of linkage results in a characteristic and separate spatial structure. Ubiquitin is conjugated via its C-terminal di-glycine motif in thio-ester bond to the relevant E2 and is then transferred to an acceptor residue in the substrate polypeptide. Lysine is the preferred, but by no means the only ubiquitin acceptor; ubiquitin conjugation

to cysteine, threonine, serine or a protein's N-terminus has been reported [19]. The genesis of the various types of poly-ubiquitin chains has been extensively reviewed [19].
A physical interaction between the dislocation substrate in the ER and the E3 of choice must occur to enable ubiquitin conjugation, as we discussed for the Hrd1p ligase in yeast (see Box 1) [20,21]. How a soluble ER protein crosses the membrane barrier to reach the enzymatic domain of the E3 ligase is unclear. The polypeptide would at least have to protrude partially from a putative dislocon to allow ubiquitylation. Therefore transfer of a part of the polypeptide to be destroyed must already have progressed to the point where a residue suitable for ubiquitylation is exposed and accessible to the E3. The force needed to extract a polypeptide from the ER is provided by cytosolic p97, which engages the substrate only after poly-ubiquitin attachment. In much the same way as yeast Kar2p (yeast BiP ortholog) ratchets proteins into the ER in the course of translation, a similar mechanism might be employed by p97 for extraction of proteins from the ER in dislocation. If we extend this parallel, their might even exist the need for a force that pushes the protein out of the ER, akin to the translating ribosome for protein import. If indeed there were such an ER-resident first mover, its identity is yet to be discovered.

Substrate ubiquitylation is more easily understood for proteins that span the ER membrane and so may provide a naturally exposed handle for ubiquitylation. For some substrates, cytosolic – not membrane-bound – E3 ligases participate in their removal; the Hsc70/CHIP E3 ligase complex is recruited to the ER to target CFTRΔF508 for degradation [22] and the HIV encoded protein Vpu recruits the cytosolic ligase complex SCFbeta-TrCP to target CD4 for dislocation and proteasomal degradation [23]. The number of mammalian E3 ligases implicated in ER quality control continues to expand, including both integral membrane as well as cytosolic E3 ligases (Tables 1 and 2). Propelled by studies of yeast Hrd1p, most of the current mechanistic information has been acquired for its mammalian ortholog HRD1, which may or may not represent all avenues open to dislocation.

It is common practice to test the involvement of any particular E3 ligase in turnover of known dislocation substrates and thus implicate the ligase in ER quality control. These experiments rely on the limited set of often artificial substrates that the E3 can be tested against. These tools provide a skewed view of substrate turnover at endogenous protein expression levels, as overexpression of the artificial substrate can modulate the landscape of the ER through activation of the UPR. Examples

Mammalian ER membrane-anchored ubiquitin ligases	Topology/Functional Domains	Corresponding in vivo dislocation substrates
HRD1 (Synoviolin) [67]	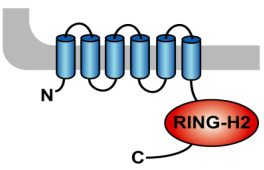	T-cell receptor subunits TCR-α and CD3-δ [67] HMG CoA reductase [67] null Hong Kong variant of apha-1-antitrypsin (premature stop codon) [68] Z variant of alpha-1-antitrypsin (E342K mutation) [69] Ig κ light chain [70] Ig μ heavy chain [70] Class I MHC heavy chain [45,70] Ribophorin$_{332}$ (deletion of transmembrane domain) [70] Hedgehog precursor and C-terminal fragment [71] Neuroserpin mutants (various point mutants) [72] Gp78 [73] Pael (Parkin-associated endothelin receptor-like) receptor [65]

Gp78 (autocrine motility factor receptor, AMFR, RNF45) [65]	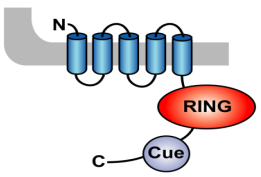	T-cell receptor subunits TCR-α and CD3-δ [65] Z variant of alpha-1-antitrypsin (E342K mutation) [65] CFTR mutant (F508 deletion in cytosolic domain) [74] Apolipoprotein B100 [65] HMG-CoA reductase [65] Insig-1 [65] KAI1 [70] Cytochrome P450 3A [75] Neuroserpin mutants (various point mutants) [72]
RMA1 (RNF5) [70]	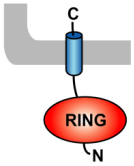	CFTR and mutant CFTR (F508 deletion in cytosolic domain) [22]
TEB4 (MARCH-VI) [65,76]	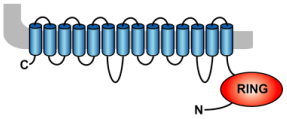	Type 2 iodothyronine deiodinase [77]
RFP2 (Leu5, Trim13) [78]	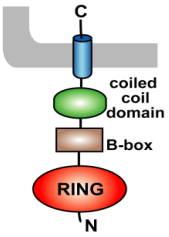	CD3-δ [78] Cav1.2 channels [79]

TRC8 (translocation in renal carcinoma, chromosome 8 gene, RNF139) [80]	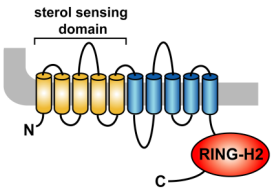	Class I MHC (cytomegalovirus US2-mediated) [80] Insig-1 [81] Sterol regulatory element binding protein precursor [81]
Kf-1 (RNF103) [82]	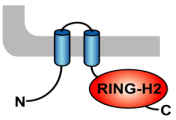	None
RNF170 [83]	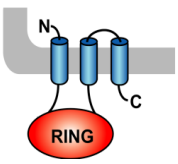	Inositol 1,4,5-trisphosphate (IP_3)[3] receptor [83]
Nixin/ZNRF4 [84]	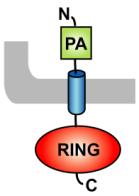	Calnexin [84]
Mammalian cytosolic ubiquitin ligases		
CHIP (C-teminus of Hsc70 interacting protein) [65]	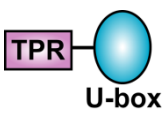	CFTR and mutant CFTR (F508 deletion in cytosolic domain) [22] Cytochrome P450 3A [75]
Parkin [65]	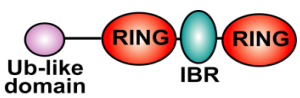	Pael (Parkin-associated endothelin receptor-like) receptor [66] Glucocerebrosidase mutants (various point mutations) [85]

SCF$^{\beta\text{-TrCP}}$ [23]	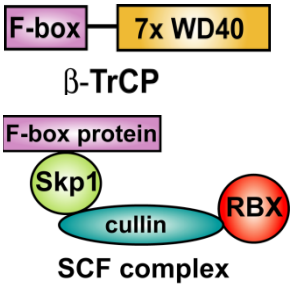	CD4 (HIV-1 Vpu-mediated) [23] Tetherin (HIV-1 Vpu-mediated) [86]
SCF^{Fbs1} (NFB42, Fbx2) [70]	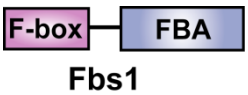	Pre-integrin β1 [87] CFTR mutant (F508 deletion in cytosolic domain) [87] TCR-α [87] **N**-methyl-D-aspartate-type glutamate receptor NR1 subunit [88] β-secretase (BACE1) [89]
SCF^{Fbs2} (Fbx6b, FBG2) [70]	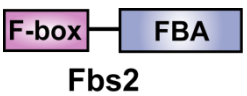	TCR-α [90]
Smurf1 (Smad ubiquitination regulatory factor 1) [91]		Wolfram syndrome protein [91]
Nrdp1 (FLRF) [92]	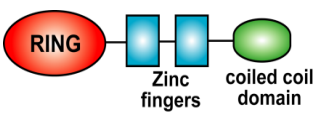	ErbB3 [92]

Yeast ubiquitin ligases		
Hrd1p [65]	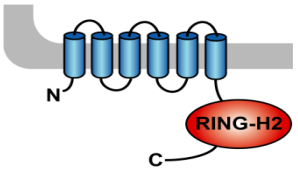	Carboxypeptidase Y mutant (CPY*) (G255R mutation) [65] Sec61-2p [65] Pdr5 mutant (Pdr5*) (C1427Y mutation) [65] Hmg2p [65] Proteinase A mutant (PrA*) (glycosylation and deletion mutants) [93] Epithelial sodium channel (EnaC) α-, β-, γ- subunits [94] Sterol regulatory element-binding protein precursor [95]
Doa10 [65,76]	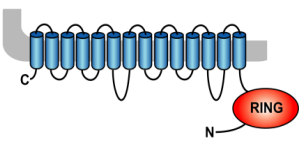	Ubc6 [96] Ste6–166 mutant (Ste*) (premature stop codon) [97] Pma1 mutant (D378N) [98] Mps2-1 mutant [99] Epithelial sodium channel (EnaC) α-, β-, γ- subunits [94]

Table 2: Mammalian and yeast ubiquitin ligases involved in ER dislocation and corresponding in vivo substrates.

The ER membrane is represented by a shaded bar with the ER lumen in the upper right corner. Except for TEB4/Doa10, the indicated membrane topologies of polytopic ubiquitin ligases are predicted based on the sequence but not experimentally confirmed. Polytopic membrane substrates are in blue, single-pass membrane substrates are in green, ER luminal substrates are in red, and tail-anchored substrates are indicated in brown color. RING (really interesting new gene); PA (protease-associated domain); TPR (tetratricopeptide repeat domain); IBR (in-between RING domain); FBA (F-box-associated domain); HECT (homologous to the E6-AP carboxyl terminus).

that approach more physiological levels of turnover include endogenous Class I MHC heavy chains [24,25], the turnover of immunoglobulin subunits [26] or degradation of proteins that undergo extensive processing in the ER such as the Hedgehog protein, which matures by autocatalytic cleavage, separating into an N-terminal signaling molecule and a C-terminal fragment that undergoes dislocation [27].

Connecting a particular E3 ligase complex with the turnover of specific ER-resident proteins tackles only one type of variability of ubiquitin-conjugation. Ubiquitin-conjugation to amino acid side chains other than lysine has been described for ER dislocation-induced ubiquitylation of TCRa [28], Class I MHC [29], as well as the NS-1 non-secreted immunoglobulin light chain [26]. Degradation of these substrates required the HRD1 ligase for ubiquitin-conjugation to serine, threonine and lysine residues. One can argue whether the identity of the acceptor amino acid plays a specific role, such as conferring susceptibility to hydrolysis of the linkage produced (amide versus thioester or hydroxy ester) or whether this is simply determined by its accessibility, caused by partial unfolding of the substrate protein. Attachment of ubiquitin may further modify the physical properties of the substrate [30], and help start it to unfold, which in return could free up preferred acceptor amino acids, if any.

Ubiquitylation is required for the dislocation reaction, but the exact role of ubiquitylation in this context remains ill-defined. Does it serve as a direct handle for extraction of the misfolded protein? Does it enable the recruitment of additional factors that continue and complete the dislocation reaction after its initial engagement? It is not clear whether p97 recruitment depends on mono-, poly- or multi-ubiquitylation of a substrate, nor do we know whether there is a single or several preferred ubiquitin-linkages. A possible complicating factor in interpretation of such experiments is the application of proteasome inhibitors, commonly used to visualize the presence of poly-ubiquitin adducts. While it is likely that poly-ubiquitin chains are present also in cells not treated with proteasome inhibitors, neither the extent nor dynamics of poly-ubiquitylation are immediately obvious in the untreated control setting. A K48-linked poly-ubiquitin tag was initially thought to determine proteasomal targeting, but a more complex picture emerged with the demonstrated involvement of all lysine linked ubiquitin-linkages in proteasomal targeting [31,32]. There may be a prominent role for K11-linked ubiquitin in ER quality control [31]. Furthermore, there is no evidence that poly-ubiquitin chains in vivo are homogeneous in linkage, leaving open the possibility of heterogeneity within a single or

between multiple chains conjugated to a given substrate, thus rephrasing the question as linkage-dominant instead of linkage-specific.

Ubiquitin-linkage specificity is largely determined by the E2 enzyme; it was recently demonstrated how the E2 UBE2S specifically builds K11-linked ubiquitin chains [33]. Mammalian E2s currently implicated in dislocation, such as UBE2J1, UBE2J2 and UBE2G2 remain to be examined from the perspective of linkage type and the E3s they serve. Monoclonal antibodies that recognize specific ubiquitin linkages will be of considerable help [34,35]. The in vivo pairing of E2s with E3s remains enigmatic, and thus resolving the extent to which the promiscuity for E2-E3 pairings observed in vitro translates to the in vivo situation is a technical challenge.

Substrate extraction and deubiquitylation.

Modification of a substrate with ubiquitin can recruit either of two multiprotein complexes that can extract the protein from the ER: p97 with its associated co-factors [12], and the 19S cap of the proteasome [36]. Although different in composition, the core of each complex consists of a ring-shaped, hexameric ATPase of the AAA family that can unfold polypeptides at the expense of ATP hydrolysis [4,12] (Figure2).

Two different types of ubiquitin receptors allow substrate engagement by the proteasome, either integrated into the structure of the proteasome itself, such as Rpn10 and Rpn13, or in the form of shuttling factors such as Rad23, Dsk2 and Ddi1 (in yeast) [4]. Upon engagement, a de-ubiquitylating activity (Rpn11) associated with the cap of the proteasome removes ubiquitin from the substrate. This allows recycling of ubiquitin and ensures compliance with size constraints of the access portal to the proteasome, which can accommodate looped polypeptides but not those with a conjugated complex ubiquitin ensemble.

The 19S cap has been reported to associate with the Sec61 translocon. Moreover, the purified cap complex supports dislocation in vitro [36,37,38]. The proposed structure of the Sec61 translocon [39] includes a narrow pore that can accommodate only unstructured polypeptides (the folding status of dislocated proteins is discussed in Box 3), and therefore the functional relevance of this physical link requires further experimental support. Whereas one can see how the short alpha-helical ‘plug’ [39] in the Sec61 pore is displaced from the ER luminal side of the

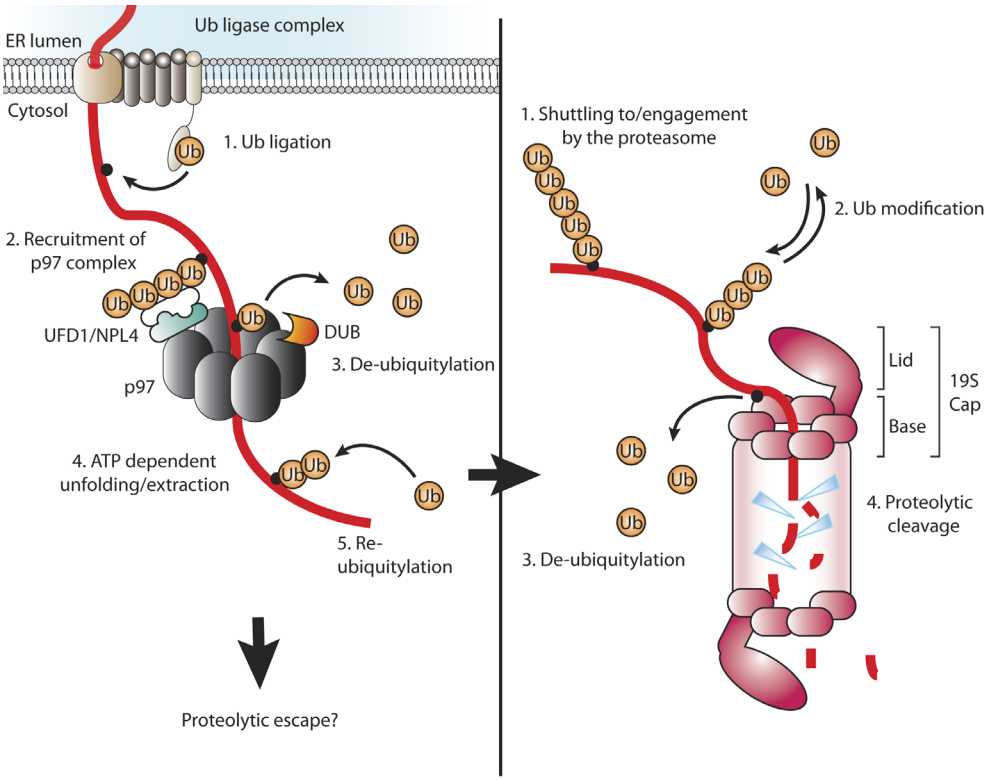

1. Ubiquitin ligase complex (see table 1)
2. UFD1/NPL4
3. YOD1, Ataxin 3, USP19
4. p97
5. Ubiquitin ligase complex? Ufd2?

1. Rad23, Dsk2, Ddi1, Rpn10, Rpn12, BAG6?
2. Uch37, Ubp6/USP14
3. Rpn11
4. Proteasome

Figure 3: Protein dislocation and/or degradation.
Left panel: A proposed model of a dislocated protein that is ubiquitylated at the ER membrane and consequently engaged by p97 via NFD1/NPL4. A de-ubiquitylating enzyme cleaves ubiquitin to allow threading of the polypeptide through the central pore of p97. A hypothesized re-ubiquitylation step post-p97 then facilitates proteasomal targeting. Right panel: A poly-ubiquitin tag targets the protein for proteasomal degradation. The poly-ubiquitin chain is probably modified before it is finally removed to allow threading of the polypeptide through the central pore of the base of the 19S cap and into the proteolytic chamber of the 20S proteasome core particle.

translocon upon protein translocation, it would presumably occlude the pore upon reverse passage. More appealing is the proposal that the proteasome can directly engage membrane proteins tagged with poly-ubiquitin[40], as has been suggested for turnover of Ubc6 in yeast. When proteasome function was selectively impaired

at one of the chymotryptic sites (pre1-1), a distinct breakdown intermediate remained associated with the ER membrane, thought to represent the trans-membrane domain of Ubc6 severed from its digested cytosolic domain [41].

P97 nucleates distinct multiprotein complexes implicated in diverse functions in the cell, ranging from dislocation and proteasomal targeting to cell cycle control and vesicular trafficking [12]. Adaptor proteins engage p97 and can either recruit or adapt it to a specific function. P97 engages ubiquitylated proteins via a dimeric adaptor consisting of NPL4 and UFD1. This dimer can engage ubiquitin and associates with the N-terminal domain of p97. Membrane-anchored auxiliaries such as VIMP [42], UBXD2 [43,44] and UBXD8 [45]^{3}- may recruit this dislocation-competent complex to the ER membrane via their p97-interacting UBX-domain. P97 can directly interact with the ligase as shown for gp78 [40]. A hierarchy in p97 cofactors was described, such that FAF1 and UBXD7 only bind to p97 when in complex with the NPL4/UFD1 dimer, but neither engages p97 alone [44]. Of note, a p97-driven dislocation reaction has been described independently of NPL4/UFD1 [46]. It will be important to determine whether a binding hierarchy exists for the p97 complex implicated in dislocation, as this can provide insight into the timing of the dislocation reaction (Table 3 lists p97 cofactors involved in dislocation). Modulation of p97 co-factors can be regulated by phosphorylation or acetylation of p97 itself [47,48].

Akin to the proteasome, the hexameric pore of p97 can accommodate a polypeptide modified with ubiquitin [49]. There is some debate as to how p97 engages the polypeptide. One model suggests the protein enters via the D1 ring, and is threaded through the structure to exit via the D2 ring (Figure 3). This is contrasted with models where the polypeptide loops into the D2 ring alone, or where the hexamer could even dissociate to release the substrate [12]. Either model suggests similar space constraints, which is most relevant for the current discussion. It is unlikely that p97 can engage a protein bearing a poly-ubiquitin chain, exactly the type of chain that is thought to facilitate transfer to the proteasome with the help of shuttling factors. Indeed, DUBs participate in the mammalian dislocation reaction, in agreement with their function at the 19S cap of the proteasome. Expression of a catalytically inactive form of the ER-membrane anchored USP19 hampered dislocation of several substrates [14]. Also, the de-ubiquitylating enzyme Ataxin 3 associates with p97 and expression of a catalytically inactive mutant causes accumulation of poly-ubiquitylated substrates in association with p97 [15]. In a rather unconventional proposal, such poly-ubiquitin chains were deemed shielded from

Ataxin 3 engagement by the p97 adaptor protein SAKS1, which could thus negatively regulate dislocation [50]. Furthermore, the de-ubiquitylating enzyme YOD1 is recruited to p97 via its UBX domain. Tampering with its function results in a near-complete blockade of dislocation [13]. Interference with dislocation/p97-associated de-ubiquitylating activity causes accumulation of misfolded proteins at a step prior to membrane extraction [13]. If de-ubiquitylating activity indeed were required to complete p97-catalyzed extraction, then such a blockade should be overcome by expression of a de-ubiquitylating enzyme that can engage these stalled poly-ubiquitinated dislocation intermediates. Exactly this was shown by co-expression of the catalytic domain of the Epstein Barr Virus large tegument protein BPFL1 (EBV DUB). Completion of the dislocation reaction thus relies on a de-ubiquitylating activity [16].

As proteasomal targeting requires ubiquitylation, it follows that substrates that undergo p97-mediated extraction, once de-ubiquitylated, require a second round of ubiquitin-modification. Do p97-associated DUBs merely trim ubiquitin-chains or do they remove them completely? Polypeptides modified with mono-ubiquitin might pass through the central pore of p97 and then engage the proteasome directly, or do so after ubiquitin chain extension by either an E3 mediated ligase reaction or via an E4-like activity (enzymes thought to engage and extend existing ubiquitin conjugates). The E4 Ufd2 has been linked to dislocation via Cdc48 in yeast [51]. In fact, soluble (dislocated) Ste6(p)* was observed in a system deprived of Ufd2 [52], where Ufd2 was suggested to increase the level of poly-ubiquitylation and thus facilitate proteasomal turnover, a suggestion that corroborates the model described above (Figure 3).

De-ubiquitylating activity at p97 opens the exciting possibility to modify the type of ubiquitin-linkage utilized, where one type of ubiquitin-build could induce extraction, followed by a switch to target the polypeptide to the proteasome.

Folding status of dislocation substrates

Translocation of proteins, as well as their threading into the central channel of the proteasome, presumably requires complete unfolding of the polypeptide chain. Whether this is also required for a misfolded protein to pass the ER membrane in the course of dislocation is still unclear. A substrate-GFP fusion protein shows no obvious loss of fluorescence while the protein undergoes dislocation [61],

Protein	Function	Interaction Domain
UFD1/NPL4 [12]	Facilitates engagement of poly-ubiquitin proteins	UBX
UBXD2 (Erasin) [43]	P97 recruitment	UBX
UBXD8 [45]	P97 recruitment	UBX
YOD1 [13]	De-ubiquitylating activity at p97	UBX
VIMP [42]	Recruits p97 to the ER membrane	Unknown
Peptide: N-glycosidase [100]	Enzymatic removal of N-linked glycans	PUB
Ataxin3 [15]	De-ubiquitylating activity at p97	VCP binding motif (VBM)
SAKS1 [50]	Mediates ubiquitin interactions	UBX

Table 3: P97 co-factors involved in mammalian dislocation

although this observation could be attributed to the ß-barrel of GFP snapping back into shape once it reaches the cytosol. Also, DHFR-substrate fusion proteins are readily dislocated even in the presence of cell-permeable analogs of methotrexate that stabilize the DHFR moiety [62], albeit with slower kinetics [63]. These observations, while by no means conclusive, raise the possibility of a dislocon that can accommodate partially folded proteins, a suggestion not easily reconciled with the structures proposed for the Sec61 channel [39]. It is important to keep in mind that multi-domain proteins deemed misfolded in quality control may still have acquired

fully folded domains. Furthermore, no protein with unfoldase activity (e.g. p97, 19S cap) has been detected on the luminal side of the ER, although a candidate in the form of the AAA ATPase TorsinA has been implicated in ER quality control [64]. The folding status of a protein undergoing dislocation across the ER membrane will remain a thorny issue until the identity of (a) putative channel(s) has been firmly established.

Soluble in the cytosol

How the cell avoids aggregation of (partly) unfolded ER glycoproteins discharged into the cytosol is poorly understood. Hydrophobic protein domains find themselves exposed to an aqueous environment upon escape from the ER. As an example, when proteasomal proteolysis is blocked, Class I MHC products with their transmembrane segment fully intact occur as soluble intermediates in the cytoplasm of cells that express viral immunoevasins [24]. The cytoplasm houses an extensive chaperone network involved in the quality control of cytosolic proteins, with Hsp70 and Hsp90 its most famous family members [53]. Both have been proposed to triage the folding of complex membrane proteins, but there is limited direct evidence that ties them to quality control/dislocation of lumenal ER proteins.

One can visualize dislocated ER proteins in the cytosol by blocking proteasomal degradation, either via chemical (as just discussed for Class I MHC) or enzymatic means [16]. Expression of the catalytic domain of the large tegument-embedded ubiquitin-specific protease domain taken from Epstein-Barr virus, EBV-DUB, impairs proteasomal degradation by preemptively removing the ubiquitin-tag from substrates. In cells that express this EBV-DUB, dislocation of ER proteins continues, albeit at a reduced rate (as expected, if ubiquitylation is a prerequisite for the first step(s) in the dislocation pathway) and the misfolded ER-derived glycoprotein accumulates as a deglycosylated product in association with the cytosolic chaperone BAG6 (BAT3) [16]. In addition, an interaction with the TRICC/CCT complex was detected. BAG6 shuttles defective translation products for degradation to the proteasome [54,55], tying it to unfolded proteins. BAG6 does not merely associate with dislocation substrates when degradation is blocked, but is required to complete the dislocation reaction itself [56].

Engagement by chaperones, combined with a de-ubiquitylation step as an ER-resident protein exits from the ER, opens a window where substrates could deviate

from the path to the proteasome. Such escape from proteolysis and the possibility of chaperone-mediated refolding could explain a set of observations where proteins (such as cholera toxin), formerly localized to the ER, escape to the cytoplasm and acquire their active conformation. Bacterial toxins may utilize dislocation machinery to reach the cytosol, be released from cytosolic chaperones -if they interact with them at all- and be allowed to reach their target for covalent modification (ADP-ribosylation, proteolysis etc).

In this thesis, I will discuss work that addresses the machinery held responsible for substrate ubiquitylation, a novel method to block the UPS by expression of a 'hyperactive' DUB, and the discovery of a cytosolic chaperone that is required for the dislocation reaction.

References

1. Braakman I, Bulleid NJ (2011) Protein folding and modification in the Mammalian endoplasmic reticulum. Annu Rev Biochem 80: 71-99.
2. Ward CL, Kopito RR (1994) Intracellular turnover of cystic fibrosis transmembrane conductance regulator. Inefficient processing and rapid degradation of wild-type and mutant proteins. J Biol Chem 269: 25710-25718.
3. Ron D, Walter P (2007) Signal integration in the endoplasmic reticulum unfolded protein response. Nat Rev Mol Cell Biol 8: 519-529.
4. Finley D (2009) Recognition and processing of ubiquitin-protein conjugates by the proteasome. Annu Rev Biochem 78: 477-513.
5. Rapoport TA (2007) Protein translocation across the eukaryotic endoplasmic reticulum and bacterial plasma membranes. Nature 450: 663-669.
6. Ploegh HL (2007) A lipid-based model for the creation of an escape hatch from the endoplasmic reticulum. Nature 448: 435-438.
7. Bernales S, McDonald KL, Walter P (2006) Autophagy counterbalances endoplasmic reticulum expansion during the unfolded protein response. PLoS Biol 4: e423.
8. Olzmann JA, Kopito RR (2011) Lipid Droplet Formation Is Dispensable for Endoplasmic Reticulum-associated Degradation. J Biol Chem 286: 27872-27874.
9. Spandl J, Lohmann D, Kuerschner L, Moessinger C, Thiele C (2011) Ancient ubiquitous protein 1 (AUP1) localizes to lipid droplets and binds the E2 ubiquitin conjugase G2 (Ube2g2) via its G2 binding region. J Biol Chem

286: 5599-5606.
10. Klemm EJ, Spooner E, Ploegh HL (2011) The dual role of ancient ubiquitous protein 1 (AUP1) in lipid droplet accumulation and ER protein quality control. J Biol Chem.
11. Engel A, Walter P (2008) Membrane lysis during biological membrane fusion: collateral damage by misregulated fusion machines. J Cell Biol 183: 181-186.
12. Stolz A, Hilt W, Buchberger A, Wolf DH (2011) Cdc48: a power machine in protein degradation. Trends Biochem Sci.
13. Ernst R, Mueller B, Ploegh HL, Schlieker C (2009) The otubain YOD1 is a deubiquitinating enzyme that associates with p97 to facilitate protein dislocation from the ER. Mol Cell 36: 28-38.
14. Hassink GC, Zhao B, Sompallae R, Altun M, Gastaldello S, et al. (2009) The ER-resident ubiquitin-specific protease 19 participates in the UPR and rescues ERAD substrates. EMBO Rep 10: 755-761.
15. Wang Q, Li L, Ye Y (2006) Regulation of retrotranslocation by p97-associated deubiquitinating enzyme ataxin-3. J Cell Biol 174: 963-971.
16. Ernst R, Claessen JH, Mueller B, Sanyal S, Spooner E, et al. (2011) Enzymatic blockade of the ubiquitin-proteasome pathway. PLoS Biol 8: e1000605.
17. Boutet SC, Disatnik MH, Chan LS, Iori K, Rando TA (2007) Regulation of Pax3 by proteasomal degradation of monoubiquitinated protein in skeletal muscle progenitors. Cell 130: 349-362.
18. Deshaies RJ, Joazeiro CA (2009) RING domain E3 ubiquitin ligases. Annu Rev Biochem 78: 399-434.
19. Kerscher O, Felberbaum R, Hochstrasser M (2006) Modification of proteins by ubiquitin and ubiquitin-like proteins. Annu Rev Cell Dev Biol 22: 159-180.
20. Carvalho P, Stanley AM, Rapoport TA (2010) Retrotranslocation of a misfolded luminal ER protein by the ubiquitin-ligase Hrd1p. Cell 143: 579-591.
21. Sato BK, Schulz D, Do PH, Hampton RY (2009) Misfolded membrane proteins are specifically recognized by the transmembrane domain of the Hrd1p ubiquitin ligase. Mol Cell 34: 212-222.
22. Younger JM, Chen L, Ren HY, Rosser MF, Turnbull EL, et al. (2006) Sequential quality-control checkpoints triage misfolded cystic fibrosis transmembrane conductance regulator. Cell 126: 571-582.
23. Binette J, Dube M, Mercier J, Halawani D, Latterich M, et al. (2007) Requirements for the selective degradation of CD4 receptor molecules by the human immunodeficiency virus type 1 Vpu protein in the endoplasmic reticu-

lum. Retrovirology 4: 75.
24. Wiertz EJ, Jones TR, Sun L, Bogyo M, Geuze HJ, et al. (1996) The human cytomegalovirus US11 gene product dislocates MHC class I heavy chains from the endoplasmic reticulum to the cytosol. Cell 84: 769-779.
25. Burr ML, Cano F, Svobodova S, Boyle LH, Boname JM, et al. (2011) HRD1 and UBE2J1 target misfolded MHC class I heavy chains for endoplasmic reticulum-associated degradation. Proc Natl Acad Sci U S A 108: 2034-2039.
26. Shimizu Y, Okuda-Shimizu Y, Hendershot LM (2010) Ubiquitylation of an ERAD substrate occurs on multiple types of amino acids. Mol Cell 40: 917-926.
27. Chen X, Tukachinsky H, Huang CH, Jao C, Chu YR, et al. (2011) Processing and turnover of the Hedgehog protein in the endoplasmic reticulum. J Cell Biol 192: 825-838.
28. Ishikura S, Weissman AM, Bonifacino JS (2010) Serine residues in the cytosolic tail of the T-cell antigen receptor alpha-chain mediate ubiquitination and endoplasmic reticulum-associated degradation of the unassembled protein. J Biol Chem 285: 23916-23924.
29. Wang X, Herr RA, Chua WJ, Lybarger L, Wiertz EJ, et al. (2007) Ubiquitination of serine, threonine, or lysine residues on the cytoplasmic tail can induce ERAD of MHC-I by viral E3 ligase mK3. J Cell Biol 177: 613-624.
30. Hagai T, Levy Y (2010) Ubiquitin not only serves as a tag but also assists degradation by inducing protein unfolding. Proc Natl Acad Sci U S A 107: 2001-2006.
31. Xu P, Duong DM, Seyfried NT, Cheng D, Xie Y, et al. (2009) Quantitative proteomics reveals the function of unconventional ubiquitin chains in proteasomal degradation. Cell 137: 133-145.
32. Saeki Y, Kudo T, Sone T, Kikuchi Y, Yokosawa H, et al. (2009) Lysine 63-linked polyubiquitin chain may serve as a targeting signal for the 26S proteasome. EMBO J 28: 359-371.
33. Wickliffe KE, Lorenz S, Wemmer DE, Kuriyan J, Rape M (2011) The mechanism of linkage-specific ubiquitin chain elongation by a single-subunit E2. Cell 144: 769-781.
34. Newton K, Matsumoto ML, Wertz IE, Kirkpatrick DS, Lill JR, et al. (2008) Ubiquitin chain editing revealed by polyubiquitin linkage-specific antibodies. Cell 134: 668-678.
35. Matsumoto ML, Wickliffe KE, Dong KC, Yu C, Bosanac I, et al. (2010) K11-linked polyubiquitination in cell cycle control revealed by a K11 linkage-specific antibody. Mol Cell 39: 477-484.

36. Kalies KU, Allan S, Sergeyenko T, Kroger H, Romisch K (2005) The protein translocation channel binds proteasomes to the endoplasmic reticulum membrane. EMBO J 24: 2284-2293.
37. Ng W, Sergeyenko T, Zeng N, Brown JD, Romisch K (2007) Characterization of the proteasome interaction with the Sec61 channel in the endoplasmic reticulum. J Cell Sci 120: 682-691.
38. Lee RJ, Liu CW, Harty C, McCracken AA, Latterich M, et al. (2004) Uncoupling retro-translocation and degradation in the ER-associated degradation of a soluble protein. EMBO J 23: 2206-2215.
39. Van den Berg B, Clemons WM, Jr., Collinson I, Modis Y, Hartmann E, et al. (2004) X-ray structure of a protein-conducting channel. Nature 427: 36-44.
40. Bagola K, Mehnert M, Jarosch E, Sommer T (2011) Protein dislocation from the ER. Biochim Biophys Acta 1808: 925-936.
41. Walter J, Urban J, Volkwein C, Sommer T (2001) Sec61p-independent degradation of the tail-anchored ER membrane protein Ubc6p. EMBO J 20: 3124-3131.
42. Ye Y, Shibata Y, Yun C, Ron D, Rapoport TA (2004) A membrane protein complex mediates retro-translocation from the ER lumen into the cytosol. Nature 429: 841-847.
43. Liang J, Yin C, Doong H, Fang S, Peterhoff C, et al. (2006) Characterization of erasin (UBXD2): a new ER protein that promotes ER-associated protein degradation. J Cell Sci 119: 4011-4024.
44. Hanzelmann P, Buchberger A, Schindelin H (2011) Hierarchical Binding of Cofactors to the AAA ATPase p97. Structure 19: 833-843.
45. Mueller B, Klemm EJ, Spooner E, Claessen JH, Ploegh HL (2008) SEL1L nucleates a protein complex required for dislocation of misfolded glycoproteins. Proc Natl Acad Sci U S A 105: 12325-12330.
46. Soetandyo N, Ye Y (2010) The p97 ATPase dislocates MHC class I heavy chain in US2-expressing cells via a Ufd1-Npl4-independent mechanism. J Biol Chem 285: 32352-32359.
47. Zhao G, Zhou X, Wang L, Li G, Schindelin H, et al. (2007) Studies on peptide:N-glycanase-p97 interaction suggest that p97 phosphorylation modulates endoplasmic reticulum-associated degradation. Proc Natl Acad Sci U S A 104: 8785-8790.
48. Ewens CA, Kloppsteck P, Forster A, Zhang X, Freemont PS (2010) Structural and functional implications of phosphorylation and acetylation in the regulation of the AAA+ protein p97. Biochem Cell Biol 88: 41-48.

49. DeLaBarre B, Christianson JC, Kopito RR, Brunger AT (2006) Central pore residues mediate the p97/VCP activity required for ERAD. Mol Cell 22: 451-462.
50. LaLonde DP, Bretscher A (2011) The UBX protein SAKS1 negatively regulates endoplasmic reticulum-associated degradation and p97-dependent degradation. J Biol Chem 286: 4892-4901.
51. Koegl M, Hoppe T, Schlenker S, Ulrich HD, Mayer TU, et al. (1999) A novel ubiquitination factor, E4, is involved in multiubiquitin chain assembly. Cell 96: 635-644.
52. Nakatsukasa K, Huyer G, Michaelis S, Brodsky JL (2008) Dissecting the ER-associated degradation of a misfolded polytopic membrane protein. Cell 132: 101-112.
53. Buchberger A, Bukau B, Sommer T (2010) Protein quality control in the cytosol and the endoplasmic reticulum: brothers in arms. Mol Cell 40: 238-252.
54. Minami R, Hayakawa A, Kagawa H, Yanagi Y, Yokosawa H, et al. (2010) BAG-6 is essential for selective elimination of defective proteasomal substrates. J Cell Biol 190: 637-650.
55. Hessa T, Sharma A, Mariappan M, Eshleman HD, Gutierrez E, et al. (2011) Protein targeting and degradation are coupled for elimination of mislocalized proteins. Nature.
56. Wang Q, Liu Y, Soetandyo N, Baek K, Hegde R, et al. (2011) A ubiquitin ligase-associated chaperone holdase maintains polypeptides in soluble States for proteasome degradation. Mol Cell 42: 758-770.
57. Wiertz EJ, Tortorella D, Bogyo M, Yu J, Mothes W, et al. (1996) Sec61-mediated transfer of a membrane protein from the endoplasmic reticulum to the proteasome for destruction. Nature 384: 432-438.
58. Schafer A, Wolf DH (2009) Sec61p is part of the endoplasmic reticulum-associated degradation machinery. EMBO J 28: 2874-2884.
59. Knop M, Finger A, Braun T, Hellmuth K, Wolf DH (1996) Der1, a novel protein specifically required for endoplasmic reticulum degradation in yeast. EMBO J 15: 753-763.
60. Horn SC, Hanna J, Hirsch C, Volkwein C, Schutz A, et al. (2009) Usa1 functions as a scaffold of the HRD-ubiquitin ligase. Mol Cell 36: 782-793.
61. Fiebiger E, Story C, Ploegh HL, Tortorella D (2002) Visualization of the ER-to-cytosol dislocation reaction of a type I membrane protein. EMBO J 21: 1041-1053.
62. Tirosh B, Furman MH, Tortorella D, Ploegh HL (2003) Protein unfolding is not a

prerequisite for endoplasmic reticulum-to-cytosol dislocation. J Biol Chem 278: 6664-6672.
63. Bhamidipati A, Denic V, Quan EM, Weissman JS (2005) Exploration of the topological requirements of ERAD identifies Yos9p as a lectin sensor of misfolded glycoproteins in the ER lumen. Mol Cell 19: 741-751.
64. Nery FC, Armata IA, Farley JE, Cho JA, Yaqub U, et al. (2011) TorsinA participates in endoplasmic reticulum-associated degradation. Nat Commun 2: 393.
65. Kostova Z, Tsai YC, Weissman AM (2007) Ubiquitin ligases, critical mediators of endoplasmic reticulum-associated degradation. Semin Cell Dev Biol 18: 770-779.
66. Imai Y, Soda M, Inoue H, Hattori N, Mizuno Y, et al. (2001) An unfolded putative transmembrane polypeptide, which can lead to endoplasmic reticulum stress, is a substrate of Parkin. Cell 105: 891-902.
67. Kikkert M, Doolman R, Dai M, Avner R, Hassink G, et al. (2004) Human HRD1 is an E3 ubiquitin ligase involved in degradation of proteins from the endoplasmic reticulum. J Biol Chem 279: 3525-3534.
68. Christianson JC, Shaler TA, Tyler RE, Kopito RR (2008) OS-9 and GRP94 deliver mutant alpha1-antitrypsin to the Hrd1-SEL1L ubiquitin ligase complex for ERAD. Nat Cell Biol 10: 272-282.
69. Wang H, Li Q, Shen Y, Sun A, Zhu X, et al. The ubiquitin ligase Hrd1 promotes degradation of the Z variant alpha 1-antitrypsin and increases its solubility. Mol Cell Biochem 346: 137-145.
70. Hirsch C, Gauss R, Horn SC, Neuber O, Sommer T (2009) The ubiquitylation machinery of the endoplasmic reticulum. Nature 458: 453-460.
71. Chen X, Tukachinsky H, Huang CH, Jao C, Chu YR, et al. Processing and turnover of the Hedgehog protein in the endoplasmic reticulum. J Cell Biol 192: 825-838.
72. Ying Z, Wang H, Fan H, Wang G The endoplasmic reticulum (ER)-associated degradation system regulates aggregation and degradation of mutant neuroserpin. J Biol Chem 286: 20835-20844.
73. Shmueli A, Tsai YC, Yang M, Braun MA, Weissman AM (2009) Targeting of gp78 for ubiquitin-mediated proteasomal degradation by Hrd1: cross-talk between E3s in the endoplasmic reticulum. Biochem Biophys Res Commun 390: 758-762.
74. Morito D, Hirao K, Oda Y, Hosokawa N, Tokunaga F, et al. (2008) Gp78 cooperates with RMA1 in endoplasmic reticulum-associated degradation of

CFTRDeltaF508. Mol Biol Cell 19: 1328-1336.
75. Kim SM, Acharya P, Engel JC, Correia MA Liver cytochrome P450 3A ubiquitination in vivo by gp78/autocrine motility factor receptor and C terminus of Hsp70-interacting protein (CHIP) E3 ubiquitin ligases: physiological and pharmacological relevance. J Biol Chem 285: 35866-35877.
76. Kreft SG, Wang L, Hochstrasser M (2006) Membrane topology of the yeast endoplasmic reticulum-localized ubiquitin ligase Doa10 and comparison with its human ortholog TEB4 (MARCH-VI). J Biol Chem 281: 4646-4653.
77. Zavacki AM, Arrojo EDR, Freitas BC, Chung M, Harney JW, et al. (2009) The E3 ubiquitin ligase TEB4 mediates degradation of type 2 iodothyronine deiodinase. Mol Cell Biol 29: 5339-5347.
78. Lerner M, Corcoran M, Cepeda D, Nielsen ML, Zubarev R, et al. (2007) The RBCC gene RFP2 (Leu5) encodes a novel transmembrane E3 ubiquitin ligase involved in ERAD. Mol Biol Cell 18: 1670-1682.
79. Altier C, Garcia-Caballero A, Simms B, You H, Chen L, et al. The Cavbeta subunit prevents RFP2-mediated ubiquitination and proteasomal degradation of L-type channels. Nat Neurosci 14: 173-180.
80. Stagg HR, Thomas M, van den Boomen D, Wiertz EJ, Drabkin HA, et al. (2009) The TRC8 E3 ligase ubiquitinates MHC class I molecules before dislocation from the ER. J Cell Biol 186: 685-692.
81. Lee JP, Brauweiler A, Rudolph M, Hooper JE, Drabkin HA, et al. The TRC8 ubiquitin ligase is sterol regulated and interacts with lipid and protein biosynthetic pathways. Mol Cancer Res 8: 93-106.
82. Maruyama Y, Yamada M, Takahashi K (2008) Ubiquitin ligase Kf-1 is involved in the endoplasmic reticulum-associated degradation pathway. Biochem Biophys Res Commun 374: 737-741.
83. Lu JP, Wang Y, Sliter DA, Pearce MM, Wojcikiewicz RJ RNF170 Protein, an Endoplasmic Reticulum Membrane Ubiquitin Ligase, Mediates Inositol 1,4,5-Trisphosphate Receptor Ubiquitination and Degradation. J Biol Chem 286: 24426-24433.
84. Neutzner A, Neutzner M, Benischke AS, Ryu SW, Frank S, et al. A systematic search for endoplasmic reticulum (ER) membrane-associated RING finger proteins identifies Nixin/ZNRF4 as a regulator of calnexin stability and ER homeostasis. J Biol Chem 286: 8633-8643.
85. Ron I, Rapaport D, Horowitz M Interaction between parkin and mutant glucocerebrosidase variants: a possible link between Parkinson disease and Gaucher disease. Hum Mol Genet 19: 3771-3781.

86. Mangeat B, Gers-Huber G, Lehmann M, Zufferey M, Luban J, et al. (2009) HIV-1 Vpu neutralizes the antiviral factor Tetherin/BST-2 by binding it and directing its beta-TrCP2-dependent degradation. PLoS Pathog 5: e1000574.
87. Yoshida Y, Chiba T, Tokunaga F, Kawasaki H, Iwai K, et al. (2002) E3 ubiquitin ligase that recognizes sugar chains. Nature 418: 438-442.
88. Kato A, Rouach N, Nicoll RA, Bredt DS (2005) Activity-dependent NMDA receptor degradation mediated by retrotranslocation and ubiquitination. Proc Natl Acad Sci U S A 102: 5600-5605.
89. Gong B, Chen F, Pan Y, Arrieta-Cruz I, Yoshida Y, et al. SCFFbx2-E3-ligase-mediated degradation of BACE1 attenuates Alzheimer's disease amyloidosis and improves synaptic function. Aging Cell 9: 1018-1031.
90. Yoshida Y, Tokunaga F, Chiba T, Iwai K, Tanaka K, et al. (2003) Fbs2 is a new member of the E3 ubiquitin ligase family that recognizes sugar chains. J Biol Chem 278: 43877-43884.
91. Guo X, Shen S, Song S, He S, Cui Y, et al. The E3 ligase Smurf1 regulates Wolfram syndrome protein stability at the endoplasmic reticulum. J Biol Chem 286: 18037-18047.
92. Fry WH, Simion C, Sweeney C, Carraway KL, 3rd Quantity Control of the ErbB3 Receptor Tyrosine Kinase at the Endoplasmic Reticulum. Mol Cell Biol 31: 3009-3018.
93. Kanehara K, Xie W, Ng DT Modularity of the Hrd1 ERAD complex underlies its diverse client range. J Cell Biol 188: 707-716.
94. Buck TM, Kolb AR, Boyd CR, Kleyman TR, Brodsky JL The endoplasmic reticulum-associated degradation of the epithelial sodium channel requires a unique complement of molecular chaperones. Mol Biol Cell 21: 1047-1058.
95. Hughes BT, Nwosu CC, Espenshade PJ (2009) Degradation of sterol regulatory element-binding protein precursor requires the endoplasmic reticulum-associated degradation components Ubc7 and Hrd1 in fission yeast. J Biol Chem 284: 20512-20521.
96. Swanson R, Locher M, Hochstrasser M (2001) A conserved ubiquitin ligase of the nuclear envelope/endoplasmic reticulum that functions in both ER-associated and Matalpha2 repressor degradation. Genes Dev 15: 2660-2674.
97. Huyer G, Piluek WF, Fansler Z, Kreft SG, Hochstrasser M, et al. (2004) Distinct machinery is required in Saccharomyces cerevisiae for the endoplasmic reticulum-associated degradation of a multispanning membrane protein and a soluble luminal protein. J Biol Chem 279: 38369-38378.
98. Wang Q, Chang A (2003) Substrate recognition in ER-associated degradation

mediated by Eps1, a member of the protein disulfide isomerase family. EMBO J 22: 3792-3802.

99. Ravid T, Kreft SG, Hochstrasser M (2006) Membrane and soluble substrates of the Doa10 ubiquitin ligase are degraded by distinct pathways. EMBO J 25: 533-543.

100. Lee JH, Choi JM, Lee C, Yi KJ, Cho Y (2005) Structure of a peptide:N-glycanase-Rad23 complex: insight into the deglycosylation for denatured glycoproteins. Proc Natl Acad Sci U S A 102: 9144-9149.

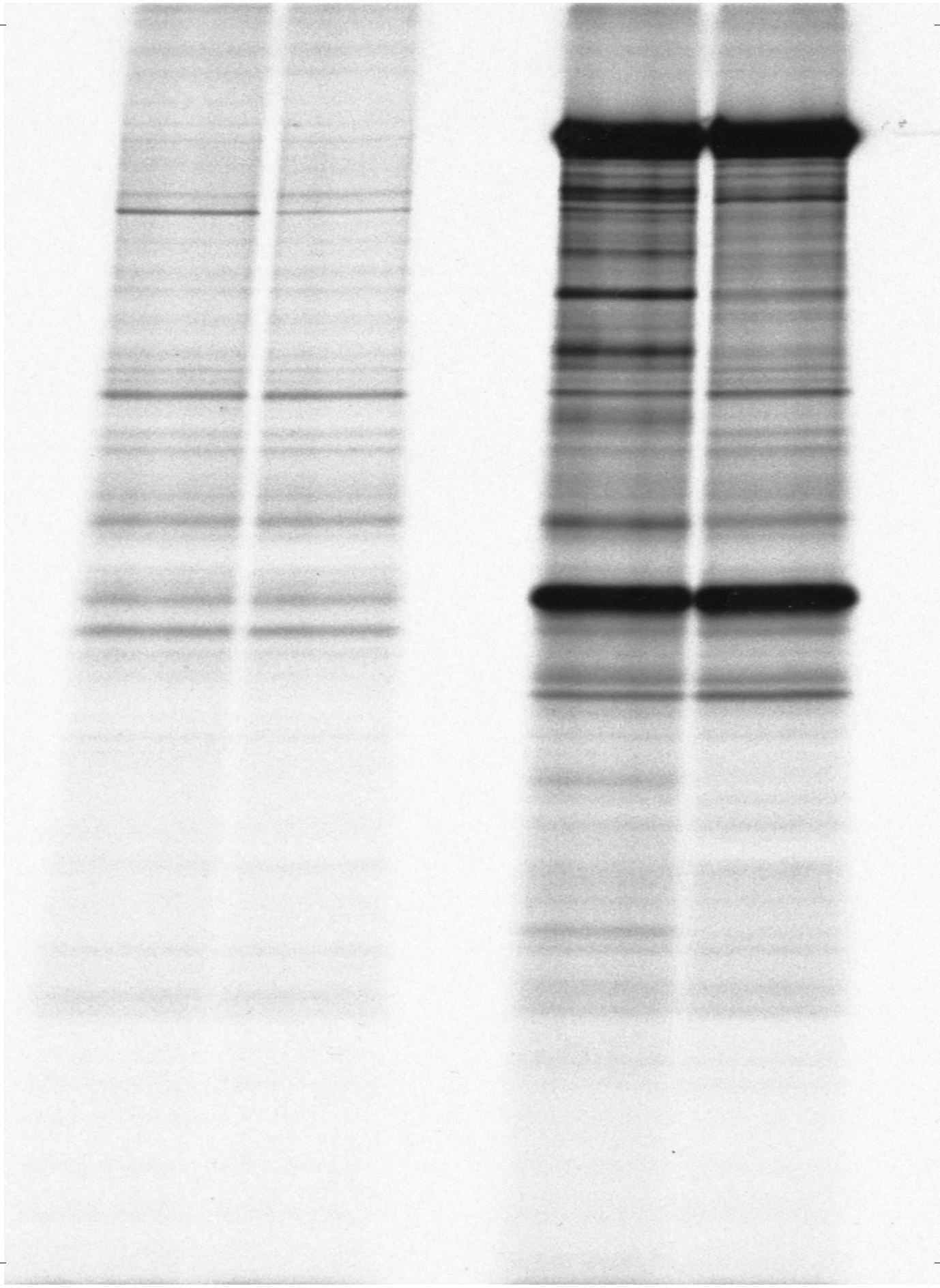

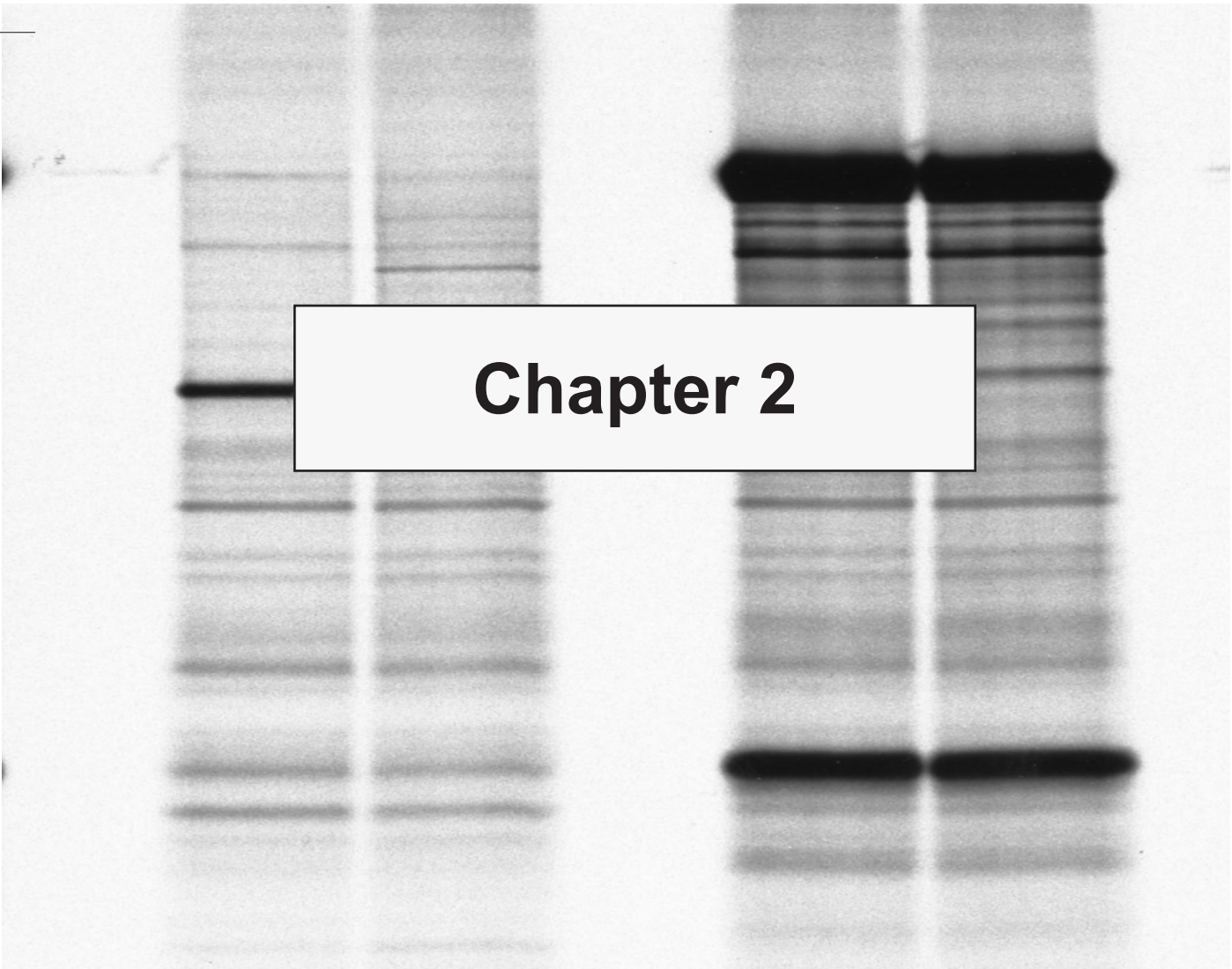

Chapter 2

The Transmembrane Domain of a Tail-anchored Protein Determines Its Degradative Fate through Dislocation from the Endoplasmic Reticulum

Jasper H.L. Claessen, Britta Mueller, Eric Spooner, Valerie L. Pivorunas, and Hidde L. Ploegh

Whitehead Institute for Biomedical Research, Department of Biology, Massachusetts Institute of Technology, Cambridge, Massachusetts, USA

Abstract

Terminally misfolded proteins that accumulate in the endoplasmic reticulum (ER) are dislocated and targeted for ubiquitin-dependent destruction by the proteasome. UBC6e is a tail-anchored E2 ubiquitin-conjugating enzyme that is part of a dislocation complex nucleated by the ER-resident protein SEL1L. Little is known about the turnover of tail-anchored ER proteins. We constructed a set of UBC6e transmembrane domain replacement mutants and found that the tail-anchor of UBC6e is vital for its function, its stability and its mode of membrane integration, the latter step dependent on the ASNA1/TRC40 chaperone. We constructed a tail-anchored UBC6e variant that requires for its removal from the ER membrane not only YOD1 and p97, two cytosolic proteins involved in the extraction of ER transmembrane or luminal proteins, but also UBXD8, AUP1 and members of the Derlin family. Degradation of tail-anchored proteins thus relies on components that are also used in other aspects of protein quality control in the endoplasmic reticulum.

Introduction

Terminally misfolded proteins that accumulate in the lumen of the endoplasmic reticulum (ER) are actively transported across the ER membrane into the cytosol. As a consequence of this dislocation (or retro-translocation), such misfolded products are targeted for proteasomal degradation in a ubiquitin-dependent manner [1].
The ER membrane is the main physical barrier that misfolded proteins must cross and is the arena where dislocation takes place. Different suggestions have been made as to how misfolded

products may traverse the ER membrane, ranging from the involvement of lipid droplets or their analogs [2], to a proteinaceous channel (reviewed in [3]. It is likely that the cell employs different methods of protein extraction, depending on the nature of the folding deficit it diagnoses [4,5] and the physiological state of the ER during differentiation or while under stress.

One well-studied dislocation complex is that exploited by the viral human cytomegalovirus protein US11 [6]. US11 is an ER-resident type I transmembrane protein that induces rapid dislocation of newly synthesized Class I major histocompatibility complex (MHC) heavy chains [7,8]. US11 recruits a dislocation complex that minimally consists of Derlin-1/2, the ubiquitin-ligase HRD1, the adaptor protein SEL1L together with the ubiquitin conjugating enzyme UBC6e, and the auxiliaries AUP1, OS9, UBXD8, [9,10,11,12,13]. The dislocation pathway employed by US11 controls more generally the degradation of aberrantly folded proteins, such as truncated ribophorin (RI_{332}), α1-antitrypsin null Hong Kong and the misfolded cystic fibrosis transmembrane conductance regulator DF508 [12,14,15].
Even though we now know the identity of many components of this dislocation complex, the temporal order and spatial relationship of interactions between these proteins remains elusive. Most of the previously mentioned players in dislocation are anchored in the ER membrane, an important plane of interaction. Misfolded secretory proteins, type I membrane proteins and polytopic membrane proteins have been the substrates of choice to examine differences and commonalities in their degradative fates, but how the turnover of tail-anchored proteins is controlled remains essentially unknown. We addressed the role of the trans-membrane domain (TMD) of UBC6e in its stability and function in an effort to address the behavior of this tail-anchored protein.

The class of tail-anchored (TA) membrane proteins -to which Ubc6e belongs- is a special category of membrane proteins, devoid of a canonical signal sequence to guide their targeting and membrane insertion. Instead, it is the TMD, or tail-anchor, located close to the C-terminus of the protein, that facilitates post-translational insertion into the target membrane, either independently or through a chaperone system [16]. With its TMD so close to its C-terminus, it is the principal UBC6e domain available for interaction with other ER proteins. Through TMD replacement, we constructed a set of UBC6e mutants that show the TMD of UBC6e not only to determine its function, but also its stability and mode of membrane insertion. Furthermore, we now describe an extraction pathway for unstable TA proteins and identify not only the de-ubiquitinating enzyme YOD1 and AAA ATPase p97 as active players in the removal of a TA protein from the ER membrane, but also UBXD8, Derlins and AUP1, other components implicated in earlier studies, thus demonstrating convergence with degradation of misfolded ER proteins.

Results

The TMD of UBC6e is important for its role in dislocation

UBC6e is a tail-anchored membrane protein. To understand the contribution of the TMD of UBC6e to its membrane insertion and stability, we made a set of mutant proteins in which we replaced the TMD of UBC6e with that of CD4 (a type I membrane protein), Cytochrome B5 (a TA-protein), UBC6 (a TA-protein) as well as a version of UBC6e without its TMD (Figure 1)
We identified UBC6e as part of a protein complex involved in dislocation of Class I MHC products in cells that express the HCMV immunoevasin US11 [11]. Overexpression of UBC6e impairs dislocation of Class I MHC HC by US11. To characterize the mutant versions of UBC6e, we introduced them into U373 astrocytoma cells that stably express US11 and examined dislocation of Class I MHC HC in a pulse-chase experiment. In control cells transduced with the empty pLHCX vector, the labeled HC population is dislocated from the ER to the cytoplasm over the 30 min chase period. We added the proteasome inhibitor ZL_3VS to stabilize the dislocated HC, which accumulates as a diagnostic deglycosylated intermediate due to the action of the cytosolic enzyme peptide N-glycanase (PNGase) [7,8]. Like the WT enzyme, overexpression of UBC6e-CD4 impaired dislocation of the HC, but none of the other UBC6e mutants produced this effect (Figure 2A,B). We conclude that the identity of the TMD appended to UBC6e determines its role in dislocation.

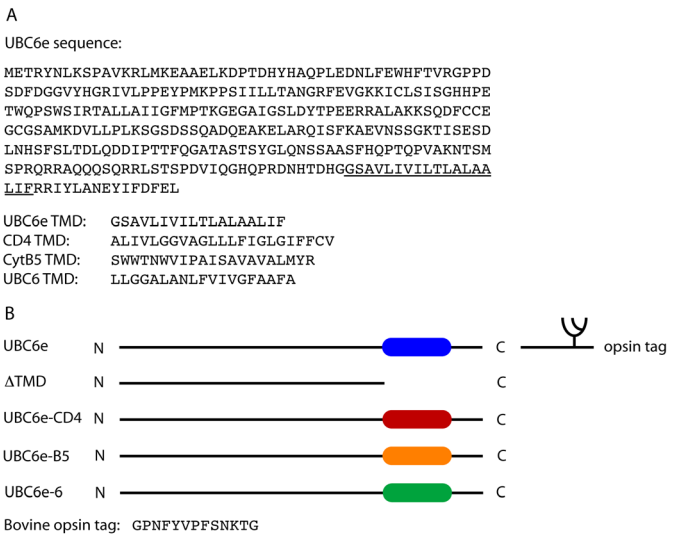

Figure 1. Sequence of UBC6e and the different trans-membrane domain variants.
(A) Sequence of UBC6e, trans-membrane domain (TMD) underlined. The sequence of the TMD replacements is given and named as indicated. (B) Schematic representation of the different TMD mutants. A 13 amino acid bovine opsin tag was appended to the C terminus of each construct, introducing a N-linked glycosylation motif.

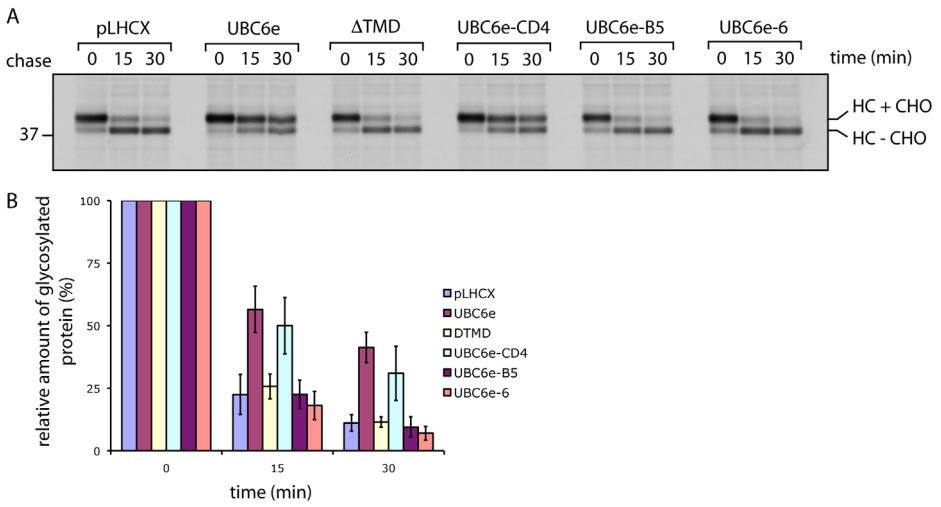

Figure 2. UBC6e and UBC6e-CD4 impair US11-mediated dislocation equally well.
(A) US11-expressing cells were transduced with either empty vector (pLHCX), UBC6e WT, ΔTMD, UBC6e-CD4, UBC6e-B5 or UBC6e-6. The six cell lines were treated with 50μM ZL3VS, pulse-labeled for 10 min with 35S, chased for indicated time points and lysed in 1% SDS; the lysates were then immunoprecipitated with anti-HC serum. The eluates were separated on a 10% SDS/PAGE gel and visualized by autoradiography. (B) Densitometric quantitation of the relative amount of glycosylated HC. Error bars represent standard deviation from the mean (n=3).

The TMD of UBC6e determines its stability

Why do some of the newly crafted tail-anchored versions of UBC6e fail to inhibit dislocation? We assessed the stability of the various UBC6e mutants in pulse-chase experiments. Whereas WT UBC6e, ΔTMD and UBC6e-CD4 are stable over a chase period of 3h, both UBC6e-B5 and UBC6e-6 are rapidly degraded. (Figure 3A) In fact, no Ubc6e-B5 or UBC6e-6 could be detected at steady state levels by immunoblotting (Figure 3B) Both unstable mutants are degraded with different but surprisingly rapid kinetics. In U373 cells, UBC6e-B5 is no longer detectable 180 min after its synthesis and UBC6e-6 is eliminated within 90 min.

The complex banding pattern observed for UBC6e is due to phosphorylation of UBC6e, as shown by treatment with alkaline phosphatase, which eliminates this heterogeneity (Figure 4) [17].

The short-lived UBC6e-B5 and UBC6e-6 mutants were both stabilized in the course of the chase by inclusion of the proteasome inhibitor ZL_3VS (Figure 3C). We conclude that UBC6e-B5 and UBC6-6 are destroyed by proteasomal degradation. This made us wonder whether these unstable UBC6e forms are actually inserted into the ER membrane at all, or whether they are immediately targeted for proteasomal degradation upon post-translational release from the ribosome.

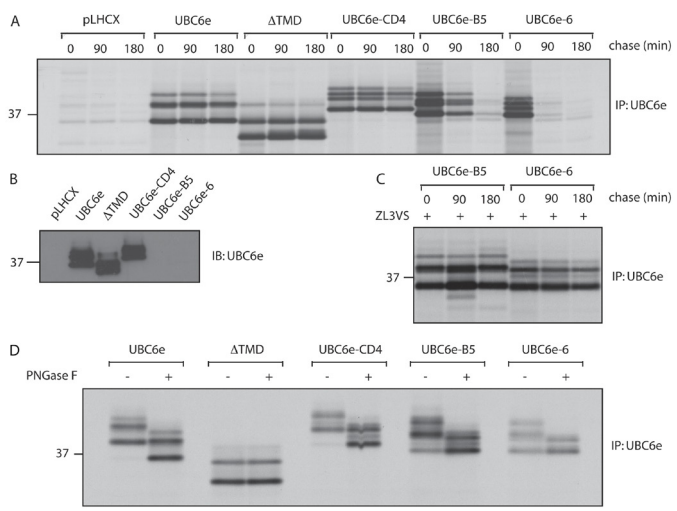

Figure 3. UBC6e and its mutants are inserted into the ER membrane but only UBC6e-B5 and UBC6e-6 are rapidly degraded.
(A) The cell lines described in Fig. 2a were pulse-labeled for 10 min with 35S, chased for indicated time points and lysed in 1% SDS; the lysate was then immunoprecipitated with anti-UBC6e serum. The eluates were separated on a 10% SDS/PAGE gel and visualized by autoradiography. (B) The cell lines described in Fig. 2a were lysed in 1% SDS; the lysate was separated on 10% SDS/PAGE and subjected to immunoblotting with anti-UBC6e serum. (C) The experiment described in (A) was repeated in the presence of 50μM ZL3VS. (D) 293T cells were transiently transfected with the indicated opsin-tagged UBC6e TMD variants. The experiment was performed as in Fig. 3a. Where indicated, the eluate was treated with PNGase F for 2h at 37°C, separated on a 10% SDS/PAGE gel and visualized by autoradiography.

All TMD mutants are inserted into the ER membrane

We explored whether the different versions of UBC6e, regardless of the TMD installed, insert themselves into the ER. To this end, we equipped these variants of UBC6e with a C-terminal bovine opsin tag, a 13 residue sequence that contains an N-linked glycosylation motif (Figure 1) [18]. Successful insertion into the ER allows N-linked glycosylation of the luminally exposed opsin tag to proceed and so reports on the efficiency of the event. The opsin-tagged constructs were transiently transfected into 293T cells, which were then pulse-labeled for 10 min and chased for 20 min to examine membrane insertion, as inferred from the acquisition of an N-linked glycan. All but ΔTMD were glycosylated, indicating successful insertion into the ER membrane (Figure 3D). To verify that N-linked glycosylation had occurred, we used treatment with PNGase, which produces a size shift if indeed an N-linked glycan is present. The slight differences in glycosylation levels between the different UBC6e TMD mutants hint at different insertion efficiency, as measured at the 20 min chase time. We conclude that those forms of UBC6e that have a TMD are inserted into the ER membrane. The short-lived tail-anchored versions of UBC6e must be extracted from the ER membrane, but how, and how are they destroyed?

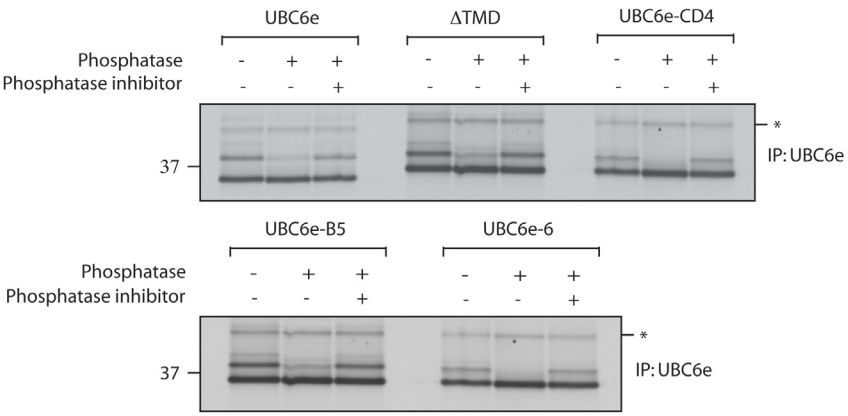

Figure 4. All UBC6e mutants are phosphorylated when expressed in mammalian cells.
293T cells were transiently transfected with the indicated UBC6e TMD mutants. Twenty-four hours post-transfection, the cells were pulse-labeled for 10 min with 35S and chased for 20 minutes to allow for membrane insertion. The cells were lysed in 1% SDS and the lysate immunoprecipitated with anti-UBC6e serum. The immunoprecipitates were treated with alkaline phosphatase (10u) in the presence or absence of phosphatase inhibitor. The eluate was separated on a 10% SDS/PAGE gel and visualized by autoradiography.

Dislocation of UBC6e-B5 depends on ER dislocation machinery

Both UBC6e-B5 and UBC6e-6 are novel and unique examples of unstable TA-proteins. Because they are targeted to the ER -as inferred from N-linked glycosylation- yet are destroyed rapidly, we asked whether any of the known components involved in dislocation play a role in the turnover of these two species. Many of the proteins involved in substrate recognition and dislocation face the ER lumen and are therefore unlikely to be involved in the active removal of UBC6e-B5 or UBC6e-6. We chose to focus on YOD1, a cytosolic de-ubiquitinating enzyme (DUB) required for the removal of misfolded species from the ER [19].
To assess the role of YOD1 in the turnover of UBC6e-B5 or UBC6e-6, we transiently transfected 293T cells with either of the dislocation substrates and co-transfected YOD1 WT or catalytically inactive YOD1, its active site cysteine mutated to a serine. Expression of YOD1 WT did not affect degradation of UBC6e-B5, whereas YOD1 C160S stabilized it (Figure 5A,C). No effect on dislocation was observed in cells transfected with UBC6e-6 (data not shown).
As YOD1 is a DUB, stabilization of UBC6e-B5 by overexpression of YOD1 C160S should lead to the accumulation of polyubiquitinated species. Does the stabilized substrate accumulate as a soluble intermediate regardless of its ubiquitination status, or is it a product that remains associated with the membrane? We transfected 293T cells with UBC6e-B5 together with HA-tagged ubiquitin and either WT or inactive YOD1. We lysed cells mechanically and subjected them to subcellular fractionation to separate the particulate from the soluble fraction. We performed immunoprecipitation with anti-UBC6e serum on each of the fractions in the presence of detergent, and visualized the ubiquitinated species by immunoblotting with an HA-antibody. As expected, co-expression of UBC6e-B5 and YOD1 C160S caused accumulation of poly-ubiquitinated UBC6e-B5 species predominantly in the membrane fraction (Figure 5E). Correct separation of the fractions was ensured by immunoblotting for UBC6e and YOD1 respectively (Figure 5E). The presence of inactive YOD1 thus stalls dislocation of UBC6e-B5 at the ER membrane.
UBC6e is an E2 enzyme with a catalytic cysteine residue at position 91. To exclude the possibility that the observed poly-ubiquitin chain is built on the active site cysteine of UBC6e, we repeated the experiment with a form of UBC6e-B5 in which the active site cysteine was mutated to a serine (Figure 5E, right panel). No differences in ubiquitination patterns were observed, showing that UBC6e-B5 indeed accumulates as a poly-ubiquitinated degradation intermediate when co-expressed with YOD1 C160S.

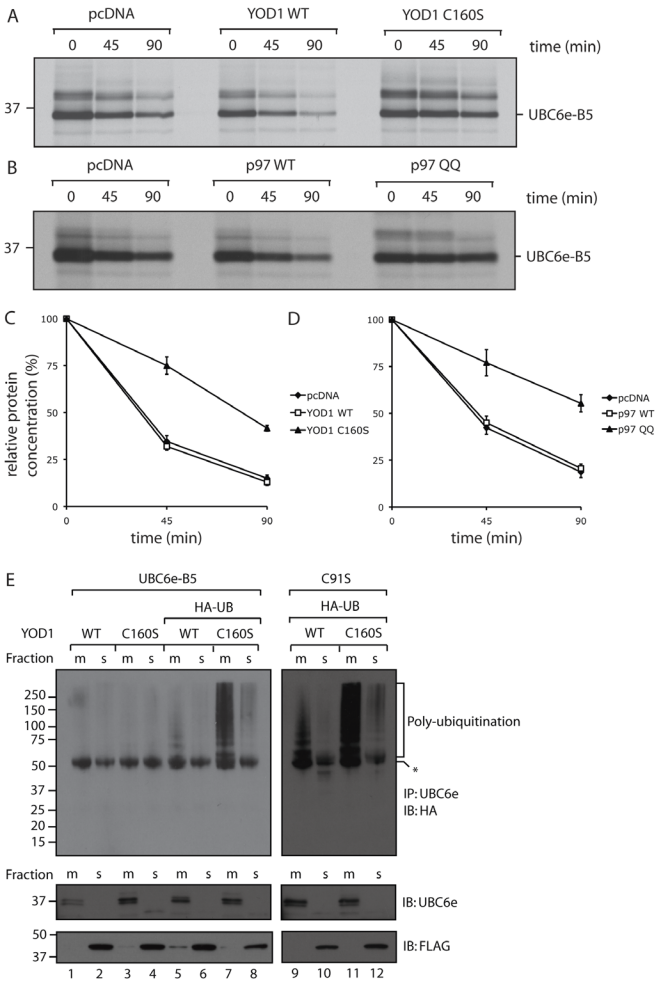

Figure 5. YOD1 and p97 contribute to dislocation of UBC6e-B5.

(A) 293T cells were co-transfected with UBC6e-B5 and empty vector, YOD1 WT or YOD1 C160S. Twenty-four hours post-transfection, the cells were pulse-labeled for 10 min with 35S, chased for indicated time points and lysed in 1% SDS; the lysate was then immunoprecipitated with anti-UBC6e serum. The eluates were separated on a 10% SDS/PAGE gel and visualized by autoradiography. This was repeated for p97 WT and p97QQ (B). (C) Densitometric quantitation of the relative amount of UBC6e-B5 in the presence of YOD1 variants (C) or p97 variants (D). Error bars represent standard deviation from the mean (n=3). (E) 293T cells were co-transfected with HA-ubiquitin, UBC6e-B5 WT or C91S and either YOD1 WT or YOD1 C160S. The cells were lysed mechanically in a hypotonic buffer. The membrane and soluble fractions were separated by high-speed centrifugation. The individual fractions were lysed in 0.5% SDS and immunoprecipitated with anti-UBC6e serum. Ubiquitinated UBC6e-B5 was visualized with anti-HA antibody. Correct separation of the membrane and soluble fractions was assessed by immunoblotting with anti-UBC6e (membrane fraction) and anti-FLAG for YOD1 (soluble fraction). The asterisk indicates nonspecifically detected polypeptides.

The AAA ATPase p97 helps remove misfolded substrates from the ER [20,21]. As YOD1 interacts with p97 through its UBX domain [19], we also tested the involvement of p97 in the degradation of UBC6e-B5. 293T cells were co-transfected with UBC6e-B5 and either p97 WT or inactive p97 QQ [20]. As expected, co-expression with inactive p97 impaired the degradation of UBC6e-B5, implicating p97 in the dislocation of a TA-protein (Figure 5B,D). We performed additional experiments that involved the use of dominant negative versions of Derlin-1, -2 and -3, expressed as GFP fusion proteins [13], as well as UBXD8-GFP and AUP1-GFP, all of which have previously been implicated in the removal of misfolded proteins from the ER [11]. With the exception of Derlin-2 GFP, all of these constructs impaired degradation of Ubc6e-B5 (Figure 6). Degradation of UBC6e-B5 thus involves at least part of the dislocation machinery involved in protein quality control in the ER.

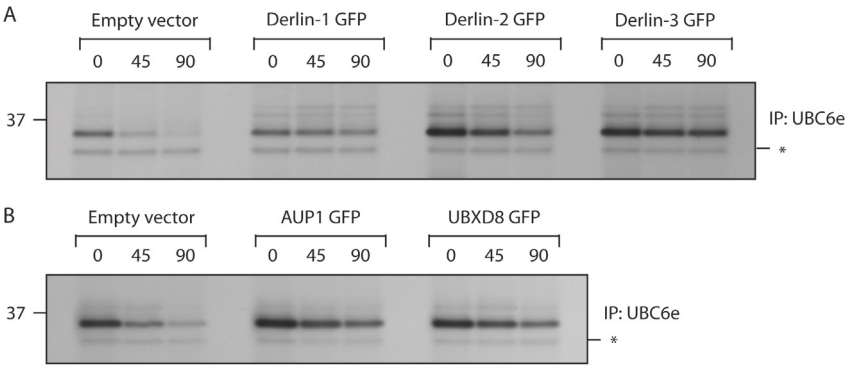

Figure 6. Dislocation of UBC6e-B5 depends on Derlin1, Derlin3, UBXD8 and AUP1.
293T cells were transiently co-transfected with UBC6e-B5 and either an empty vector control, Derlin-1 GFP, Derlin-2 GFP or Derlin-3 GFP. The experiment was performed as in Fig. 5a. The asterisks indicate nonspecifically bound polypeptides. (B) 293T cells were transiently co-transfected with UBC6e-B5 and either an empty vector control, AUP1 GFP or UBXD8 GFP. The experiment was performed as in Fig. 5a.

ASNA1 targets UBC6e to the ER membrane

Tail-anchored membrane proteins are characterized by post-translational membrane insertion, which occurs either in a manner assisted by, or independently of a chaperone system, the composition and function of which are only now being unraveled. In mammalian cells, the client tail anchored protein can be inserted through ASNA1 (TRC40), heat shock protein 40/heat shock cognate 70, signal recognition particle, or independent of chaperone assistance, depending on the hydrophobicity of the trans-membrane segment [16]. We identified ASNA1 by MS/MS

(47% sequence coverage, 10 unique peptides) as an interaction partner of UBC6e in a large-scale immunopurification. In this experiment, C-terminally HA-tagged UBC6e was transduced into 293T cells. UBC6e was isolated by immunoprecipitation from digitonin extracts and the eluate subjected to SDS/PAGE, followed by MS/MS analysis of the individual polypeptides recovered in a complex with Ubc6e. Having recovered ASNA1 as a strong hit, we therefore set out to examine whether membrane insertion of UBC6e is in fact dependent on ASNA1.

ASNA1 is an ATPase involved in posttranslational targeting of membrane proteins [18,22]. The crystal structure of Get3, the yeast homologue of ASNA1, provides insight into the binding of a tail anchored substrate and its regulated release under the control of ATP hydrolysis [23,24]. Accordingly, we made an ATPase-deficient G46R mutant of ASNA1.

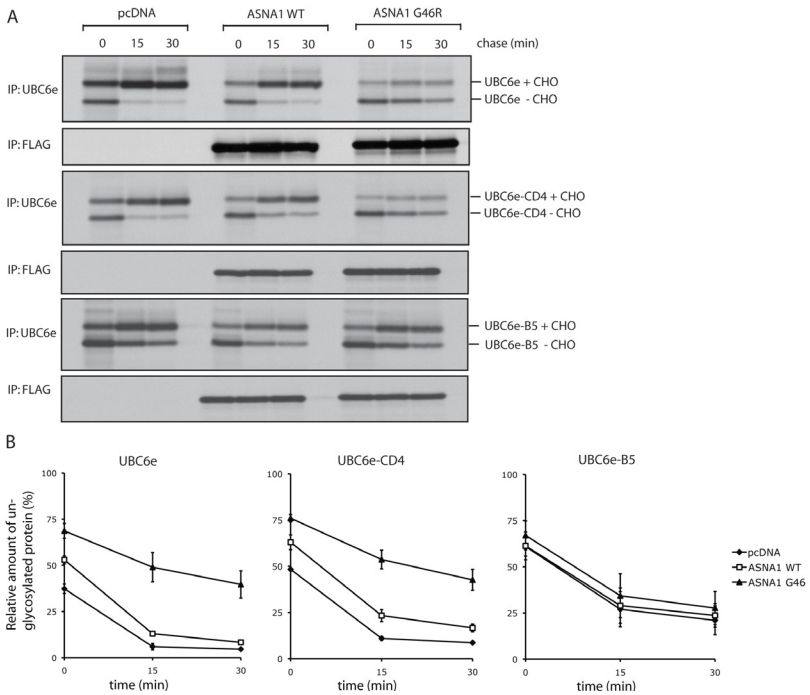

Figure 7. UBC6e and UBC6e-CD4 are targeted to the ER membrane by ASNA1.

(A) 293T cells were co-transfected with the indicated opsin-tagged UBC6e TMD variants and empty vector, ASNA1 WT or ASNA1 G46R. Twenty-four hours post-transfection, the cells were pulse-labeled for 5 min with 35S, chased for indicated time points and lysed in 1% SDS; the lysate was then immunoprecipitated with anti-UBC6e serum. The precipitated protein was treated for 1h with alkaline phosphatase at 37°C to reduce the complexity of the banding pattern. The eluates were separated on a 10% SDS/PAGE gel and visualized by autoradiography. ASNA1 expression was assessed through immunoprecipitation with anti-FLAG antibody. (B) Densitometric quantitation of the amount of non-glycosylated UBC6e variant relative to total protein. Error bars represent standard deviation from the mean (n=3).

To test whether UBC6e is dependent on ASNA1 for membrane targeting and insertion, we examined membrane insertion in the presence of either ASNA1 WT or ASNA1 G46R, using N-linked glycosylation as a read-out for insertion of the opsin tagged TA UBC6e variants into the ER membrane. A short pulse of 5 min allowed us to follow the fate of the newly synthesized population of UBC6e. Within 30 min of chase, virtually all of the newly synthesized UBC6e was inserted into the ER membrane in control cells (Figure 7A,B). Expression of ASNA1 WT did not impair ER membrane integration. However, expression of ASNA1 G46R reduced membrane integration of UBC6e. We performed a similar experiment with UBC6e-CD4 and UBC6e-B5. Again, UBC6e-CD4 behaved as UBC6e WT and required ASNA1 for membrane integration. In contrast, expression of ASNA1 G46R did not affect insertion of UBC6e-B5 (Figure 7A,B). We conclude that UBC6e is a TA protein targeted to the ER membrane by ASNA1.

Discussion

The TMD of UBC6e determines its function and its stability. We crafted different mutants of UBC6e in which we replaced its TMD with that of other membrane proteins, including TA and type I membrane proteins. A comparison of different TMD mutants of UBC6e showed that the identity of the TMD determines its role in US11-mediated dislocation of MHC Class I HC products and markedly affects the stability of that version of UBC6e itself.

Expression of either active or inactive UBC6e disturbs the function of the dislocation complex nucleated by Sel1L, presumably by disrupting the proper stoichiometry of the multi-protein complex that serves as (part of) the translocon [11]. Our data show that the TMD of UBC6e is crucial for this property. Deprived of its TMD, UBC6e is no longer targeted to the ER and therefore fails to engage other components of the complex. This is in line with our hypothesis that UBC6e engages its interaction partners within the ER membrane [11]°A<. When we substituted the TMD of UBC6e with that of other trans-membrane proteins, the nature of the replacement TMD affected both function and stability of the resultant product. Irrespective of the nature of the TMD, all forms of UBC6e were inserted successfully into the ER membrane. It is unclear whether UBC6e interacts directly with other members of the HRD1/SEL1L dislocation complex or whether it does so via an as yet unidentified scaffold protein, as proposed for the yeast Hrd1/Hrd3-ubiquitin ligase [25]. The nature of the TMD could affect either one of these interactions. The physico-

chemical properties of the TMD may also affect location and trafficking of its bearer within the plane of the membrane [26].

A UBC6e mutant with the TMD of CD4 mimics the WT enzyme in both function and stability. WT UBC6e and UBC6e-CD4 are TA-proteins targeted to the ER by ASNA1.
Replacement of the TMD of UBC6e with that of CytB5 or UBC6 results in highly unstable proteins that fail to engage the dislocation complex, as inferred form their inability to affect US11-dependent dislocation of class I MHC products. After insertion, UBC6e-B5 and UBC6e-6 are rapidly removed from the ER and targeted for proteasomal degradation. Furthermore, UBC6e-B5 does not utilize the ASNA1-dependent pathway for membrane insertion. This unique trait allowed us to use these proteins as substrates to study quality control and active removal of TA-proteins (Figure 8).

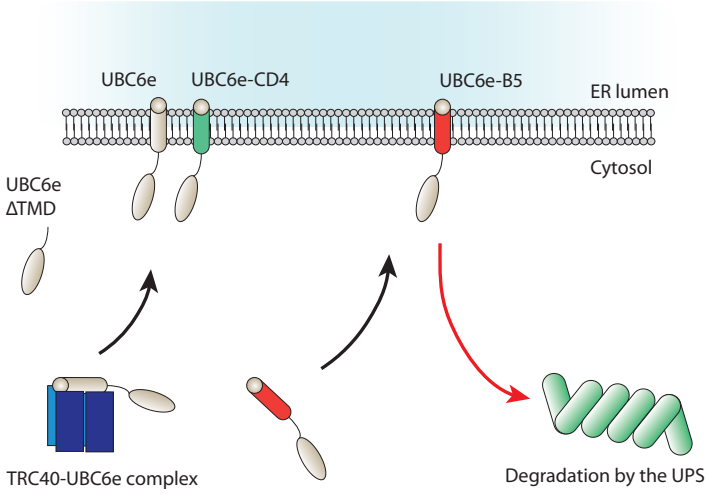

Figure 8. Schematic representation of UBC6e protein insertions.
After synthesis, UBC6e wt is inserted in the ER membrane with the help of ASNA1/TRC40, as is the UBC6e-CD4 mutant. Upon deletions of its TMD, UBC6eΔTMD remains stable in the cytosol. The UBC6e-B5 TMD mutant is inserted into the ER, independent of ASNA1/TRC40, and then rapidly degraded by the ubiquitin proteasome system.

Both YOD1 and p97 are required for the dislocation of UBC6e-B5 (Figure 5). In addition, we implicate Derlin-1 and Derlin-3, as well as UBXD8 and AUP1 (Figure 6), -all of which contribute to dislocation [11,13]- in the rapid turnover of UBC6e-B5. This places several known players involved in ER dislocation in a pathway for TA-protein degradation [19,20]. The involvement of YOD1, p97 and other proteins

that participate in dislocation suggests that the degradation pathway of TA-proteins converges with the currently known mechanisms of disposal of misfolded proteins from the ER lumen: ubiquitination triggers active removal of the substrate, which is then targeted to the proteasome. The observed convergence of quality control pathways for ER luminal proteins and for TA-proteins must occur downstream of the initial decision to remove the protein from the membrane compartment. The nature of TA-proteins places their functional domain on the cytosolic side of the ER membrane. We hypothesize that the initial triage of inserted TA-proteins must occur through the action of proteins with a similar cytosolic orientation compared to the ER membrane, or within the plane of the ER itself. The latter possibility would be entirely consistent with the involvement of the Derlins and AUP1 in particular. It is difficult to envision involvement of the typical ER-resident luminal chaperones such as PDI, OS9, BiP, calreticulin, calnexin and possibly others.

Both UBC6e-B5 and UBC6e-6 are degraded with rapid but different kinetics. It is unclear why these proteins are dysfunctional and removed, unlike their UBC6e-CD4 counterpart. One possibility is that these TMDs no longer allow interactions with other components of the dislocation complex, triggering an as yet unidentified intra-membrane quality control mechanism. Another possibility is that these proteins are mis-targeted to the wrong ER membrane subdomains as they no longer engage ASNA1, which targets the tail-anchored UBC6e to the ER membrane, presumably the location where specific receptors for ASNA1 are present. The notion that specific subdomains of the ER may be relegated to quality control and turnover of misfolded proteins is supported by data on the degradation of mutant forms of the polytopic protein Ste6 in yeast [27]. By strict analogy with the GET system in yeast [28], membrane receptors could facilitate not only the specific targeting of TA-proteins to organelles, but also to unique membrane domains within those organelles. Mis-targeting would then result in active removal of the protein. The involvement of YOD1 and p97 in the removal of UBC6e-B5 but not UBC6e-6, may account for the different kinetics for removal and degradation.

Materials and methods

Antibodies, Cell lines, Constructs

Antibodies to Class I MHC heavy chains (HC) and UBC6e have been described [11]. Antibodies against the hemagglutinin (HA) epitope tag were purchased from Roche (3F10), anti-FLAG tag was purchased from Sigma-Aldrich. US11- express-

ing cell lines have been described [12]. 293T cells were purchased from ATCC. Cell transduced with pLHCX-based vectors were selected and maintained in 125μg/ml hygromycin B (Roche).

The UBC6e, Derlin-1 GFP, Derlin-2 GFP, Derlin-3 GFP, AUP1 GFP, UBXD8 GFP, YOD1 and p97 constructs used for transfection experiments have been described [11,13,19]. The TMD of UBC6e was replaced by that of CD4 (T4 surface glycoprotein precursor), Cytochrome B5 (type A) or UBC6 by standard PCR-based cloning methods and verified by sequencing (see also figure 1).

A cDNA clone for ASNA1 was obtained from Open Biosystems (LIFESEQ1405919) and cloned into pcDNA3.1(+) (Invitrogen) with a C-terminal FLAG epitope tag. Site-directed mutagenesis of ASNA1 G46R and UBC6e-B5 C91S was performed with the QuickChange II Mutagenesis Kit according to the manufacturer's instructions (Stratagene).

Transient Transfection, Viral transduction

293T cells were transiently transfected using Trans-IT (Takara Mirus Bio) according to the manufacturer's instructions. Virus production in 293T cells and viral transduction has been described [29].

Pulse-chase experiments, Immunoprecipitation, SDS/PAGE

Cells were detached by trypsin treatment and then incubated with methionine- and cysteine-free DME with or without the proteasome inhibitor ZL_3VS (50mM) for 45 min at 37°C. Cells were labeled with 10 mCi/ml [^{35}S]metionine/cysteine (1175 Ci/mmol; Perkin Elmer) at 37°C for the indicated times and chased with DME supplemented with nonradiolabeled methionine (2.5mM) and cysteine (0.5mM) at 37°C for the indicated times. Cells were lysed in 1% SDS. Immunoprecipitations were performed using 30μl immobilized rProtein A (IPA 300, Repligen) with the relevant antibodies or with 10μl ANTI-FLAG M2-Agarose (Sigma) for 3h at 4°C with gentle agitation. Immune complexes were eluted by boiling in reducing sample buffer, subjected to SDS/PAGE (10%) and visualized by autoradiography. Densitometric quantification of radioactivity was performed on a phosphoimager (Fujifilm BAS-2500) using Image Reader BAS-2500 V1.8 software (Fujifilm) and Multi Gauge V2.2 (Fujifilm) software for analysis.

Immunoblotting

For immunoblot analysis, cell lysates were prepared by solubilizing cell pellets in 1% SDS. Protein concentrations of the lysates were determined by using the BCA assay (Pierce), and equivalent amounts of total cellular protein were used for immunoblotting.

Fractionation

For subcellular fractionation assays, cells were homogenized by passage through a 23G needle in hypotonic buffer (20mM HEPES pH 7.5, 5mM KCl, 5 mM $MgCl_2$, 1 mM DTT, supplemented with a protease inhibitor cocktail [Roche]). The particulate and soluble fractions were separated by centrifugation at 156.600g in a Beckman TLA 100 centrifuge. All samples were adjusted to 0.5% SDS and analyzed by SDS-PAGE (10%).

PNGase F and Phosphatase treatment

PNGase F digestion or Phosphatase treatment (10u) of radiolabeled UBC6e variants was performed after immunoprecipitation according to the recommendations of the manufacturer (New England Biolabs and Fermentas respectively). Phosphatase inhibitor cocktail was acquired from Roche and used according to the instructions of the manufacturer.

References

1. Ellgaard L, Helenius A (2003) Quality control in the endoplasmic reticulum. Nat Rev Mol Cell Biol 4: 181-191.
2. Ploegh HL (2007) A lipid-based model for the creation of an escape hatch from the endoplasmic reticulum. Nature 448: 435-438.
3. Hebert DN, Bernasconi R, Molinari M (2009) ERAD substrates: Which way out? Semin Cell Dev Biol.
4. Carvalho P, Goder V, Rapoport TA (2006) Distinct ubiquitin-ligase complexes define convergent pathways for the degradation of ER proteins. Cell 126: 361-373.
5. Vashist S, Ng DT (2004) Misfolded proteins are sorted by a sequential checkpoint mechanism of ER quality control. J Cell Biol 165: 41-52.
6. Ahn K, Angulo A, Ghazal P, Peterson PA, Yang Y, et al. (1996) Human cytomegalovirus inhibits antigen presentation by a sequential multistep process. Proc Natl Acad Sci U S A 93: 10990-10995.
7. Wiertz EJ, Jones TR, Sun L, Bogyo M, Geuze HJ, et al. (1996) The human cytomegalovirus US11 gene product dislocates MHC class I heavy chains from the endoplasmic reticulum to the cytosol. Cell 84: 769-779.
8. Wiertz EJ, Tortorella D, Bogyo M, Yu J, Mothes W, et al. (1996) Sec61-mediated transfer of a membrane protein from the endoplasmic reticulum to the proteasome for destruction. Nature 384: 432-438.
9. Lilley BN, Ploegh HL (2004) A membrane protein required for dislocation of mis-

folded proteins from the ER. Nature 429: 834-840.
10. Ye Y, Shibata Y, Yun C, Ron D, Rapoport TA (2004) A membrane protein complex mediates retro-translocation from the ER lumen into the cytosol. Nature 429: 841-847.
11. Mueller B, Klemm EJ, Spooner E, Claessen JH, Ploegh HL (2008) SEL1L nucleates a protein complex required for dislocation of misfolded glycoproteins. Proc Natl Acad Sci U S A 105: 12325-12330.
12. Mueller B, Lilley BN, Ploegh HL (2006) SEL1L, the homologue of yeast Hrd3p, is involved in protein dislocation from the mammalian ER. J Cell Biol 175: 261-270.
13. Lilley BN, Ploegh HL (2005) Multiprotein complexes that link dislocation, ubiquitination, and extraction of misfolded proteins from the endoplasmic reticulum membrane. Proc Natl Acad Sci U S A 102: 14296-14301.
14. Oda Y, Okada T, Yoshida H, Kaufman RJ, Nagata K, et al. (2006) Derlin-2 and Derlin-3 are regulated by the mammalian unfolded protein response and are required for ER-associated degradation. J Cell Biol 172: 383-393.
15. Younger JM, Chen L, Ren HY, Rosser MF, Turnbull EL, et al. (2006) Sequential quality-control checkpoints triage misfolded cystic fibrosis transmembrane conductance regulator. Cell 126: 571-582.
16. Rabu C, Schmid V, Schwappach B, High S (2009) Biogenesis of tail-anchored proteins: the beginning for the end? J Cell Sci 122: 3605-3612.
17. Oh RS, Bai X, Rommens JM (2006) Human homologs of Ubc6p ubiquitin-conjugating enzyme and phosphorylation of HsUbc6e in response to endoplasmic reticulum stress. J Biol Chem 281: 21480-21490.
18. Favaloro V, Spasic M, Schwappach B, Dobberstein B (2008) Distinct targeting pathways for the membrane insertion of tail-anchored (TA) proteins. J Cell Sci 121: 1832-1840.
19. Ernst R, Mueller B, Ploegh HL, Schlieker C (2009) The otubain YOD1 is a deubiquitinating enzyme that associates with p97 to facilitate protein dislocation from the ER. Mol Cell 36: 28-38.
20. Ye Y, Meyer HH, Rapoport TA (2001) The AAA ATPase Cdc48/p97 and its partners transport proteins from the ER into the cytosol. Nature 414: 652-656.
21. Ye Y, Meyer HH, Rapoport TA (2003) Function of the p97-Ufd1-Npl4 complex in retrotranslocation from the ER to the cytosol: dual recognition of nonubiquitinated polypeptide segments and polyubiquitin chains. J Cell Biol 162: 71-84.
22. Stefanovic S, Hegde RS (2007) Identification of a targeting factor for posttrans-

lational membrane protein insertion into the ER. Cell 128: 1147-1159.
23. Mateja A, Szlachcic A, Downing ME, Dobosz M, Mariappan M, et al. (2009) The structural basis of tail-anchored membrane protein recognition by Get3. Nature 461: 361-366.
24. Suloway CJ, Chartron JW, Zaslaver M, Clemons WM, Jr. (2009) Model for eukaryotic tail-anchored protein binding based on the structure of Get3. Proc Natl Acad Sci U S A 106: 14849-14854.
25. Horn SC, Hanna J, Hirsch C, Volkwein C, Schutz A, et al. (2009) Usa1 functions as a scaffold of the HRD-ubiquitin ligase. Mol Cell 36: 782-793.
26. Ronchi P, Colombo S, Francolini M, Borgese N (2008) Transmembrane domain-dependent partitioning of membrane proteins within the endoplasmic reticulum. J Cell Biol 181: 105-118.
27. Nakatsukasa K, Huyer G, Michaelis S, Brodsky JL (2008) Dissecting the ER-associated degradation of a misfolded polytopic membrane protein. Cell 132: 101-112.
28. Schuldiner M, Metz J, Schmid V, Denic V, Rakwalska M, et al. (2008) The GET complex mediates insertion of tail-anchored proteins into the ER membrane. Cell 134: 634-645.
29. Soneoka Y, Cannon PM, Ramsdale EE, Griffiths JC, Romano G, et al. (1995) A transient three-plasmid expression system for the production of high titer retroviral vectors. Nucleic Acids Res 23: 628-633.

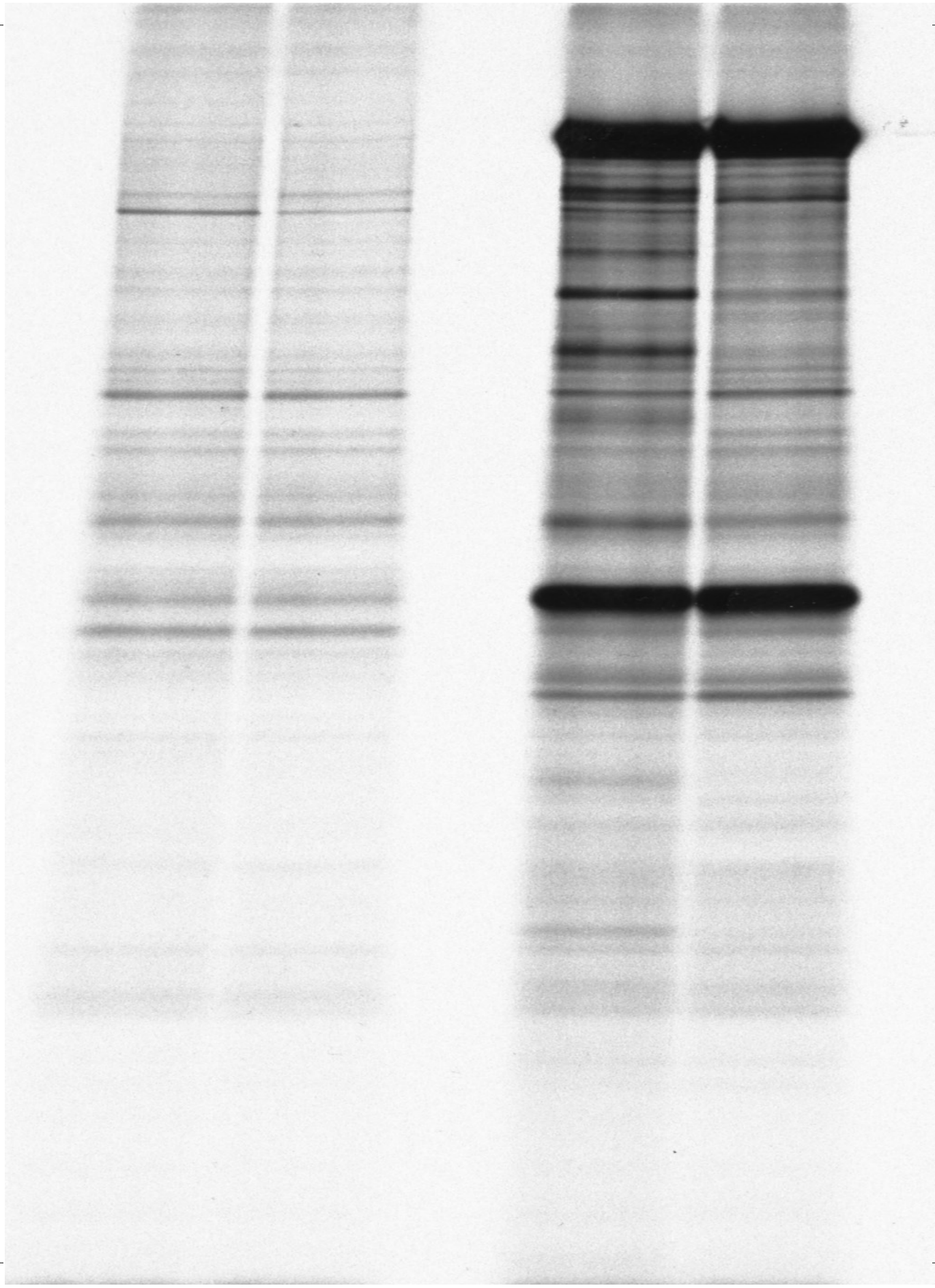

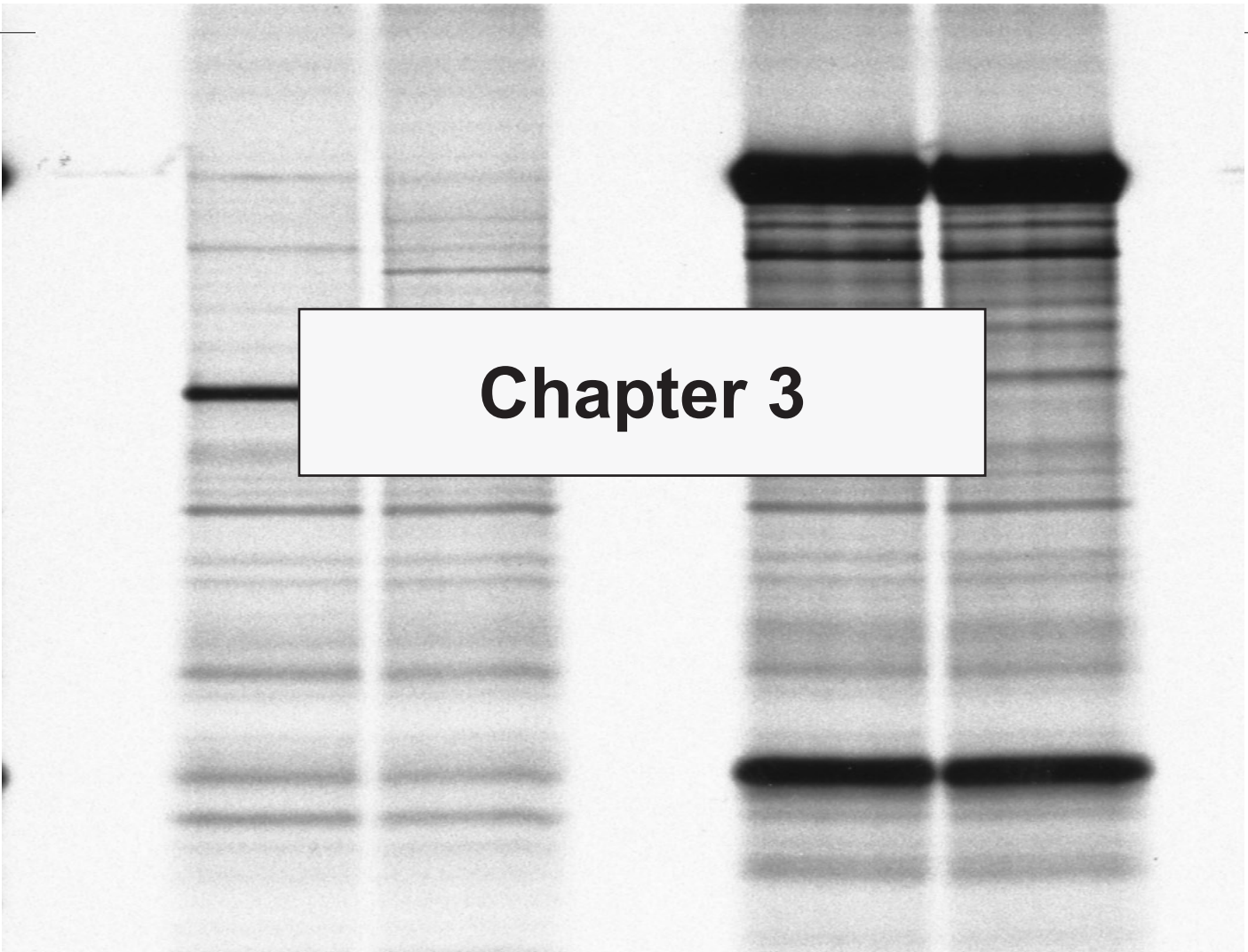

Chapter 3

Enzymatic Blockade of the Ubiquitin-Proteasome Pathway

Robert Ernst*[1], Jasper H.L. Claessen*[1], Britta Mueller[1], Sumana Sanyal[1], Eric Spooner[1], Annemarthe G. van der Veen[1], Oktay Kirak[1], Christian D. Schlieker, Wilhelm A. Weihofen[2], Hidde L. Ploegh[1]

(*= equal first author)

[1] Whitehead Institute for Biomedical Research, Department of Biology, Massachusetts Institute of Technology, Cambridge, Massachusetts, USA
[2] Department of Molecular and Cellular Biology, Harvard University, Cambridge, Massachusetts,USA

Abstract

Ubiquitin-dependent processes control much of cellular physiology. We show that expression of a highly active, Epstein-Barr virus-derived deubiquitylating enzyme (EBV-DUB) blocks proteasomal degradation of cytosolic and ER-derived proteins by preemptive removal of ubiquitin from proteasome substrates, a treatment less toxic than the use of proteasome inhibitors. Recognition of misfolded proteins in the ER lumen, their dislocation to the cytosol, and degradation are usually tightly coupled but can be uncoupled by the EBV-DUB: a misfolded glycoprotein that originates in the ER accumulates in association with cytosolic chaperones as a deglycosylated intermediate. Our data underscore the necessity of a DUB activity for completion of the dislocation reaction and provide a new means of inhibition of proteasomal proteolysis with reduced cytotoxicity.

Introduction

Protein quality control and ubiquitin-dependent degradation are essential for cellular homeostasis and survival [1]. The ubiquitin-proteasome-system (UPS) is responsible for the turnover of most cytosolic proteins. Likewise, secreted and membrane proteins that do not fold properly or fail to associate with their requisite partners in the ER are delivered to the cytosol and then destroyed by the UPS [2]. To facilitate this reaction, one or several dedicated receptors recognize misfolded ER-luminal proteins, which are then recruited to the dislocation machinery and rendered accessible to the cytosolic ubiquitylation apparatus. For both cytosolic and ER-derived substrates, attachment of polyubiquitin (poly-Ub) chains by an enzymatic E1-E2-E3 cascade is the signal for proteasomal degradation [3]. Poly-Ub chains serve as a recognition signal also for protein dislocation from the ER [4]. When an ER-derived misfolded protein gains access to the cytosol, the attachment of a poly-Ub chain recruits the cytosolic ATPase p97/VCP/CDC48 (Swiss-Prot ID: **P55072)** and its associated co-factors Ufd1-Npl4 [5–7], believed to provide the force required for extraction of substrate from the ER. It is not known whether these Ub-chains are utilized as a handle to exert a mechanical force or whether they target the dislocated protein directly to the proteasome [5,6,8].

The 19S lid of the 26S proteasome and p97/VCP/CDC48 both occur in association with ubiquitin ligase and deubiquitylating activities [9,10]. Ubiquitylation is a dynamic process, tightly controlled by a collection of associated ubiquitin-processing factors, both at the level of the proteasome and at the level of p97 [9,10]. Ubiquitylation and its reverse reaction, catalyzed by deubiquitylating enzymes (DUBs), are crucial for p97-mediated dislocation and for proteasome function [3,5]. Impairment of p97-associated DUB activity can block substrate dislocation [11,12]. The removal of poly-Ub chains by DUBs associated with the proteasomal lid precedes the threading of unfolded proteins through a narrow pore into the proteolytic chamber of the core 20S proteasome [1,13,14]. The removal of Ub prior to degradation also recycles this essential modifier and replenishes the cellular pool of free Ub. It follows that DUB activity can have distinct outcomes for proteasomal turnover of proteins: some DUBs facilitate degradation, whereas others may stabilize proteins destined for degradation.

Removal of glycoproteins from the ER involves multiple distinct enzymatic reactions: ubiquitylation, deubiquitylation, deglycosylation, and ATP-dependent dislocation [2]. How are the opposing activities of ubiquitylation and debuiquitylation coupled in the course of extraction from the ER and delivery to the proteasome?

The activity of DUBs is no less carefully controlled than that of the ligases that carry out ubiquitylation. The catalytic domains of DUBs, both cellular and viral, are flanked by often sizable segments that likely mediate such control [12,15,16]. We reasoned that the expression of a highly active DUB protease domain, excised from its normal context, might preemptively remove Ub from substrates targeted for degradation and stabilize them. We chose the protease domain of the Epstein-Barr Virus (EBV) large tegument protein (BPLF1, Swiss-Prot ID: **P03186**) for that purpose. We use this EBV-DUB to cause an enzymatic blockade of the UPS and show that its expression uncouples dislocation from degradation. Our data demonstrate that protein dislocation from the ER requires a DUB activity upstream of p97-mediated extraction from the ER. Furthermore, a side-by-side comparison of different experimental strategies that impede degradation of a misfolded ER-luminal substrate enabled us to identify this substrate's interactors at distinct stages en route to degradation. This allows us to propose a timeline for the discrete steps involved. We further identify the ER-luminal machinery for disulfide bridge formation as a putative target of eeyarestatin-I, a small-molecule inhibitor of dislocation. The cytosolic co-chaperone recruiter BAT3 (Swiss-Prot ID: P46379) surfaces as a specific interactor of an ER-derived—and now cytosolic—substrate when the UPS is blocked by the EBV-DUB. Our data suggest a previously unanticipated function of cytosolic chaperones, namely to cope with ER-derived misfolded proteins that arrive in the cytosol. The consequences of EBV-DUB expression are less toxic than those caused by pharmacological proteasome inhibitors and might find wide application in cell biology.

Results

EBV-DUB is a highly active, viral ubiquitin-specific protease

We aimed to shift the balance of ubiquitylation towards deubiquitylation through enforced expression of a highly active DUB. To this end we employed the protease domain (aa1-270) of the EBV BPLF1 gene (Figure 1A) [16]. The isolated protease domain (EBV-DUB) hydrolyzed K_{48} Ub-linkages more readily (>10-fold) than preparations of the cellular DUB YOD1 (Swiss-Prot ID: **Q5VVQ6)** (Figure 1B). The EBV-DUB was an excellent substrate for the activity-based probe HA-Ub-VME [17], but not when the putative catalytic cysteine was substituted to alanine (C61A) or when Ub-binding was abolished through blocking the catalytic cleft of the EBV-DUB by an I173W mutation (Figure 1A,C). BPFL1 is active towards both K_{48}- and K_{63}-linked

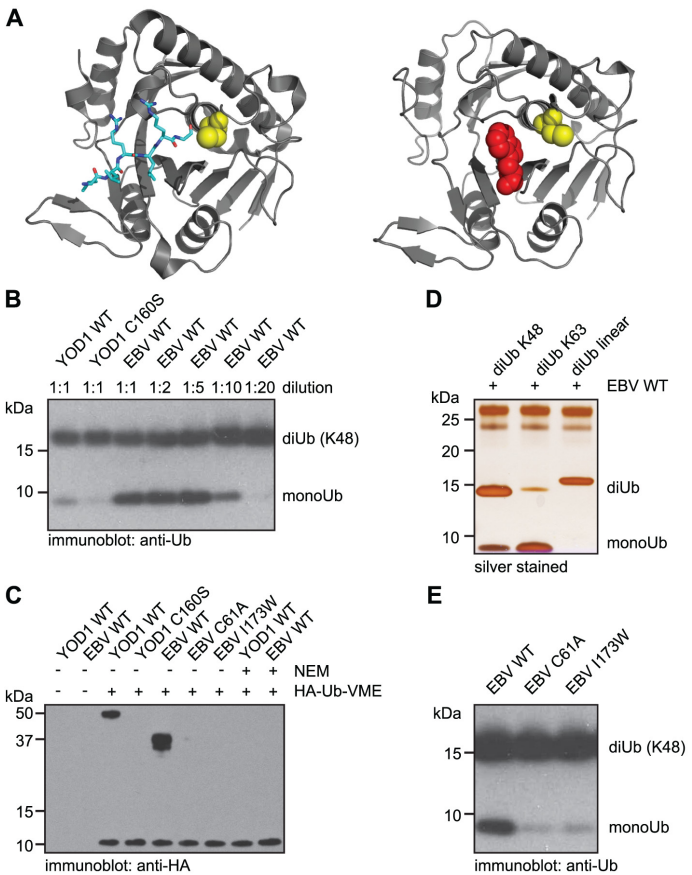

Figure 1. EBV-DUB is a highly active enzyme in vitro.

(A) The left panel shows the crystal structure of the M48 protease from mouse cytomegalovirus (MCMV) [16]. Depicted in cyan is the extended C-terminus of Ub in the M48 active-side cleft pointing towards the catalytic cysteine (C23), shown in yellow. The right panel shows a structural model based of EBV-DUB I173W, with the catalytic cysteine (C61) depicted in yellow and the tryptophane 173 point mutation, blocking the catalytic cleft, shown in red. (B) YOD1 WT, YOD1 C160S, and EBV-DUB WT (1 µg) were incubated with 0.5 µg of K48-linked diUb for 3 h at 37 ºC. The amount and concentration of the EBV-DUB WT was titrated as indicated. The reaction was stopped by boiling in sample buffer, subjected to SDS-PAGE, and immunoblotted with anti-Ub antibody. (C) Purified YOD1 and EBV-DUB (WT and indicated mutants) were incubated at a molar ratio of 1:1 with HA-Ub-VME, an activity-based probe [17], and subjected to SDS-PAGE. When indicated, NEM was included in the reaction mixture. HA-Ub-VME adduct formation was visualized by immunoblotting with anti-HA antibodies. Purified EBV-DUB is proteolytically processed and runs as a double band, however both forms promote adduct formation with the HA-Ub-VME probe. (D) K48-linked, K63-linked, or linear diUb (0.5 µg) was incubated for 3 h at 37 ºC in a total volume of 10 µl with EBV-DUB WT (1 µg). The reaction mixture was subjected to SDS-PAGE and silverstained. (E) EBV-DUB WT, the C61A mutant, and the I173W mutant of the EBV-DUB were incubated with K48-linked diUb (0.5 µg) for 3 h at 37 ºC. The reaction mixture was subjected to SDS-PAGE and immunoblotted with anti-Ub antibody.

di-Ub, as well as NEDD8 [18], but not against linear di-Ub despite its topological similarity to K_{63}-linked Ub (Figure 1D) [19]. The cellular function of BPLF1's DUB activity remains largely unknown [20]. Our experiments do not address the hydrolysis of poly-Ub chains of other linkage types, including K_{11}, or chains of mixed topologies, all of which could contribute to proteasomal targeting to different degrees [21]. K_{63} linkages have been linked primarily to endocytosis and other non-proteasomal events [22] but could contribute to protein homeostasis as well [23,24]. As a control for all subsequent experiments, we employed the I173W mutant unable to bind and hydrolyze Ub-chains (Figure 1A,C,E).

Expression of a FLAG tagged variant of the wild-type EBV-DUB in 293T cells resulted in a substantial downward shift of polyubiquitylation in HA-ubiquitin expressing cells (Figure 2A). In contrast, the expression of a cellular, less active DUB (YOD1 WT) failed to do so. Consistent with previous observations, the catalytically inactive mutant (YOD1 C160S) caused accumulation of polyubiquitylated proteins, presumably due to stalled dislocation [11]. The efficiency with which the viral DUB eliminated polyubiquitylated conjugates in living cells is even more apparent when the activity of the proteasome is blocked by prior exposure of cells to ZL3VS: polyubiquitylated proteins now accumulated in control cells but were largely absent from EBV-DUB WT cells when examined at similar sensitivity of detection (Figure 2A). To corroborate our findings, we repeated our experiments in the absence of co-transfected HA-Ub. Immunoblots using antibodies directed against ubiquitin or specific for Lys48-linked ubiquitin revealed diminished polyubiquitylation in EBV-DUB WT cells, but not in control cells (Figure S1).

A strong reduction in polyubiquitylation should affect protein turnover globally. Therefore we analyzed the effect of EBV-DUB expression on steady-state levels of two short-lived, cytosolic GFP variants: the ubiquitin-fusion degradation (UFD) substrate Ub-G76V-GFP and the N-end rule substrate Ub-R-GFP (Figure 2B) [25]. Both proteins are unstable and their detection improves upon inhibition of the UPS. Ub-R-GFP is processed by cellular ubiquitin hydrolases, which results in exposure of arginine as the N-terminal destabilizing residue [26]. Ub-G76V-GFP cannot be processed by cellular hydrolases, but the fusion with ubiquitin itself serves as a degradation signal [27]t;accession-num>11917093</accession-num><urls><related-urls><url>http://www.ncbi.nlm.nih.gov/entrez/query.fcgi?cmd=Retrieve&db=PubMed&dopt=Citation .

Co-expression of Ub-G76V-GFP and EBV-DUB WT gave rise to a population with high GFP fluorescence, best illustrated by the 5.3-fold higher median fluorescence intensity of GFP-positive cells (MFI) as compared to control cells and the 1.8-fold

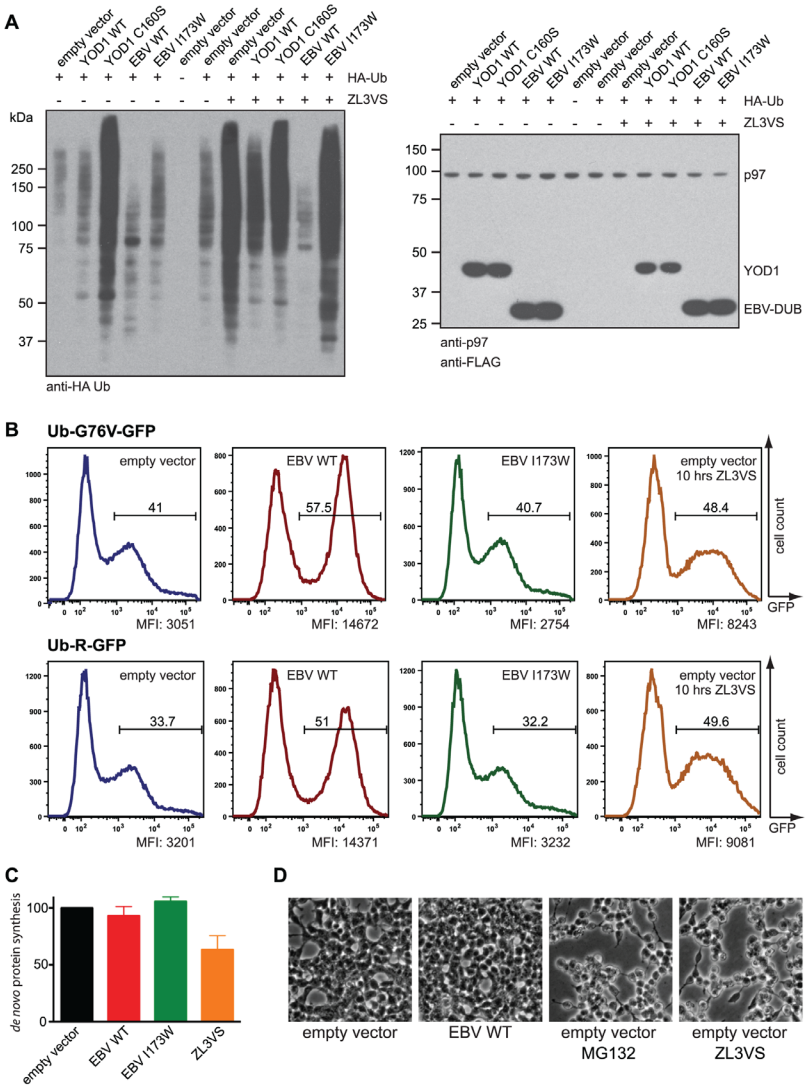

Figure 2. A viral DUB switches the cellular ubiquitylation balance towards deubiquitinylation and blocks proteasomal degradation.

(A) Lysates of 293T cells transfected as indicated and immunoblotted with anti-HA, anti-p97, and anti-Flag antibodies. Where indicated, cells were treated with for 10 h with 10 μM ZL3VS. (B) Flow-cytometric analysis of 293T cells treated and co-transfected with as indicated. The gate was set to identify GFP-positive, live cells. Quantified is the median fluorescence intensity (MFI) of GFP-positive cells. (C) Pulse-labeling experiment and quantification of de novo protein synthesis. Where indicated, cells were starved and radiolabeled in the presence of 50 μM ZL3VS. Radioactivity incorporated by control cells was normalized to 100%. The error bars depict the standard deviation (n = 4). (D) Morphology changes of 293T cells 26 h after transfection and after treatment for 20 h with 10 μM of indicated proteasome inhibitors.

increased MFI compared to cells treated with the proteasome inhibitor ZL3VS (Figure 2B). Similarly, Ub-R-GFP and EBV-DUB co-expressing cells exhibited a 4.4-fold higher MFI compared to control cells and a 1.6-fold higher MFI compared to ZL3VS-treated cells, apparent also when titrating ZL3VS (Figure S2). As expected, the relative fraction of GFP-positive cells increased when protein degradation was impaired (Figure 2B). ZL3VS is an efficient inhibitor of the chymotryptic and the peptidyl-glutamyl peptide hydrolyzing activities of the proteasome and impairs its tryptic activity by ~50% [25,28]. Taking this into account, our flow cytometric data on two well-established, short-lived proteins suggest a near complete blockade of the UPS [25,29]. Both the N-end rule and UFD pathway are affected, likely at an ubiquitinyl-dependent step in commitment of the substrate to the proteasome. Ubiquitylation and protein turnover are central to many cellular processes. Overexpression of a highly active DUB or proteasomal inhibition by small molecules might affect the physiology of a cell in many ways. Pharmacological inhibition of the proteasome impairs *de novo* protein synthesis [30,31]. In our hands, treatment of cells with ZL3VS for 40 min resulted in ~40% reduced incorporation of radioactivity in a 10 min pulse labeling experiment when compared to control and EBV-DUB expressing cells (Figure 2C). Thus, *de novo* protein synthesis was impaired upon pharmacological inhibition but remained unperturbed in EBV-DUB cells. Prolonged treatment (20 h) of cells with proteasome inhibitors caused growth arrest and changes in cell morphology, consistent with the known ability of proteasome inhibitors to induce apoptosis and cell cycle arrest [25,32]. EBV-DUB cells appeared normal at times of cultivation where ZL3VS treated cells were morphologically aberrant (>26 h) (Figure 2D), but after much longer cultivation they, too, succumbed, presumably because the continued operation of the UPS is essential for cell survival.

Expression of EBV-DUB blocks protein turnover

Does expression of the viral DUB affect protein degradation directly? To allow a direct comparison of an ER-derived and cytosolic substrate, we employed RI_{332}, a C-terminally truncated form of ribophorin-I that is commonly used as a model to study dislocation and degradation of ER-luminal proteins [11,33,34]. When devoid of its N-terminal signal sequence (DSS-RI_{332}) the protein fails to enter the ER, cannot be glycosylated, and remains cytosolic, but is otherwise identical to RI_{332} (see schematic representation in Figure 3E). The cytosolic UPS substrate DSS-RI_{332} is turned over in both control and EBV-DUB I173W cells ($t_{1/2}$ = 20 min), but its deg

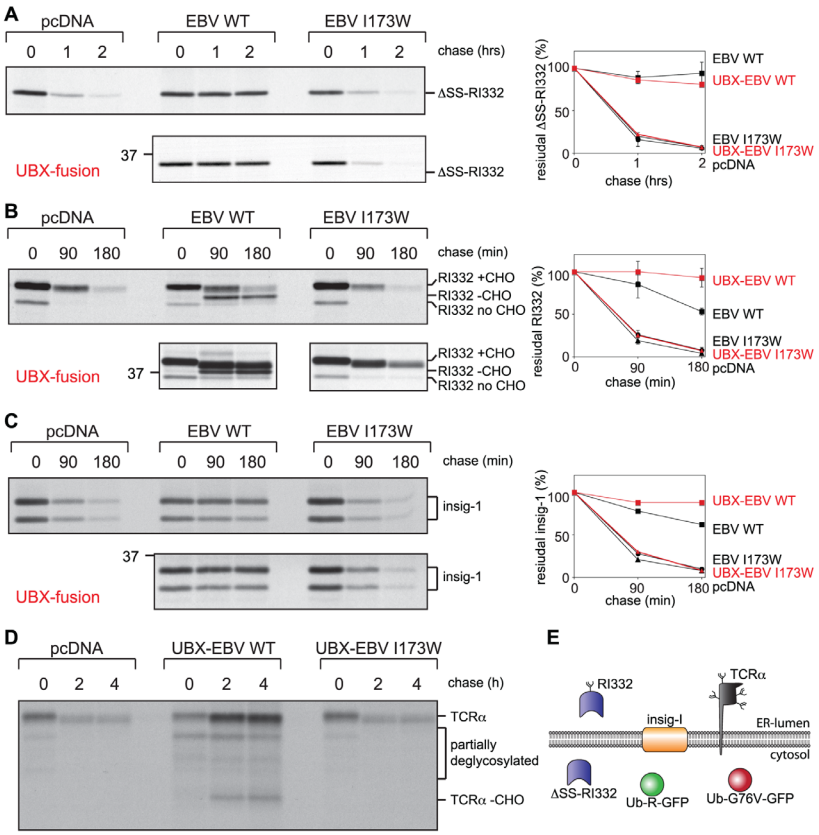

Figure 3. Expression of a viral DUB blocks degradation of cytosolic, ER-luminal, and ER-membrane proteins.

(A–C) Pulse-chase analysis with unstable model substrates: (A) cytosolically localized DSS-RI332, (B) the ER-luminal glycoprotein RI332, (C) Insig-1, a multi-spanning membrane protein of the ER, and (D) TCRa, a glycosylated protein with one transmembrane helix. (E) Unstable model proteins used throughout this study are shown schematically. After indicated chase times, the model substrates were immunoprecipitated, subjected to SDS-PAGE, and quantified (right panels). The influence of targeting the EBV-DUB to p97 through installation of an UBX-domain (red symbols) versus non-targeted EBV-DUB (black symbols) is tested by direct comparison of model substrate stabilization. The error bars correspond to the standard deviation (n = 3). See Figure S3 for UBX-mediated targeting to p97.

radation was blocked by expression of EBV-DUB WT (Figure 3A). This confirms our flow cytometric data on Ub-R-GFP and Ub-G76V-GFP (Figure 2B) and demonstrates an efficient blockade of the UPS imposed by EBV-DUB WT. An arrest of the UPS should also affect the degradation of ER-derived proteins. When equipped with its natural signal sequence, RI_{332} is translocated into the ER and glycosylated

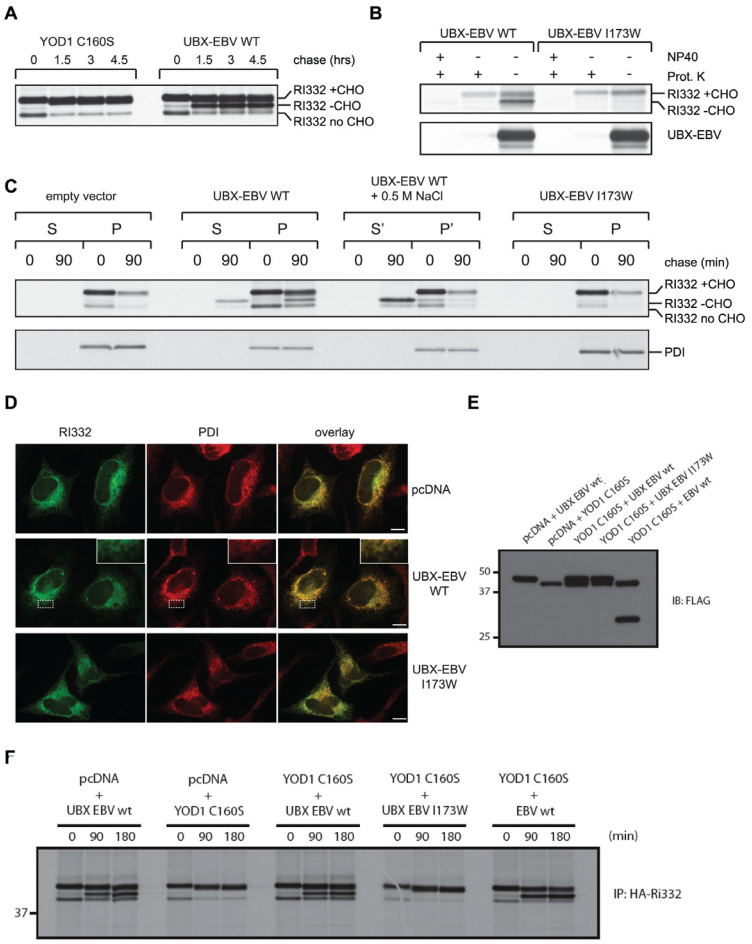

Figure 4. ER-dislocation and protein degradation are uncoupled by p97-targeted EBV-DUB.
(A) 293T cells were co-transfected with RI332 and the indicated constructs and subjected to pulse chase analysis. (B) 293T cells were co-transfected with the indicated constructs, disrupted mechanically, and treated with proteinase K and/or NP40 as indicated. The UBX-EBV-DUB served as control for a cytosolic protein. (C) 293T cells were co-transfected as indicated and pulse labeled. After 0 min or 90 min of chase, the cells were subjected to a subcellular fractionation experiment, after selective permeabilization of the plasma membrane with Perfringolysin O. RI332 and PDI were retrieved after fractionation via immunoprecipitation. When shown (S'/P'), the fractionation was performed in the presence of high salt (0.5 M). (D) Immunofluorescence of HeLa cells co-transfected with RI332 and the indicated constructs. Endogenous PDI (red) served as an ER-marker and RI332 (green) was detected via the HA-epitope tag. Scale bar = 10 µm. (E) 293T cells were co-transfected with indicated YOD1, EBV-DUB, and RI332 constructs. Expression levels of YOD1 and the EBV-DUB were determined from SDS-lysastes after immunoblotting against the N-terminal Flag-epitope. (F) A pulse chase experiment was performed with 293T transfected as in Figure 4E. The block in dislocation induced by YOD1 C160S can be rescued by co-expression of UBX-EBV WT.

but rapidly destroyed in control and EBV-DUB I173W cells ($t_{1/2}$ = 44 min) (Figure 3B) [33].

The banding pattern observed in these experiments requires explanation. The lower band at the 0 min chase time point corresponds to ER-luminal, non-glycosylated RI_{332} (RI332 no CHO) with its signal sequence removed, while the upper band is the glycosylated form of RI_{332} (RI332 +CHO) [11]. Removal of the *N*-linked glycan by cytosolic *N*-glycanase converts asparagine at the site of glycan attachment to aspartate (N275D) [35]. As a consequence, deglycosylated RI_{332} (RI332CHO) shows altered electrophoretic mobility. This form was readily apparent in EBV-DUB WT cells after a 90 min chase and beyond (Figures 3B, S3) and can arise only as a consequence of glycan removal from previously glycosylated RI_{332}. Such deglycosylated intermediates are normally rapidly degraded by the proteasome and therefore escape detection, unless the activity of the proteasome is compromised [33]. Co-expression of the EBV-DUB stabilized RI_{332}, but did not do so completely (Figure 3B). Since dislocation and proteolysis are at least to some extent coupled processes [33,36], we reasoned that some Ub-chains present on ER-derived dislocation substrates might not be accessible to the EBV-DUB. We therefore targeted the viral DUB domain to p97, the “motor of dislocation,” by equipping it with the UBX domain of YOD1 to copy the strategy employed by this cellular DUB. This chimeric protein (UBX-EBV WT) associated with p97 (Figure S4) and blocked degradation of the ER-derived RI_{332} substrate completely (Figure 3B, UBX-fusion).

The degradation of two unrelated membrane proteins—the polytopic transmembrane protein insig-1 and the glycosylated a-chain of the T-cell receptor (TCRa) with one transmembrane helix (Figure 3E)—were likewise affected. Expression of UBX-EBV WT halted the turnover of myc-tagged insig-1, an ER-localized transmembrane protein that regulates cholesterol synthesis (Figure 3C) [8]. Of note, insig-1-myc is not a glycoprotein but has two alternative start codons yielding two translation products with distinct electrophoretic mobilities [37]. Also the degradation TCRa, an unstable protein when expressed in the absence of other T-cell receptor subunits, was blocked upon co-expression of UBX-EBV WT (Figure 3D).

In summary, the EBV-DUB arrests turnover of cytosolic and ER-derived proteins. In all cases, targeting of the viral DUB to p97 improved the stabilization of ER-derived substrates, but its activity towards cytosolic substrates of the UPS persisted (Figures 3, S5).

Uncoupling protein dislocation and degradation

The occurrence of the deglycosylated RI_{332} intermediate that accumulated in UBX-EBV WT and in EBV WT cells (RI_{332} −CHO; Figure 3B) was informative. Since *N*-glycanase is confined to the cytosol [35,38], this observation immediately suggested that the single *N*-linked glycan of RI_{332} gained cytosolic exposure and therefore that dislocation must have occurred, entirely or in part. However, when turnover of RI_{332} was inhibited by expression of YOD1 C160S, the deglycosylated form RI_{332} was not observed, even after long chase periods (Figure 4A), indicating its confinement to the ER. The appearance of deglycosylated intermediates was not specific for the ER-luminal RI_{332} but was readily observable as well for TCRa when co-expresssed with UBX-EBV WT (Figure 3D). For reasons that remain to be determined, we consistently observe greater recovery of label for TCRa at later chase points. It is possible that detergent extraction of newly synthesized TCRa is somehow less efficient than material that has left the site of membrane insertion. We do not observe a similar discrepancy for the other substrates analyzed, insig-1 and RI_{332}.

We confirmed cytosolic accessibility of the deglycosylated RI_{332} intermediate by a proteinase K protection experiment in mechanically disrupted cells (Figure 4B). In the absence of detergent, only deglycosylated RI_{332} (RI332 − CHO) was accessible to protease. The glycosylated, ER-luminal form (RI332 + CHO) was not affected by the protease under identical conditions and serves as an internal control for membrane integrity (Figure 4B). Proteinase K sensitivity of deglycosylated RI_{332} implied that a substantial portion of RI_{332}, if not RI_{332} in its entirety, was exposed to the cytosol in UBX-EBV WT expressing cells. To further corroborate this result, we performed a fractionation experiment in which we made use of the pore-forming toxin Perfringlolysin O (PFO) [39]. UBX-EBV WT cells were pulse labeled and the radiolabeled, deglycosylated intermediate of RI_{332} was enriched during a 90 min chase period (Figure 4C). After selective permeabilization of the plasmamembrane by PFO, the cytosolic fraction was separated from cellular remnants by centrifugation, in the presence or absence of added high salt to ensure release of peripherally membrane-associated materials. Only for UBX-EBV WT cells did we see release of the deglycosylated RI_{332} (RI332 − CHO) into the supernatant fraction (S), even more pronounced in the presence of high salt (S'). However, glycosylated RI_{332} (RI332 + CHO) was retained in the pellet fraction under all conditions, consistent with an ER-luminal localization. PFO permeabilization did not damage intracellular compartments, as verified by complete retention of the ER-resident chaperone PDI

(Figure 4C) in the particulate fraction.
We conclude that the deglycosylated form of RI_{332} was indeed dislocated from the ER and arrived in the cytosol. Combined, our observations show that expression of UBX-EBV WT uncouples dislocation and degradation of RI_{332}. We wondered if the deglycosylated intermediate of RI_{332} once cytosolic would remain associated with the ER or whether it might travel to a different location. Immunofluorescence microscopy showed that RI_{332} localized to the ER in UBX-EBV WT expressing cells, with no evidence of obvious aggregation (Figure 4D). In light of the fractionation data, this suggests that upon dislocation, a sizable fraction of deglycosylated RI_{332} remains loosely associated with the cytosolic face of the ER-membrane.

A DUB-catalyzed reaction is essential for protein dislocation

We blocked dislocation from the ER by the expression of YOD1 C160S, which causes stabilization of ER resident, glycosylated RI_{332} [11]. We previously proposed that p97-mediated dislocation is stalled under these conditions, because Ub removal is required to allow threading of the dislocation substrate through p97's central pore [11]. If this interpretation is correct, then it should be possible to reverse this block by expression of a DUB capable of attacking the hypothetical stalled intermediate and to overcome the YOD1 C160S-imposed block. Indeed, co-expression of comparable levels of UBX-EBV WT and YOD1 C160S (Figure 4E) resulted in the accumulation of the deglycosylated intermediate of RI_{332} indicative of dislocation (Figure 4F). Co-expression of the inactive mutant UBX-EBV I173W failed to do so, thus excluding simple competition of the UBX-fusion protein with other p97-interactors as the explanation. Consistently, even the non-targeted EBV-DUB without fused UBX-domain could relieve the blockade of dislocation imposed by YOD1 C160S (Figure 4F).
We conclude that a DUB-catalyzed reaction is essential for protein dislocation from the ER. Because ubiquitylation by HRD1-SEL1L is required for the initial engagement of the cytosolic dislocation apparatus [2,34,40], premature removal of ubiquitin might also inhibit the earliest steps in this pathway, if EBV-DUB has access to these ubiquitylated intermediates. The rate of dislocation as determined by the disappearance of glycosylated RI_{332} (Figure 3B; RI332 + CHO) was not affected compared to control cells in EBV-WT expressing cells, but was lower in cells expressing the p97-targeted variant (Figure 3B, UBX-fusion; Figure S3). Thus, the non-targeted form of the EBV-DUB interfered exclusively with the degradation of already dislocated RI_{332}, while the ER-targeted variant stabilized RI_{332} at the initia-

tion of dislocation and through prevention of delivery to the proteasome by preemptive removal of poly-Ub chains from the substrate. Nevertheless, both variants, p97-targeted or not, caused accumulation of deglycosylated, dislocated RI_{332} in the cytosol.

Staging a misfolded ER-derived glycoprotein on its path to destruction

What keeps the breakdown intermediate(s) of RI_{332} from aggregation? To address this question and to gain a more global perspective on the natural history of a misfolded protein, we staged the different steps in degradation through identification of proteins that interact with RI_{332} and its various dislocation intermediates. Through interference with dislocation and degradation by different means, we generated discrete intermediates in the breakdown pathway of RI_{332} as explained in the preceding sections. Using affinity tagged RI_{332} as a bait, we retrieved interacting proteins from UBX-EBV WT, YOD1 C160S, or p97 QQ-expressing (an ATPase-deficient form of p97) cells [6], and from cells exposed to the proteasome inhibitor ZL3VS or eeyarestatin I, an inhibitor of dislocation and possibly membrane insertion [29,41,42]. As controls, we performed immunoprecipitations from cells that either did not express RI_{332} or that co-expressed RI_{332} with YOD1 DZnf C160S, YOD1 WT, or UBX-EBV I173W, none of which significantly perturb the dislocation/degradation process [11]. We performed a total of nine independent large-scale immunopurifications and analyzed each by LC/MS/MS. We identified 836 candidate interactors and enumerated the number of peptides that originated from each one of them. We sought to identify interactions enriched upon inhibition of dislocation/degradation to gain insight into their spatial and temporal occurrence. We therefore normalized our dataset as follows. Each candidate protein was represented by multiple peptide fragments in different experimental conditions, and the maximum number of peptides (MNOP) for a given candidate was based on the condition that yielded the highest peptide count. All interactions between RI_{332} and its candidate interactors (retrieved from independent immunoprecipitation experiments) were expressed as a percentage of the MNOP. Such a normalized interaction matrix should facilitate the identification of groups of proteins that responded similarly if certain discrete steps of the dislocation/degradation pathways are perturbed.
After application of a stringent set of rules (inclusion requirement based on a threshold number of peptides and absence from normal serum controls; see Text S1 for details) a total of 33 candidate interactors remained (Table S1). The candidates were arranged in three groups via k-means clustering and are depicted in a

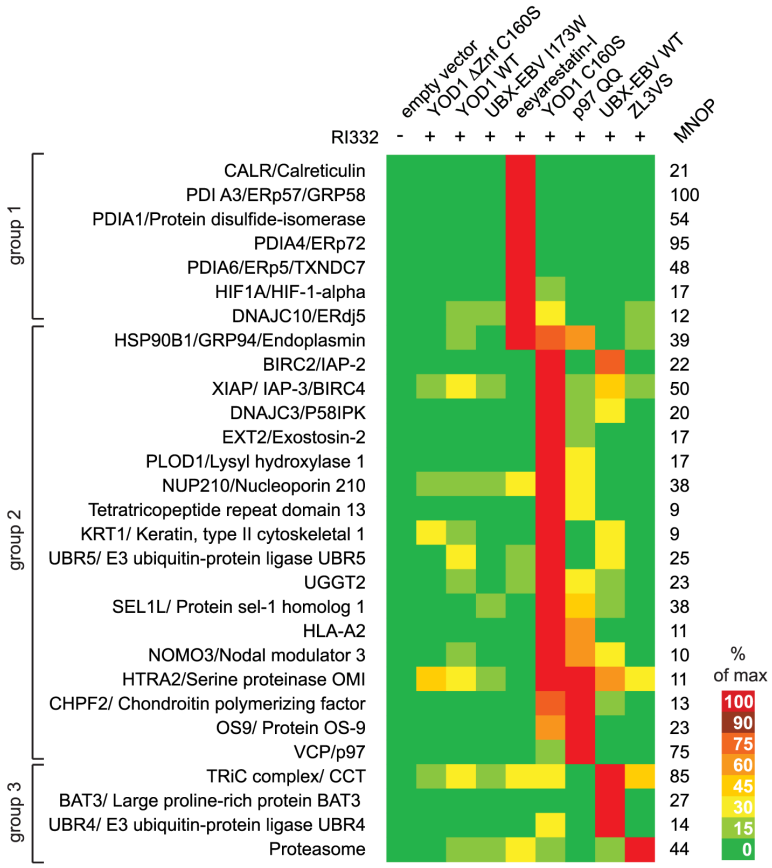

Figure 5. The natural history of an unstable, ER-luminal glycoprotein.
RI332 was immunoprecipitated from cells transfected with indicated constructs or treated with eeyarestatin-I or ZL3VS (10 μM each). As control, one batch of cells (empty vector) was not transfected with RI332. Co-immunoprecipitated interactors of RI332 were identified by LC/MS/MS. The maximum number of peptides (MNOP) associated with RI332 for a given condition was set to 100% and peptides recovered from the other experimental conditions expressed as percentage of the maximum for each candidate accordingly. After selection using a strict set of rules (see Materials and Methods), the candidates were grouped via K-means clustering. See also the list of candidate interactors in Table S1. The color-coding represents a quantitative measure for the interaction from bright red (maximal interaction) to dark green (minimal/no interaction).

heat map (Figure 5). The heat map is a graphical representation of the normalized interaction matrix and visualizes the conditions under which a particular interactor co-precipitated with RI_{332}.

Group 1 comprised those interactors of RI_{332} that were specifically retrieved from eeyarestatin-I treated cells (Figure 5). Consistent with an ER-luminal accumula-

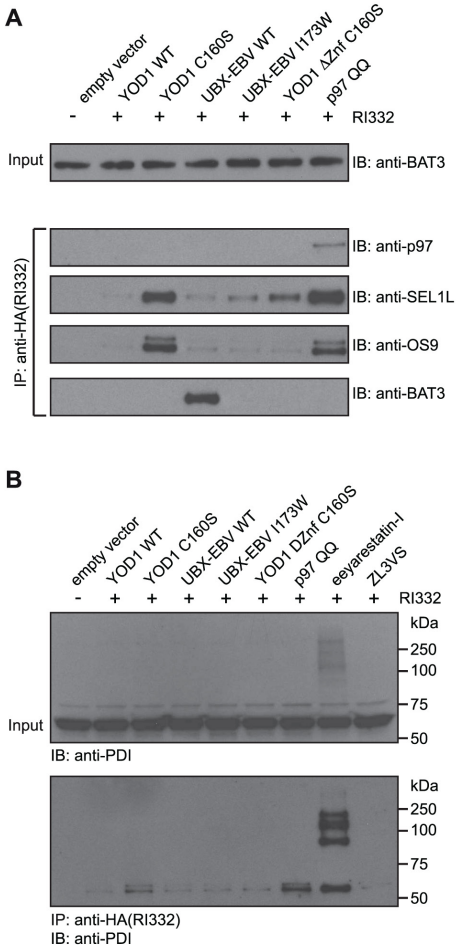

Figure 6. BAT3 interacts with the cytosolic dislocation intermediate of RI332 and eeyarestatin-I induces adducts of PDI.
(A, B) 293T cells transiently transfected as indicated were homogenized in NP40 lysis buffer and subjected to immunoprecipitation with anti-HA antibodies. As control, one batch of cells was not transfected with RI332. Co-precipitated interactors were identified by immunoblotting using the antibodies anti-BAT3, anti-p97, anti-SEL1L, anti-OS9 (left panels), and anti-PDI (right panel). To control for equal loading, lysates were subjected to immunoblotting using (A) anti-BAT3 and (B) anti-PDI antibodies. See also the structural formula of eeyarestatin-I in Figure S6.

tion of RI_{332}, we observe the ER-luminal disulfide shuffling and/or PDI-domain containing proteins (ERdj5, ERp72, ERp57, ERp5, PDI, and Calreticulin) in association with RI_{332} (see Table S1 for Swiss-Prot IDs of candidate interactors) [42,43].

When a protein is terminally misfolded, a family of substrate recognition molecules targets the substrate to the dislocation machinery. A snapshot of this type of intermediate was provided by co-expression of YOD1 C160S or mutant p97 (QQ). Specifically enriched interaction partners of RI_{332} under these conditions clustered in group 2 and include glycan-binding and modifying proteins (OS9, UGGT2), general ER-luminal substrate recruiting factors and chaperones (SEL1L, Endoplasmin/GRP94, DNAJC3/P58IPK), p97, and the cytosolic UBR5, implicated in ubiquitylation according to the N-end rule [6,44–46]. Our unbiased proteomic approach supports our earlier proposal that YOD1 C160S blocks the dislocation reaction itself [11]. RI_{332} is recognized as misassembled by OS9, SEL1L, and GRP94, associates with p97, but cannot be extracted in YOD1 C160S and p97 QQ cells [11,34,40,45]. Interactors that clustered in group 2 comprised both ER-luminal and cytosolic components of the ER-quality control machinery and UPR signaling.

After successful dislocation, misfolded proteins are targeted to the cytosolic proteasome. Group 3 comprised those

proteins that were co-immunoprecipitated with RI_{332} from UBX-EBV WT or ZL3VS treated cells. Our mass spectrometry data suggested that the deglycosylated intermediate of RI_{332} associates with cytosolic chaperones, namely the co-chaperone recruiter BAT3 and the TRiC complex/CCT. The TRiC complex is important for transient stabilization of nascent polypeptide chains prior to their translocation into the ER [47,48], and BAT3 was recently implicated in integration of tail-anchored proteins into the ER membrane [49]. Not surprisingly, we can demonstrate an interaction of RI_{332} with the proteasome when its activity was blocked by the action of ZL3VS. The identified cytosolic interactors of RI_{332} fully support our biochemical characterization and suggest that dislocation and degradation are uncoupled in UBX-EBV WT expressing cells.

A cytosolic chaperone associates with an ER-derived dislocated protein

As corroboration of the mass spectrometry experiments, we verified interactors of RI_{332} (Figure 6A) by different means. After immunoprecipitation of RI_{332} from cells transfected/treated as in the large-scale pulldown experiments, we confirmed an interaction of RI_{332} with p97 when the ATPase activity of p97 was blocked by mutation (p97 QQ). We likewise confirmed the association of SEL1L and OS9 with RI_{332} when co-expression of either YOD1 C160S or p97 QQ blocked its dislocation from the ER. We established the association of RI_{332} with BAT3, which required the co-expression of UBX-EBV WT. These data hint at the existence of a chaperone-mediated buffer to sequester dislocated proteins from the canonical degradation pathway.

The mass spectrometry experiment predicted a strikingly enriched association of PDI/PDIA1 with RI_{332}, when cells were treated with eeyarestatin-I. Indeed, we could verify an interaction of these proteins when co-expressed with either YOD1 C160S or p97 QQ or when cells were treated with eeyarestatin-I (Figure 6B). More surprisingly, eeyarestatin-I induced the formation of SDS- and b-mercaptoethanol-resistant adducts of PDI. The enrichment of these adducts relative to monomeric PDI in immunoprecipitates of RI_{332} was indicative for adduct formation between RI_{332} and PDI upon eeyarestatin-I treatment. Similar observations were also made for PDIA3/ERp57 (unpublished data).

Discussion

To explore the contributions of ubiquitin addition and removal in protein extraction from the ER, we developed an enzyme-based method to disrupt ubiquitin-dependent protein degradation. We used a biochemical approach to analyze its effect on protein turnover and dislocation from the ER.

A novel tool to block ubiquitin-dependent proteasomal degradation

The expression of a highly active viral DUB markedly shifts the cellular balance towards deubiquitylation (Figures 2A, S1). Similar to pharmacological inhibition of the proteasome, accelerated or premature Ub removal from substrates should affect their ubiquitin-dependent degradation. Indeed, overexpression of the EBV-DUB blocks the degradation of several model substrates, but without the immediate cytotoxic effects that are commonly observed upon treatment of cells with pharmacological proteasome inhibitors (Figure 2C,D). In view of Ub's role in cell cycle control, through K_{11}-linked Ub-chain assembly by the ubiquitin ligase APC/C [50], the ultimate demise of cells with an arrested UPS is of course hardly surprising. The greater cytotoxicity of pharmacological inhibition could perhaps be related to ubiquitin-independent functions of the proteasome or reflect the critical importance of free Ub in the cell [3,51]. Interference with the UPS by blocking proteolysis with small molecules or by enzymatic interference with proteasomal targeting are two fundamentally different approaches. Small molecule proteasome inhibitors cause an accumulation of polyubiquitylated proteins and deplete cells of free Ub [52]. Cell viability critically depends on a pool of free Ub and its depletion kills cells [51]. Shifting the cellular balance towards deubiquitylation, as achieved by the EBV-DUB, does not result in accumulation of polyubiquitylated proteins (Figure 2A) and represents a novel means of inhibiting the UPS. Unlike the EBV-DUB, pharmacological inhibition of the proteasome reduces *de novo* protein synthesis even after relatively short times of exposure (Figure 2C) [30,31]. Translation, protein folding, secretion, and dislocation are interdependent processes and the ability to block proteasomal protein degradation without immediately affecting translation provides an additional benefit.

Deubiquitylation is essential for protein dislocation from the ER

We showed previously that YOD1 C160S causes complete retention of RI_{332} in the

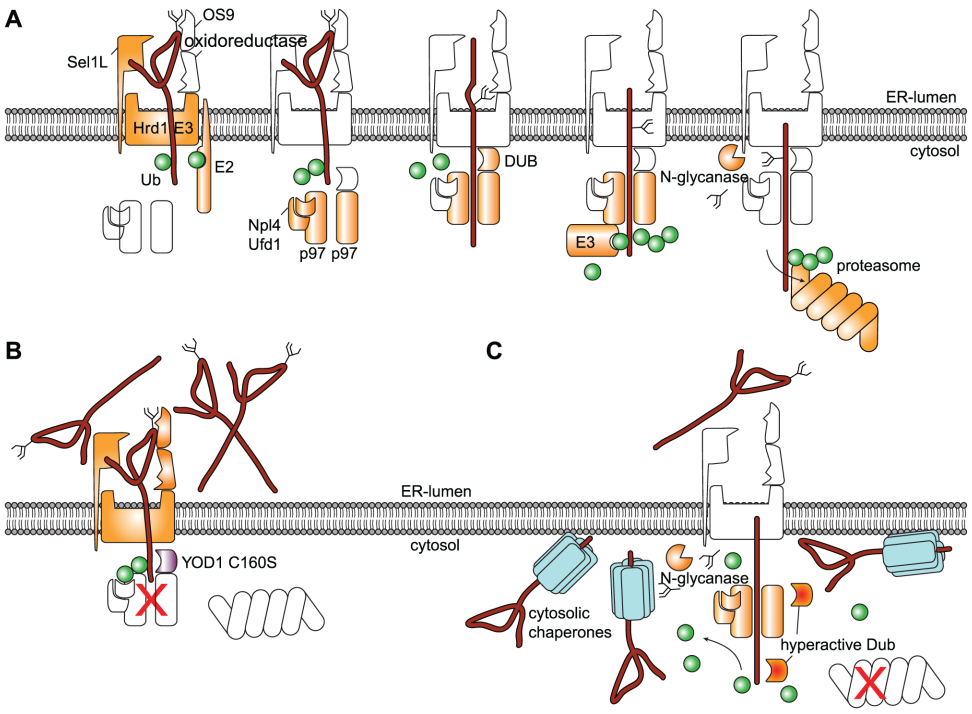

Figure 7. A misfolded glycoprotein on its path to destruction.
(A) Model of two consecutive ubiquitylation cycles that initiate dislocation and target the substrate to the proteasome, respectively. (B) Expression of catalytically inactive YOD1 C160S impairs deubiquitylation upstream of the p97 AAA ATPase. This jams the central pore of p97 and processive threading of the dislocation substrate is arrested. In consequence, misfolded, glycosylated proteins accumulate in the ER-lumen and as partially dislocated intermediates at the site of dislocation. (C) Expression of the highly active EBV-DUB deubiquitylates misfolded proteins upstream of p97 and thus facilitates processive dislocation mediated by p97. Lack of proper proteasome commitment results in accumulation of a deglycosylated, cytosolic intermediate of the misfolded protein.

ER, a substrate otherwise extracted and targeted for degradation (Figure 7A,B) [11]. This retention can be reversed at least in part by expression of the p97-targeted EBV-DUB (Figures 4F, 7C). Combined, these results demonstrate a need for removal of Ub to achieve dislocation. Ramping down the p97-associated DUB activity blocks dislocation but can be rescued by an active DUB. This immediately suggests that DUBs can have opposing functions for the degradation of ER-derived proteins. Some DUBs might impair dislocation by reversing ubiquitylation; others might facilitate dislocation and subsequent degradation. Indeed, TCRa-GFP is stabilized by knockdown of USP13 but destabilized by knockdown of Ataxin-3 [12]. Moreover, the observed uncoupling of dislocation and degradation by the

EBV-DUB suggests that a persistently ubiquitylated state is not essential for the physical extraction of substrate from the ER. Misfolded proteins are escorted to the proteasome by ubiquitin binding proteins [53,54]. It is therefore no surprise that the removal of Ub-chains by the EBV-DUB abrogates proteasomal turnover of these proteins. By analogy, p97-mediated extraction would be arrested by the EBV-DUB to a similar extent if persistent substrate modification with Ub-chains were required to exert a mechanical force for such extraction. Indeed, protein dislocation is slowed down, but clearly the reaction continues in cells that express EBV-DUB (Figures 4A, S3). Together with the evident requirement of a DUB-catalyzed reaction upstream of p97 (Figure 4E), these findings suggest that Ub-chains are not required to exert a mechanical force on the dislocation substrate [7] but may instead be required only as recognition signal [5].

Our data are consistent with the following model (Figure 7A). Dislocation substrates are targeted to a dislocon that connects with an Ub ligase activity, as exemplified by the HRD1-SEL1L complex [2,34,45]. Consistent with its requirement for dislocation, substrate ubiquitylation recruits p97 and the Ub-recognizing co-factors Ufd1 and Npl4 to initiate dislocation [6,7,11,12,55]. Once the dislocation machinery is recruited, one or several p97-associated DUBs remove the initial Ub tag to enable ATP-dependent threading through the central pore of p97 [7,11,12,55]. Unless p97 is coupled directly to the proteasome, for which there is no firm experimental support at present [56], a second round of ubiquitylation would be required to target the unfolded protein to the proteasome, again necessitating removal of the Ub-chain prior to its insertion into the proteolytic chamber [14]. There is of course also a structural resemblance between the 6-fold symmetrical p97 complex, present in association with Ub-recognizing and -processing factors, and the similarly equipped proteasomal cap complex [53].

The first round of ubiquitylation would be responsible for the engagement and proper assembly of the p97-Ufd1-Npl4 dislocation complex and may involve K_{11}-linked ubiquitin chains [21,57]. The second round would then target the dislocated, now cytosolic protein to the proteasome like any other p97-dependent, cytosolic substrate of the UPS [12,29,57]. Ubiquitylation-dependent events occur both upstream and downstream of p97 [53,54]. Two consecutive rounds of ubiquitylation are conceptually similar to the use of multiple independent ubiquitylation sites on many standard proteasomal substrates: modification of more than a single site on a given substrate requires sequential engagement by a given ligase, or the involvement of more than one ligase.

The p97-targeted EBV-DUB interferes with degradation of ER-derived substrates

at two distinct steps (Figure 7C). First, it interferes with proper initiation of dislocation by premature removal of ubiquitin. Second, it blocks substrate degradation by removal of the poly-Ub chains that would otherwise have mediated delivery of the misfolded protein to the proteasome. In the absence of a fused UBX-domain, the EBV-DUB affects to a lesser extent the initial stages of dislocation but still strongly inhibits proteasomal proteolysis of cytosolic substrates and ER-derived substrates (Figures 2B, 3A,B). The EBV-DUB can even facilitate the dislocation reaction when dislocation is otherwise stalled by expression of YOD1 C160S (Figures 4F, 7B). Our data establish the necessity of a DUB-catalyzed reaction upstream of p97-mediated protein extraction from the ER. These observations are most consistent with a model of two consecutive rounds of ubiquitylation and deubiquitylation.

The natural history of an ER-luminal glycoprotein dislocation substrate

Using different tools to block protein dislocation and degradation, we identified interacting partners of a misfolded, ER-derived glycoprotein at different stations on its road to destruction. Starting in the ER, eeyarestatin-I was first identified as an inhibitor of dislocation [42]. However, there is no consensus on the identity of its molecular targets or its exact mode of action [29,41,58]. Eeyarestatin-I contains two halogenated benzene rings (Figure S6). Bromobenzene, a hepatotoxic compound, is metabolized to reactive metabolites (e.g. bromobenzene-3,4-oxide) and forms covalent adducts with cellular proteins, including PDIA1, PDIA6, and PDIA3 [59,60]. Also other halogenated aromatic derivatives covalently modify proteins in a reaction mechanism similar to that involving bromobenzene [61]. If the two halogenated benzene rings of eeyarestatin-I would react similarly, formation of covalently cross-linked adducts of PDI might ensue, consistent with our observations that eeyarestatin-I induces SDS-resistant adducts of PDI (Figure 6B). We therefore suggest the possibility that the two halogenated benzene rings of eeyarestatin-I might promote crosslinking of proteins in the ER lumen and that its targets include the machinery for disulfide shuffling. If the machinery for disulfide shuffling in the ER is indeed a molecular target of eeyarestatin-I, then both import into and export from the ER are likely to be affected, explaining the seemingly divergent observations reported for eeyarestatin-I's mechanism of action [29,41,42].
By staging the process of dislocation and degradation we identified several novel and intriguing candidate interactors for the RI_{332} dislocation substrate, including proteins important in the maturation of extracellular matrix components (PLOD1, CHPF2, EXT2). Whether the machineries for heparan sulfate synthesis, chondroitin

sulfate synthesis, and collagen polymerization merely undergo rapid turnover and are processed via p97 or whether they are otherwise involved in the dislocation reaction remains to be established.

We validated BAT3 as a cytosolic interactor of the deglycosylated intermediate of RI_{332}. This result implies not only that RI_{332} is dislocated from the ER but also that it remains associated with chaperones, possibly to prevent aggregation. This type of interaction may be an example of how cells cope with dislocated proteins that escape degradation. Could it be that the machineries for translocation and dislocation share certain co-factors? Intriguingly, BAT3 has recently been implicated in proteasomal degradation of newly synthesized defective polypeptides [62]. This might suggest that cytosolic quality control machineries handle defective, ribosome-derived nascent chains similarly to how they deal with defective polypeptides that originate from the ER. The specifically enriched association of the TRiC/CCT with RI_{332} in UBX-EBV WT expressing cells (Figure 5) further supports this interpretation: Cytosolic chaperone complexes implicated in the stabilization and quality control of folding intermediates prior to translocation in the ER [47,48] also interact with an ER-derived, dislocated protein.

The approach developed here—expression of the EBV-DUB—stabilizes a range of proteins that are normally degraded in an Ub-dependent manner. Although capable of blocking Ub-dependent protein degradation globally and efficiently, the EBV-DUB is less toxic to cells than pharmacological proteasome inhibitors, providing an extended window of observation. We show that dislocation and degradation of ER-derived misfolded substrates can be uncoupled by the expression of the viral DUB domain and so allows the unprecedented visualization of a deglycosylated dislocation intermediate in the absence of pharmacological proteasome inhibitors. We identify the necessity of a DUB-catalyzed reaction for protein dislocation from the ER and place this activity upstream of p97. The determination of the sets of interacting partners of a misfolded, ER-derived glycoprotein at different stations on its road to destruction helped us characterize the order of events during dislocation and degradation. The expression of this highly active DUB has provided new mechanistic insights into protein quality control. Given its low toxicity and the possibility of achieving cell-type or tissue-specific expression in vivo, the EBV-DUB and variants derived from it may prove to be an attractive alternative to the use of small molecule inhibitors of the proteasome.

Materials and methods

Antibodies, Cell Lines, Constructs, Experimental Procedures

Antibodies against the HA-epitope were purchased from Roche (3F10); anti-Flag, anti-Ubiquitin antibodies were purchased from Sigma-Aldrich; and Lys48-specific anti-Ubiquitin antibodies (anti-K48-Ub, clone Apu2) were purchased form Millipore. Anti-p97 and anti-BAT3 antibodies were purchased from Fitzgerald Industries and Abcam, respectively. Polyclonal anti-OS9 and anti-SEL1L antibodies were described previously [45,63]. A.E. Johnson (Texas A&M University, TX) provided a plasmid encoding perfringolysin O. Polyclomal anti-PDI serum (rabbit) was generated with bacterially expressed human PDI. 293T cells were cultured and transfected as previously described [63]. The deletion constructs and mutants of YOD1 have been described elsewhere [11]. All p97-targetting constructs were cloned into the pcDNA3.1(+) vector system (Invitrogen) with a Kozak sequence (GCCACC) inserted directly upstream to the Start-Codon, and encoded for a N-terminal Flag-tag (DYKDDDK) followed by the UBX domain of YOD1 (aa1–131). For the UBX-GFP construct, these aa1–131 of YOD1 were followed by a LEGS linker sequence and the aa2–239 of enhanced GFP (EGFP). The UBX-EBV-DUB fusion construct comprised the aa1–128 of YOD1, a GGGS linker sequence and the DUB domain of the EBV large tegument protein BPLF1 (aa1–270). The construct coding catalytically impaired p97 (p97 QQ) was described earlier [11]. Site directed mutagenesis of the EBV-DUB was performed with the QuikChange II mutagenesis kit (Stratagene). The predicted catalytic cysteine residue at position 61 of the original EBV protein BPLF1 was mutated to alanine (C61A), threonine (C61T), serine (C61S), or lysine (C61K). The isoleucine at position 173 and alanine at position 178 were mutated to tryptophane (I173W) and to arginine (A178R), respectively. Maria Masucci provided the Ub-R-GFP and the Ub-G76V-GFP construct. Untagged RI_{332} was a generous gift from N. Erwin Ivessa. The Plasmid pCMV-INSIG-1-Myc was obtained from the American Type Culture Collection (ATCC number 88099). HA-RI_{332} was cloned into pcDNA3.1(+) via *HindIII* and *XbaI* restriction sites. The HA-epitope (YPYDVPDYA) and a GSLE linker sequence were inserted between aa27 and aa28 of the signal sequence.

Pulse-Chase Experiments, Immunoprecipitations, Gel Electrophoresis, Immunoblotting, and Transient Transfections

Pulse chase experiments were performed as previously described [38]. Prior to pulse labeling, the cells were starved for 30 min in methionine/cysteine-free DMEM at 37 °C. Cells were then labeled for 10 min at 37 °C with 250 µCi of [^{35}S]methio-

nine/cysteine (PerkinElmer). De novo protein synthesis was quantitated in a pulse labeling experiment. Where indicated, 50 μM ZL3VS was applied to the cells during the starvation, pulse labeling, and chase period. Incorporated radioactivity was quantified after SDS-mediated cell lysis and TCA precipitation.

Transient transfection, cell lysis, immunoprecipitations and transfections, SDS-PAGE, and fluorography were performed as described earlier [34]. All quantifications were performed on a phosphoimager.

For the protease protection assay cells were homogenized by passing through a 23 × g needle in hypotonic buffer (20 mM Hepes pH 7.5, 5 mM KCl, 5 mM $MgCl_2$, 1 mM DTT, and a protease protection cocktail (Roche)). Proteinase K was added to a final concentration of 100 μg/ml in the presence and absence of 0.5% NP40. After 20 min on ice, the proteinase K was inactivated by inclusion of PMSF (5 mM) and samples were analyzed by SDS-PAGE.

Selective Plasmamembrane Permeabilization and Subcellular Fractionation

For selective permeabilization of the plasmamembrane, cell 293T cells were trypsinized harvested and washed with PBS. Perfringolysin O was added to a final concentration of 0.5 μM at 0 ºC followed by an incubation of the cells at 37 ºC for 15 min to induce pore-formation. Where indicated, the mixture was adjusted to 0.5 M NaCl. Centrifugation (5 min, 9000 × g) separated cytosolic proteins in the supernatant from cellular remnants in the pellet. The pellet was washed with ice-cold PBS and lysed in PBS/1% SDS to solubilize membrane proteins and release organelle contents.

Structural Modeling

Structural modeling is described in Text S1.

Data Analysis and Clustering

Data analysis and clustering are described in the Supporting Information section.

Confocal Microscopy

Cells were grown on coverslips, fixed in 4% paraformaldehyde, quenched with 20 mM glycerine, 50 mM NH_4Cl, and permeabilized in 0.1% Triton X-100 at room temperature. Fixed and permeabilized cells were blocked in 4% BSA and incubated either with anti-HA antibodies (3F10, rat monoclonal, Roche) or anti-PDI (Abcam) antibodies as described [45]. Images were acquired by using a spinning disk confocal microscope, a Nikon 60x magnification, and a 1× numerical aperture oil lens.

Flow Cytometry

Cells were harvested by trypsinization 10 h after addition of proteasome inhibitors and 20 h after transient transfection. Cells were washed and incubated for 30 min at 4 ºC with a LIFE/DEAD cell viability stain (Invitrogen). Subsequently, cells were

washed and fixed with 2% paraformaldehyde. Fluorescence intensity of GFP was measured with LSR I flow cytometer (BD Biosciences). Data were collected with CellQuest (BD Biosciences) and analyzed with FlowJo (Tree Star).

Cell Morphology

Cells were transiently transfected with EBV-DUB WT or empty vector. After 6 h, pharmacological proteasome inhibitors (10 μM MG132 or 10 μM ZL3VS) were applied to the cells. Photographs were taken 20 h post-treatment.

References

1. Reyes-Turcu FE, Ventii KH, Wilkinson KD (2009) Regulation and cellular roles of ubiquitin-specific deubiquitinating enzymes. Annu Rev Bio chem 78: 363-397.
2. Vembar SS, Brodsky JL (2008) One step at a time: endoplasmic reticulum-associated degradation. Nat Rev Mol Cell Biol 9: 944-957.
3. Glickman MH, Ciechanover A (2002) The ubiquitin-proteasome proteolytic pathway: destruction for the sake of construction. Physiol Rev 82: 373-428.
4. Hiller MM, Finger A, Schweiger M, Wolf DH (1996) ER degradation of a misfolded luminal protein by the cytosolic ubiquitin-proteasome pathway. Science 273: 1725-1728.
5. Flierman D, Ye Y, Dai M, Chau V, Rapoport TA (2003) Polyubiquitin serves as a recognition signal, rather than a ratcheting molecule, during retrotranslocation of proteins across the endoplasmic reticulum membrane. J Biol Chem 278: 34774-34782.
6. Ye Y, Meyer HH, Rapoport TA (2001) The AAA ATPase Cdc48/p97 and its partners transport proteins from the ER into the cytosol. Nature 414: 652-656.
7. Ye Y, Meyer HH, Rapoport TA (2003) Function of the p97-Ufd1-Npl4 complex in retrotranslocation from the ER to the cytosol: dual recognition of nonubiquitinated polypeptide segments and polyubiquitin chains. J Cell Biol 162: 71-84.
8. Ikeda Y, Demartino GN, Brown MS, Lee JN, Goldstein JL, et al. (2009) Regulated endoplasmic reticulum-associated degradation of a polytopic protein: p97 recruits proteasomes to Insig-1 before extraction from membranes. J Biol Chem 284: 34889-34900.
9. Crosas B, Hanna J, Kirkpatrick DS, Zhang DP, Tone Y, et al. (2006) Ubiquitin chains are remodeled at the proteasome by opposing ubiquitin ligase and

deubiquitinating activities. Cell 127: 1401-1413.
10. Rumpf S, Jentsch S (2006) Functional division of substrate processing cofactors of the ubiquitin-selective Cdc48 chaperone. Mol Cell 21: 261-269.
11. Ernst R, Mueller B, Ploegh HL, Schlieker C (2009) The otubain YOD1 is a deubiquitinating enzyme that associates with p97 to facilitate protein dislocation from the ER. Mol Cell 36: 28-38.
12. Sowa ME, Bennett EJ, Gygi SP, Harper JW (2009) Defining the human deubiquitinating enzyme interaction landscape. Cell 138: 389-403.
13. Lee BH, Lee MJ, Park S, Oh DC, Elsasser S, et al. (2010) Enhancement of proteasome activity by a small-molecule inhibitor of USP14. Nature 467: 179-184.
14. Pickart CM, Cohen RE (2004) Proteasomes and their kin: proteases in the machine age. Nat Rev Mol Cell Biol 5: 177-187.
15. Leggett DS, Hanna J, Borodovsky A, Crosas B, Schmidt M, et al. (2002) Multiple associated proteins regulate proteasome structure and function. Mol Cell 10: 495-507.
16. Schlieker C, Korbel GA, Kattenhorn LM, Ploegh HL (2005) A deubiquitinating activity is conserved in the large tegument protein of the herpesviridae. J Virol 79: 15582-15585.
17. Borodovsky A, Kessler BM, Casagrande R, Overkleeft HS, Wilkinson KD, et al. (2001) A novel active site-directed probe specific for deubiquitylating enzymes reveals proteasome association of USP14. Embo J 20: 5187-5196.
18. Gastaldello S, Hildebrand S, Faridani O, Callegari S, Palmkvist M, et al. (2010) A deneddylase encoded by Epstein-Barr virus promotes viral DNA replication by regulating the activity of cullin-RING ligases. Nat Cell Biol.
19. Komander D, Reyes-Turcu F, Licchesi JD, Odenwaelder P, Wilkinson KD, et al. (2009) Molecular discrimination of structurally equivalent Lys 63-linked and linear polyubiquitin chains. EMBO Rep 10: 466-473.
20. Whitehurst CB, Ning S, Bentz GL, Dufour F, Gershburg E, et al. (2009) The Epstein-Barr virus (EBV) deubiquitinating enzyme BPLF1 reduces EBV ribonucleotide reductase activity. J Virol 83: 4345-4353.
21. Xu P, Duong DM, Seyfried NT, Cheng D, Xie Y, et al. (2009) Quantitative proteomics reveals the function of unconventional ubiquitin chains in proteasomal degradation. Cell 137: 133-145.
22. Kerscher O, Felberbaum R, Hochstrasser M (2006) Modification of proteins by ubiquitin and ubiquitin-like proteins. Annu Rev Cell Dev Biol 22: 159-180.
23. Peth A, Uchiki T, Goldberg AL (2010) ATP-dependent steps in the binding of

ubiquitin conjugates to the 26S proteasome that commit to degradation. Mol Cell 40: 671-681.

24. Saeki Y, Kudo T, Sone T, Kikuchi Y, Yokosawa H, et al. (2009) Lysine 63-linked polyubiquitin chain may serve as a targeting signal for the 26S proteasome. EMBO J 28: 359-371.
25. Dantuma NP, Lindsten K, Glas R, Jellne M, Masucci MG (2000) Short-lived green fluorescent proteins for quantifying ubiquitin/proteasome-dependent proteolysis in living cells. Nat Biotechnol 18: 538-543.
26. Bachmair A, Finley D, Varshavsky A (1986) In vivo half-life of a protein is a function of its amino-terminal residue. Science 234: 179-186.
27. Johnson ES, Ma PC, Ota IM, Varshavsky A (1995) A proteolytic pathway that recognizes ubiquitin as a degradation signal. J Biol Chem 270: 17442-17456.
28. Groll M, Heinemeyer W, Jager S, Ullrich T, Bochtler M, et al. (1999) The catalytic sites of 20S proteasomes and their role in subunit maturation: a mutational and crystallographic study. Proc Natl Acad Sci U S A 96: 10976-10983.
29. Wang Q, Li L, Ye Y (2008) Inhibition of p97-dependent protein degradation by Eeyarestatin I. J Biol Chem 283: 7445-7454.
30. Ding Q, Dimayuga E, Markesbery WR, Keller JN (2006) Proteasome inhibition induces reversible impairments in protein synthesis. FASEB J 20: 1055-1063.
31. Mazroui R, Di Marco S, Kaufman RJ, Gallouzi IE (2007) Inhibition of the ubiquitin-proteasome system induces stress granule formation. Mol Biol Cell 18: 2603-2618.
32. Hideshima T, Richardson P, Chauhan D, Palombella VJ, Elliott PJ, et al. (2001) The proteasome inhibitor PS-341 inhibits growth, induces apoptosis, and overcomes drug resistance in human multiple myeloma cells. Cancer Res 61: 3071-3076.
33. de Virgilio M, Weninger H, Ivessa NE (1998) Ubiquitination is required for the retro-translocation of a short-lived luminal endoplasmic reticulum glycoprotein to the cytosol for degradation by the proteasome. J Biol Chem 273: 9734-9743.
34. Mueller B, Lilley BN, Ploegh HL (2006) SEL1L, the homologue of yeast Hrd3p, is involved in protein dislocation from the mammalian ER. J Cell Biol 175: 261-270.
35. Hirsch C, Blom D, Ploegh HL (2003) A role for N-glycanase in the cytosolic

turnover of glycoproteins. EMBO J 22: 1036-1046.
36. Mancini R, Fagioli C, Fra AM, Maggioni C, Sitia R (2000) Degradation of unassembled soluble Ig subunits by cytosolic proteasomes: evidence that retrotranslocation and degradation are coupled events. FASEB J 14: 769-778.
37. Yang T, Espenshade PJ, Wright ME, Yabe D, Gong Y, et al. (2002) Crucial step in cholesterol homeostasis: sterols promote binding of SCAP to INSIG-1, a membrane protein that facilitates retention of SREBPs in ER. Cell 110: 489-500.
38. Wiertz EJ, Jones TR, Sun L, Bogyo M, Geuze HJ, et al. (1996) The human cytomegalovirus US11 gene product dislocates MHC class I heavy chains from the endoplasmic reticulum to the cytosol. Cell 84: 769-779.
39. Waheed AA, Shimada Y, Heijnen HF, Nakamura M, Inomata M, et al. (2001) Selective binding of perfringolysin O derivative to cholesterol-rich membrane microdomains (rafts). Proc Natl Acad Sci U S A 98: 4926-4931.
40. Christianson JC, Shaler TA, Tyler RE, Kopito RR (2008) OS-9 and GRP94 deliver mutant alpha1-antitrypsin to the Hrd1-SEL1L ubiquitin ligase complex for ERAD. Nat Cell Biol 10: 272-282.
41. Cross BC, McKibbin C, Callan AC, Roboti P, Piacenti M, et al. (2009) Eeyarestatin I inhibits Sec61-mediated protein translocation at the endoplasmic reticulum. J Cell Sci 122: 4393-4400.
42. Fiebiger E, Hirsch C, Vyas JM, Gordon E, Ploegh HL, et al. (2004) Dissection of the dislocation pathway for type I membrane proteins with a new small molecule inhibitor, eeyarestatin. Mol Biol Cell 15: 1635-1646.
43. Appenzeller-Herzog C, Ellgaard L (2008) The human PDI family: versatility packed into a single fold. Biochim Biophys Acta 1783: 535-548.
44. Hirsch C, Gauss R, Horn SC, Neuber O, Sommer T (2009) The ubiquitylation machinery of the endoplasmic reticulum. Nature 458: 453-460.
45. Mueller B, Klemm EJ, Spooner E, Claessen JH, Ploegh HL (2008) SEL1L nucleates a protein complex required for dislocation of misfolded glycoproteins. Proc Natl Acad Sci U S A 105: 12325-12330.
46. Tasaki T, Kwon YT (2007) The mammalian N-end rule pathway: new insights into its components and physiological roles. Trends Biochem Sci 32: 520-528.
47. Leznicki P, Clancy A, Schwappach B, High S (2010) Bat3 promotes the membrane integration of tail-anchored proteins. J Cell Sci.
48. Plath K, Rapoport TA (2000) Spontaneous release of cytosolic proteins from posttranslational substrates before their transport into the endoplasmic

reticulum. J Cell Biol 151: 167-178.
49. Mariappan M, Li X, Stefanovic S, Sharma A, Mateja A, et al. (2010) A ribosome-associating factor chaperones tail-anchored membrane proteins. Nature 466: 1120-1124.
50. Jin L, Williamson A, Banerjee S, Philipp I, Rape M (2008) Mechanism of ubiquitin-chain formation by the human anaphase-promoting complex. Cell 133: 653-665.
51. Swaminathan S, Amerik AY, Hochstrasser M (1999) The Doa4 deubiquitinating enzyme is required for ubiquitin homeostasis in yeast. Mol Biol Cell 10: 2583-2594.
52. Patrick GN, Bingol B, Weld HA, Schuman EM (2003) Ubiquitin-mediated proteasome activity is required for agonist-induced endocytosis of GluRs. Curr Biol 13: 2073-2081.
53. Elsasser S, Finley D (2005) Delivery of ubiquitinated substrates to protein-unfolding machines. Nat Cell Biol 7: 742-749.
54. Richly H, Rape M, Braun S, Rumpf S, Hoege C, et al. (2005) A series of ubiquitin binding factors connects CDC48/p97 to substrate multiubiquitylation and proteasomal targeting. Cell 120: 73-84.
55. Gerega A, Rockel B, Peters J, Tamura T, Baumeister W, et al. (2005) VAT, the thermoplasma homolog of mammalian p97/VCP, is an N domain-regulated protein unfoldase. J Biol Chem 280: 42856-42862.
56. Wang Q, Li L, Ye Y (2006) Regulation of retrotranslocation by p97-associated deubiquitinating enzyme ataxin-3. J Cell Biol 174: 963-971.
57. Alexandru G, Graumann J, Smith GT, Kolawa NJ, Fang R, et al. (2008) UBXD7 binds multiple ubiquitin ligases and implicates p97 in HIF1alpha turnover. Cell 134: 804-816.
58. Wang Q, Mora-Jensen H, Weniger MA, Perez-Galan P, Wolford C, et al. (2009) ERAD inhibitors integrate ER stress with an epigenetic mechanism to activate BH3-only protein NOXA in cancer cells. Proc Natl Acad Sci U S A 106: 2200-2205.
59. Koen YM, Hanzlik RP (2002) Identification of seven proteins in the endoplasmic reticulum as targets for reactive metabolites of bromobenzene. Chem Res Toxicol 15: 699-706.
60. Lau SS, Monks TJ, Gillette JR (1984) Multiple reactive metabolites derived from bromobenzene. Drug Metab Dispos 12: 291-296.
61. Hinson JA, Roberts DW (1992) Role of covalent and noncovalent interactions in cell toxicity: effects on proteins. Annu Rev Pharmacol Toxicol 32: 471-

510.
62. Minami R, Hayakawa A, Kagawa H, Yanagi Y, Yokosawa H, et al. (2010) BAG-6 is essential for selective elimination of defective proteasomal substrates. J Cell Biol 190: 637-650.
63. Lilley BN, Ploegh HL (2005) Multiprotein complexes that link dislocation, ubiquitination, and extraction of misfolded proteins from the endoplasmic reticulum membrane. Proc Natl Acad Sci U S A 102: 14296-14301.

Supporting Information

Material and Methods

Structural Modeling

Model coordinates of EBV-DUB were generated using the X-ray structure of M48USP as template (pdb code 2J7Q) after aligning the two sequences in ClustalW (23% sequence identity). MODELLER [1] was used for threading and subsequent refinement with molecular dynamics using simulated annealing. Model quality was assessed using QMEAN [2] and WHATCHECK [3], both showing reliable modeling within the enzyme core region. Ub was docked manually to the EBV-DUB and *in silico* mutations assessed for probable interference with Ub binding. Refined models of mutant EBV-DUB were created using the same procedure as for WT EBV-DUB.

Data Analysis and Clustering.

In order to reduce the number of false positive hits we applied a set of stringent rules: 1) All candidates for which only redundant peptides (peptides that could not be assigned to one specific protein) were excluded (3.6 % of total). 2) All non-human candidates (e.g. rabbit immunoglobulin) were excluded (0.7 % of total). 3) Nonspecifically bound proteins retrieved from cells not expressing RI_{332} were excluded (16.7 % of total). 4) Candidates for which less than nine unique peptides could be detected were excluded (64 % of total). 5) Candidates that had only two-fold or less higher peptides counts upon inhibition of dislocation/degradation as compared to unperturbed dislocation/degradation (YOD1 WT, YOD1 DZnf C160S, and UBX-EBV I173W cells) were excluded (10.6 % of total). By applying this very stringent set of rules, we reduced the number of candidate interactors from 836 to 33 (**SOM T1**). Several subunits of the TRiC complex/CCT (Chaperonin containing TCP1) and the ATPase subunit 1 of the 26S proteasome were identified in the final

list of candidate proteins (**Su T1**). As these proteins are part of known protein complexes, all peptides derived from subunits of these complexes were considered for further analysis. The final list of candidates was arranged according to their normalized interaction matrix into three groups via K-means clustering (similarity metric: euclidean distance) using the Cluster 3.0 software [4]

References

1. Sali A, Blundell TL (1993) Comparative protein modelling by satisfaction of spatial restraints. J Mol Biol 234: 779-815.
2. Benkert P, Tosatto SC, Schomburg D (2008) QMEAN: A comprehensive scoring function for model quality assessment. Proteins 71: 261-277.
3. Hooft RW, Vriend G, Sander C, Abola EE (1996) Errors in protein structures. Nature 381: 272.
4. de Hoon MJ, Imoto S, Nolan J, Miyano S (2004) Open source clustering software. Bioinformatics 20: 1453-1454.

Name	Swiss-Prot	MNOP / % Coverage	MNOP taken from	Function	Local
IAP-2	Q13490	22/31	YOD1 C160S	E3/Apo	Cyt
XIAP	P98170	50/66	YOD1 C160S	E3/Apo	Cyt
BAT3/	P46379	27/23	UBX EBV WT	F/QC	Cyt
CALR/ Calreticulin	P27797	21/25	Eeyarestatin-I	F/QC	ER
TCP1, subunit 2	P78371	16/28	UBX EBV WT	F/QC	Cyt
TCP1, subunit 3	P49368	15/28	UBX EBV WT	F/QC	Cyt
TCP1, subunit 4	P50991	15/23	UBX EBV WT	F/QC	Cyt
TCP1, subunit 5	P48643	10/19	UBX EBV WT	F/QC	Cyt
TCP1, subunit 8	P50990	19/38	UBX EBV WT	F/QC	Cyt
CHPF2/ Chondroitin polymerizing factor	Q9P2E5	13/20	P97QQ	ECM	
DNAJC10/ ERdj5	Q8IXB1	12/11	Eeyarestatin-I	F/QC	ER
DNAJC3/ P58IPK	Q13217	20/41	YOD1 C160S	F/QC	ER
EXT2/ Exostosin-2	Q93063	17/29	YOD1 C160S	ECM	
HIF1A/ HIF-1-alpha	Q16665	17/19	Eeyarestatin-I	SIG	Cyt
HLA-A2	P01892	11/22	YOD1 C160S	AP	ER
HSP90B1/ GRP94/ Endoplasmin	P14625	39/34	YOD1 C160S	QC	ER
HTRA2/ Serine proteinase OMI	O43464	11/12	P97 QQ / YOD1 C160S	Apo	Cyt
KRT1/ Keratin, type II cytoskeletal 1	P04264	9/13	YOD1 C160S	IF	Cyt
NOMO3/ Nodal modulator 3	P69849	10/11	YOD1 C160S	SIG	ER
NUP210/ Nucleoporin 210	Q8TEM1	38/21	YOD1 C160S	NPC	
OS9/ Protein OS-9	Q13438	23/24	P97 QQ	QC	ER
PDIA3/ ERp57/ GRP58	P30101	100/44	Eeyarestatin-I	F/QC	ER
PDIA1/Protein disulfide-isomerase	P07237	54/43	Eeyarestatin-I	F/QC	ER
PDIA4/ ERp72	P13667	95/41	Eeyarestatin-I	F/QC	ER
PDIA6/ ERp5/ TXNDC7	Q15084	48/28	Eeyarestatin-I	F/QC	ER
PLOD1/ Lysyl hydroxylase 1	Q02809	17/28	YOD1 C160S	ECM	ER
Proteasome 26S subunit ATPase 1	P62191	9/24	ZL3VS	UPS/QC	Cyt
SEL1L/ Protein sel-1 homolog 1	Q9UBV2	38/36	YOD1 C160S	QC	ER
Tetratricopeptide repeat domain 13	Q8NBP0	9/13	YOD1 C160S		
E3 ubiquitin-protein ligase UBR4	Q5T4S7	14/4	UBX EBV WT	UPS/E3	Cyt
E3 ubiquitin-protein ligase UBR5	O95071	25/13	YOD1 C160S	UPS/E3	Cyt
UGGT2	Q9NYU1	23/16	YOD1 C160S	QC	ER
VCP/p97 26S ATPase subunit 1	P55072	9/24	P97 QQ	UPS/QC	Cyt

Table S1. Interactome of RI_{332}. List of proteins exhibiting enriched interaction with RI_{332} when protein degradation and/or dislocation were blocked by different means (listed in Figure 4). The table gives the protein/gene names, Swiss-Prot accession number, the number of peptides that could be identified under optimal conditions in an LC/MS/MS experiment, the conditions under which the MNOP was observed, and the resulting sequence coverage.

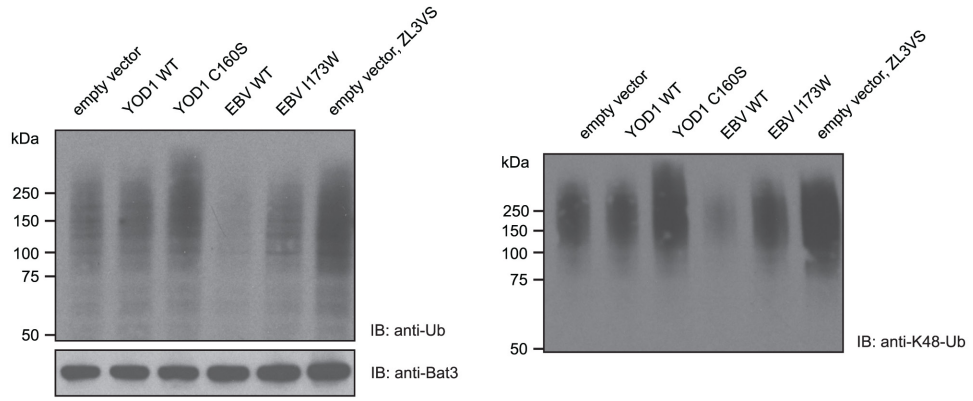

Figure S1. EBV-DUB switches the cellular ubiquitylation balance towards deubiquitylation. 293T cells were transfected as indicated and immunobloted with anti-Ub (left panel) and anti-K_{48}-Ub antibodies (right panel). An immunoblot with anti-BAT3 antibodies serves as loading control. Where indicated, cells were treated for 1 h with 50 μM ZL3VS.

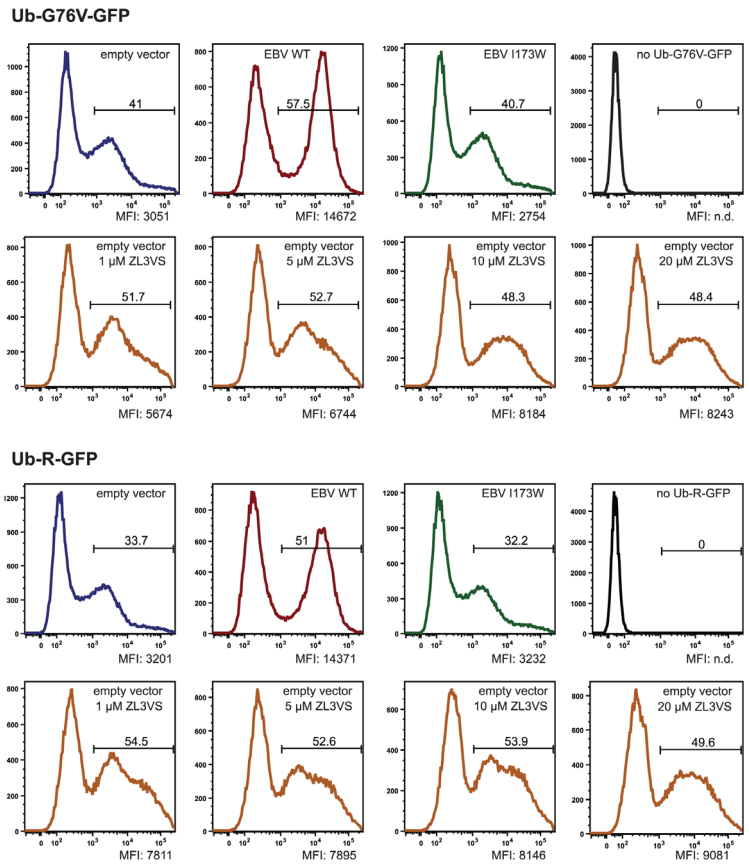

Figure S2. EBV-DUB blocks proteasomal degradation of Ub-G76V-GFP and Ub-R-GFP. Flow-cytometric analysis of 293T cells treated and co-transfected as indicated. The gate was set to identify GFP-positive, live cells. The fraction of GFP-positive cells is given for each panel. Quantified is the median fluorescence intensity (MFI) of GFP-positive cells. Where indicated, the cells were treated with ZL3VS for 10 hrs prior to formaldehyde-fixation.

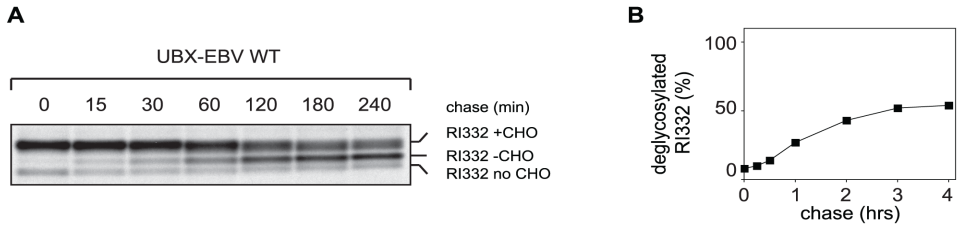

Figure S3. EBV-DUB uncouples dislocation and degradation. 293T cells were co-transfected with RI_{332} and UBX-EBV WT and subjected to a pulse chase experiment. After indicated time points, RI_{332} was immunoprecipitated, subjected to SDS-PAGE and quantified. The fraction of deglycolated RI_{332} (RI332 -CHO) was determined and plotted versus the chase time (right panel).

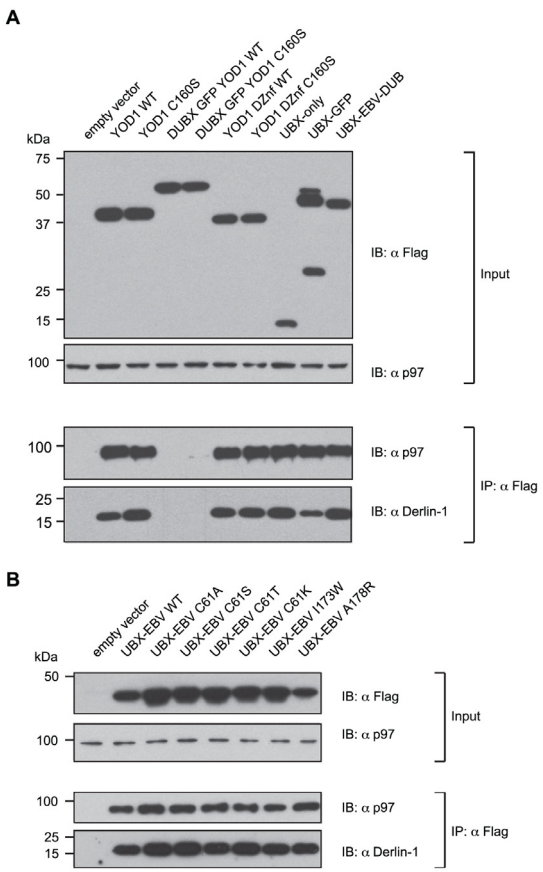

Figure S4. EBV-DUB can be targeted to p97 by N-terminal attachment of an UBX domain. (**A**) 293T cells were transiently transfected with the indicated constructs and homogenized in NP40-containing lysis buffer 24 hrs after transfection. To control for expression of YOD1 variants and chimeric fusions of the YOD1 UBX-domain to GFP and the EBV-DUB the lysates were subjected to immunoblotting with anti-FLAG antibodies. Anti-p97 antibodies were used to control for equal loading (two upper panels). Retrieved p97 and Derlin-1 from anti-FLAG immunoprecipitates was detected by immunoblotting with anti-p97 and anti-Derlin-1 antibodies, respectively (lower panels). (**B**) 293T cells were transiently transfected with the indicated constructs. Cell lysates were prepared as in (A). Retrieved p97 and Derlin-1 in anti-FLAG immunoprecipitates was detected by immunoblotting with anti-p97 and anti-Derlin-1 antibodies, respectively (lower panels). The numbers on the left of individual figures represent the molecular weight standard in kDa.

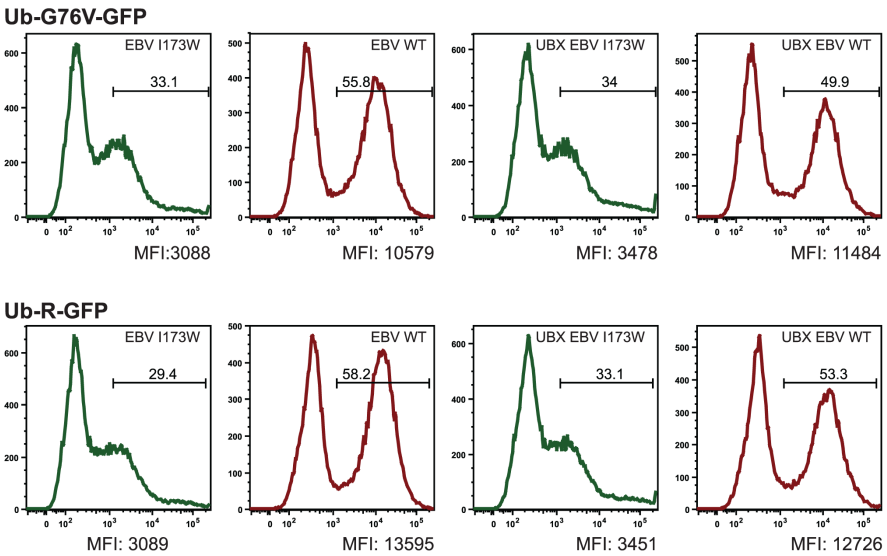

Figure S5. EBV-DUB and the p97-targeted UBX-EBV-DUB block degradation of cytosolic substrates. Flow-cytometric analysis of 293T cells treated and co-transfected as indicated. The gate was set to identify GFP-positive, live cells. The fraction of GFP-positive cells is given for each panel. Quantified is the median fluorescence intensity (MFI) of GFP-positive cells.

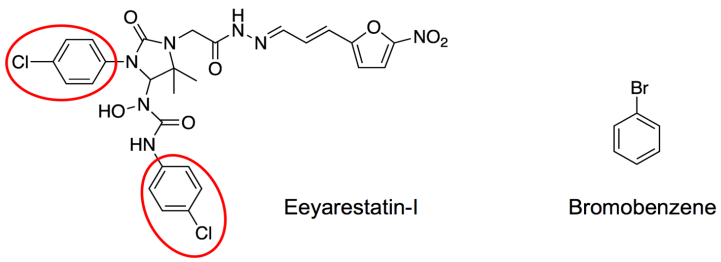

Figure S6. Structural formulas of eeyarestatin-I and bromobenzene. The two halogenated benzene rings of eeyarestatin-I are highlighted with red ellipses.

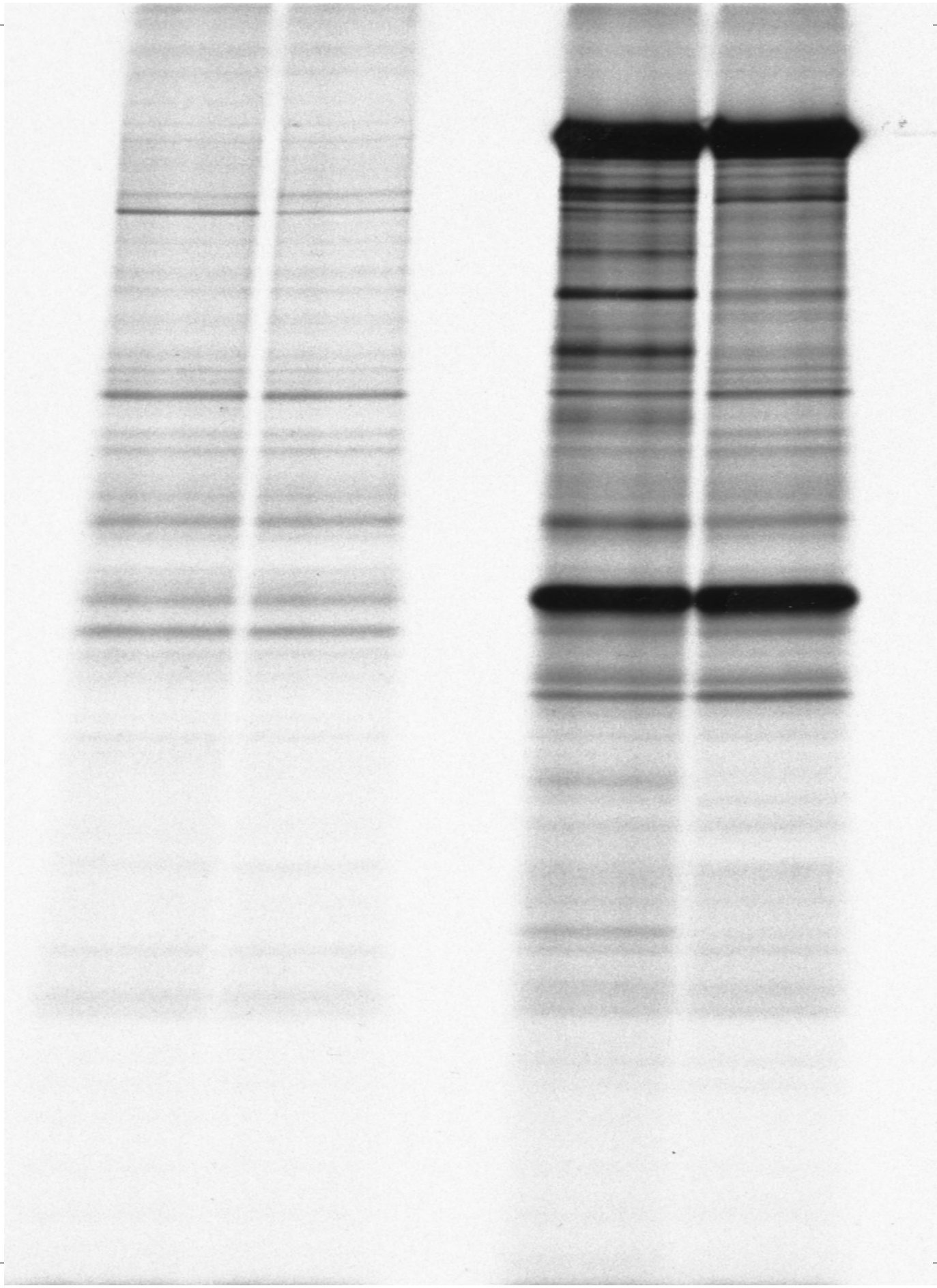

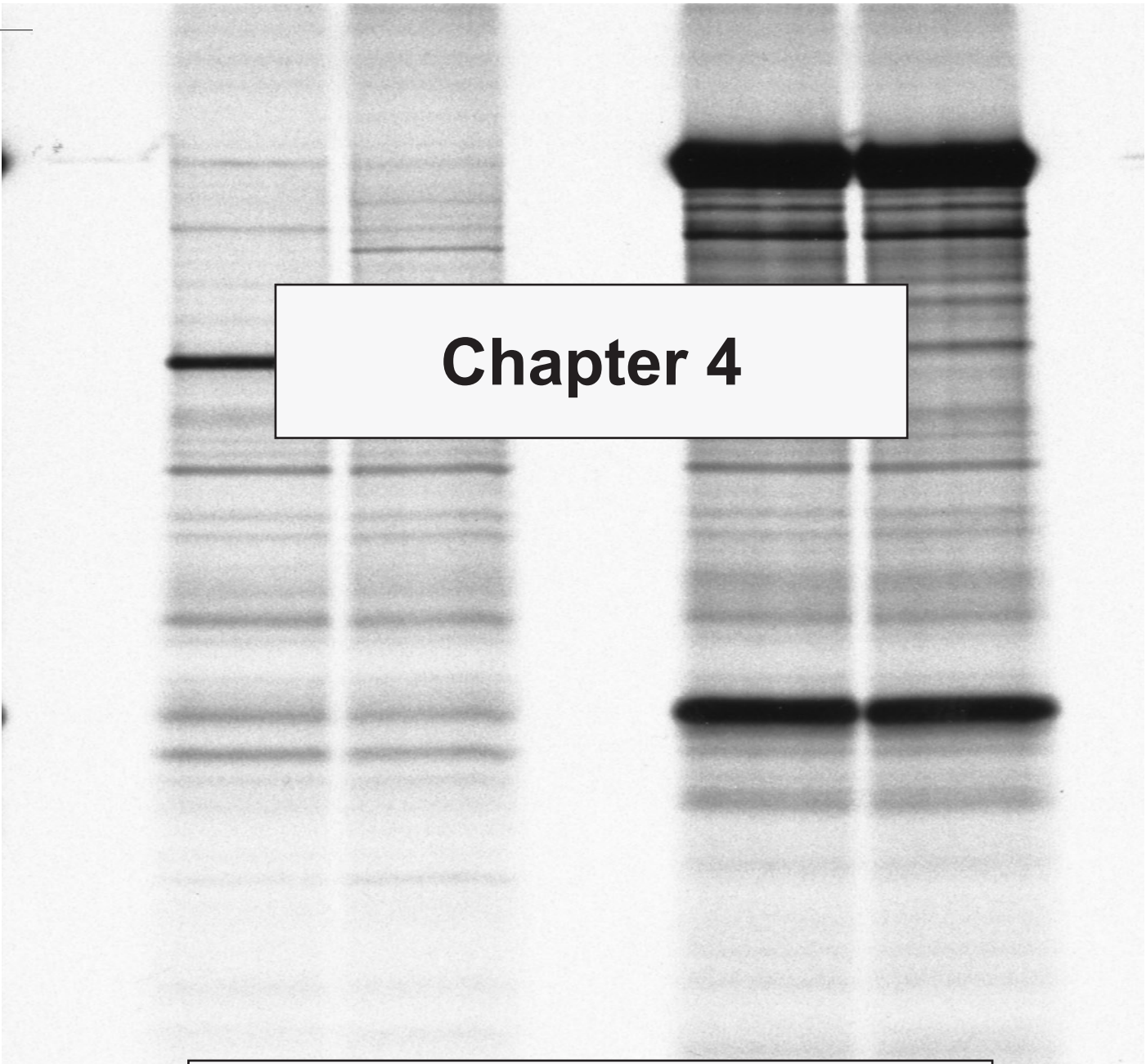

Chapter 4

BAT3 Guides Misfolded Glycoproteins Out of the Endoplasmic Reticulum

Jasper H.L. Claessen, Hidde L. Ploegh

Whitehead Institute for Biomedical Research, Department of Biology, Massachusetts Institute of Technology, Cambridge, Massachusetts, USA

Abstract

Secretory and membrane proteins that fail to acquire their native conformation within the lumen of the Endoplasmic Reticulum (ER) are usually targeted for ubiquitin-dependent degradation by the proteasome. How partially folded polypeptides are kept from aggregation once ejected from the ER into the cytosol is not known. We show that BAT3, a cytosolic chaperone, is recruited to the site of dislocation through its interaction with Derlin2. Furthermore, we observe cytoplasmic BAT3 in a complex with a polypeptide that originates in the ER as a glycoprotein, an interaction that depends on the cytosolic disposition of both, visualized even in the absence of proteasomal inhibition. Cells depleted of BAT3 fail to degrade an established dislocation substrate. We thus implicate a cytosolic chaperone as an active participant in the dislocation of ER glycoproteins.

Introduction

Protein folding in the endoplasmic reticulum (ER) is an inherently fallible process. Terminally misfolded ER glycoproteins leave the folding cycle and are often targeted for dislocation to the cytosol, followed by ubiquitin-dependent degradation by the proteasome (reviewed in [1]). Many ER luminal proteins have been identified that are involved in shuttling misfolded polypeptides to the hypothesized dislocon, the identity and composition of which remain to be defined more fully in molecular terms. BiP, OS-9, XTB3-B, PDI, and members of the EDEM family are thought to target the polypeptide to the dislocon [1]. At the same time they help maintain solubility to prevent detrimental build-up of aggregated, misfolded translation products inside the ER lumen [2].

Unfolded polypeptides interact with chaperones to prevent exposure of hydrophobic amino acids or putative transmembrane domains prior to the completion of protein folding or membrane insertion, cotranslational protein translocation into the ER being a prime example [3]. Misfolded ER glycoproteins exit from the ER in a process called dislocation (or retrotranslocation) [4,5]. Although different modes of escape have been proposed, a conserved dislocation reaction that involves polyubiquitylation, followed by extraction by the dedicated AAA ATPase p97, operates in both yeast and mammals [6,7,8]. Misfolded proteins that undergo dislocation almost certainly display features of a partly unfolded polypeptide. The definition of dimensional restrictions imposed by the putative dislocon must await its more complete molecular characterization. In any case, polypeptides that are fed into p97 AAA ATPase, as well as those entering the proteolytic core of the proteasome require complete unfolding [9,10,11].

How the cell avoids aggregation of ER glycoproteins discharged into the cytosol is poorly understood. When proteasomal proteolysis is blocked, a soluble version of Class I MHC products -bona-fide type I membrane proteins- occurs in the cytoplasm of cells that express viral immunoevasins, with the transmembrane segment, normally inserted into a lipid bilayer, fully intact [4,5]. Tight coupling between proteasomal proteolysis and dislocation may prevent exposure of transmembrane segments to an aqueous environment, or perhaps chaperones temporarily shield such segments until the proteasome (or an other protease) can be engaged.
We previously showed that expression of a highly active, Epstein-Barr virus-derived deubiquitylating enzyme domain (EBV-DUB) blocks proteasomal degradation

of cytosolic and ER-derived proteins by preemptive removal of ubiquitin from proteasome substrates [12]. Upon EBV-DUB expression, a misfolded ER glycoprotein accumulates in association with the cytosolic chaperone BAT3 (BAG6/Scythe) as a deglycosylated cytosolic intermediate [12].
We now place BAT3 in the extraction pathway for ER glycoproteins. We find that it associates with Derlin2 at the ER membrane and engages misfolded ER proteins, whereas depletion of BAT3 hampers their degradation. We thus assign a role for a cytosolic chaperone in the dislocation reaction. While these experiments were in progress, Ye and colleagues [13] published data fully consistent with the earlier proposal that cytosolic chaperones associate with cytoplasmic dislocation products [12] and our observations agree with this report [13].

Results

BAT3 associates with Derlin2

Dislocation and degradation of ER glycoproteins can be uncoupled by expression of a highly active DUB. The misfolded ER luminal glycoprotein truncated Ribophorin I (Ri332) accumulates in the cytosol as a deglycosylated dislocation intermediate when expressed together with the EBV-DUB [12]. Because this deglycosylated species accumulated in association with BAT3, we investigated whether BAT3 merely serves as a buffer for dislocation substrates stalled in the cytoplasm to maintain them in disaggregated form, or whether BAT3 plays an active role in the dislocation reaction itself.
To validate the observed interaction, we first reproduced it in an *in vitro* setting. Ri332 was synthesized in an *in vitro* translation system and retrieved by an immunoprecipitation reaction after mild lysis. BAT3 was readily retrieved in complex with Ri332, but this interaction was not observed when translation was carried out in the presence of microsomal membranes (Figure 1A). Under these conditions Ri332 was translocated into the lumen of the microsomes, as indicated by cleavage of its signal sequence. This indicates that the observed interaction between Ri332 and BAT3 depends on the cytosolic disposition of both interacting partners.
BAT3 could still be involved in the dislocation reaction when in close proximity to the ER membrane, because at least some of the dislocation intermediate observed upon expression of the EBV-DUB remains loosely associated with the ER membrane [12]. We therefore examined whether BAT3 engages any of the known dislocation components that localize to the ER membrane. We readily retrieved BAT3 in

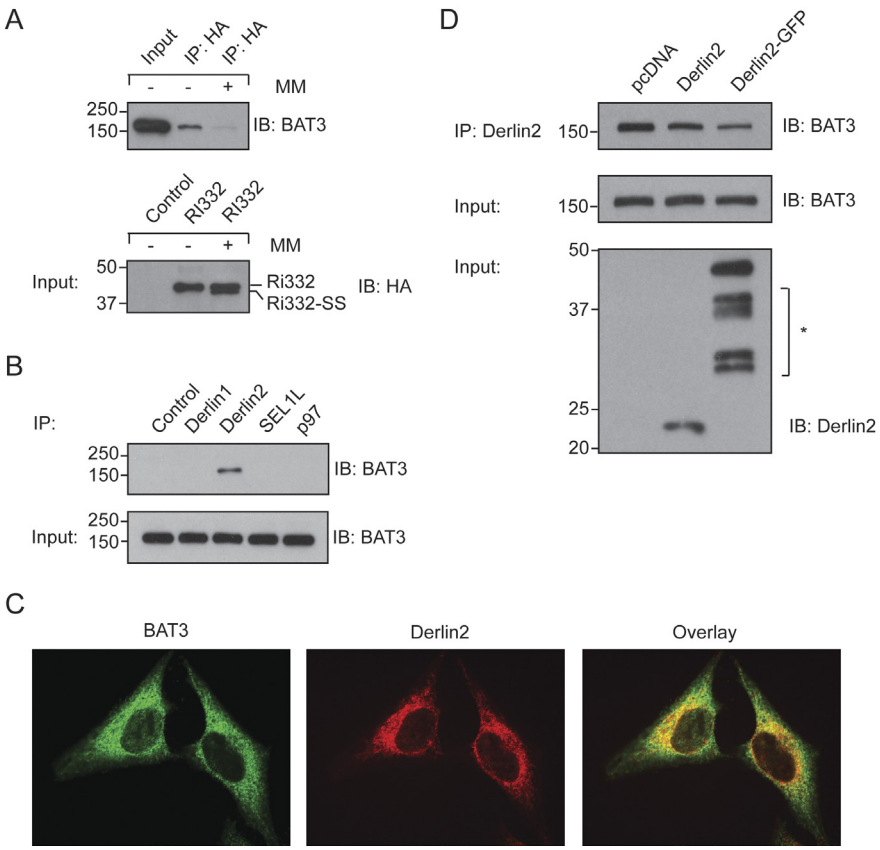

Figure 1. BAT3 associates with Derlin2.

(A) HA-Ri332 was synthesized in a rabbit reticulocyte lysate in the presence or absence of canine pancreatic microsomal membranes (MM). Following NP40-mediated lysis, Ri332 was retrieved by immunoprecipitation. The immunoprecipitate and input samples were blotted for either BAT3 or HA as indicated. (B) 293T cells were subjected to NP40 lysis, followed by retrieval of the indicated proteins. Pre-immune serum served as a control. The eluates were blotted for BAT3, as were the input control samples. (C) Immunofluorescence of Hela cells using antibodies against endogenous BAT3 (green) and Derlin2 (red). Scale bar = 5µm. (D) 293T cells were transiently transfected with the indicated constructs, subjected to NP40 lysis followed by an immunoprecipitation for Derlin2. Immunoprecipitates were blotted for BAT3. Input samples were blotted for BAT3 and Derlin2. The asterisk indicates non-specific polypeptides.

association with Derlin2, a small membrane protein implicated in ER quality control (Figure 1B) [14,15].

Although BAT3 is reported to localize to the nucleus [16], we demonstrated additional co-localization with Derlin2 by immunofluorescence microscopy (Figure 1C), in line with assigned roles for BAT3 in the cytosol [13,17]. In order to characterize this interaction further, we examined the consequences of overexpression of

Derlin2. The stoichiometry of multi-protein complexes can be disturbed by over-expression of one of its components. We recovered a reduced amount of BAT3 upon overexpression of Derlin2, and we observed an even more obvious reduction when we overexpressed a Derlin2-GFP fusion protein (Figure 1D). The latter effect we ascribe to the bulk of the appended GFP moiety, which would sterically hinder these interactions.
We conclude that BAT3 can interact with a dislocation substrate and that it is recruited to the site of dislocation through interactions with Derlin2, although our data do not distinguish between direct and indirect interactions. Of note, members of the Derlin family have been speculated to form a channel that facilitates passage of misfolded polypeptides from the lumen of the ER across the ER membrane to the cytoplasm [18,19].

Visualizing a dislocation complex

Having shown interactions between BAT3 and Ri332, and between BAT3 and Derlin2, we set out to visualize these complexes by microscopy. As Ri332 is rapidly destroyed, we reasoned that we could best visualize any such complex by inhibiting degradation. To this end, we interfered with degradation by expression of a dominant negative version of YOD1 (YOD1 C160S) [20] or the EBV protease domain targeted to p97 (UBX-EBV) [12].
Hela cells were transiently transfected with Ri332, upon which the various types of blockade were imposed. After fixation, cells were permeabilized and triple-labeled for Ri332 (HA), Derlin2 and BAT3. We directed our attention to cells with a strong signal for the dislocation substrate, as an indication of successful inhibition of degradation.
In control cells, we observed clear co-localization of Ri332, BAT3 and Derlin2 (white color) consistent with the notion that BAT3 can engage a misfolded ER luminal glycoprotein at the site of dislocation (Figure 2A).
Irrespective of the type of blockade imposed, we see near complete co-localization between Ri332 and BAT3 (Figure 2B, C). Ri332 is thought to accumulate partly if not mostly inside the ER lumen when degradation is blocked. However, if stalled dislocation substrates were to accumulate at the luminal site of dislocation, such localization would result in the observed staining pattern. Under conditions of ongoing proteasomal proteolysis, Ri332 does not accumulate in such complexes, because its levels rapidly drop due to proteasomal activity. We conclude that BAT3 localizes to a dislocation substrate at the site of a dedicated dislocation component.

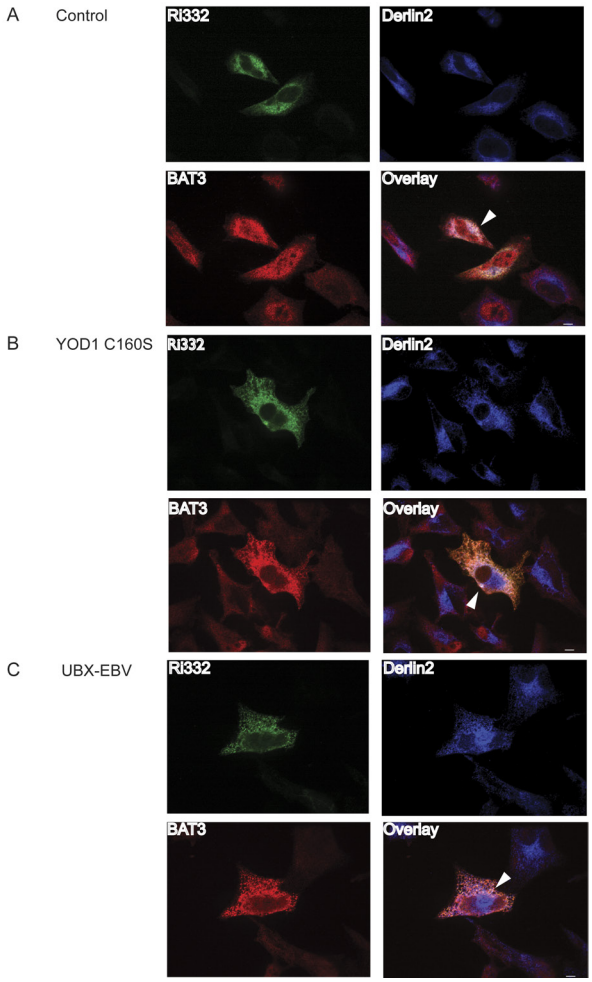

Figure 2. BAT3 localizes to a complex with Derlin2 and Ri332. Hela cells were plated on coverslips and transiently transfected with HA-Ri332 and empty vector (A), YOD1 C160S (B) or UBX-EBV (C). After paraformaldehyde fixation, cells were labeled for HA (green), BAT3 (red), and Derlin2 (blue). Scale bar = 5μm.

BAT3 is required for dislocation of TCRα

Having shown that BAT3 can associate with a misfolded, dislocated ER glycoprotein in vitro and that BAT3 can occur in a complex with both the degradation substrate and Derlin2 when proteasomal degradation is inhibited, we examined whether there was a direct requirement for BAT3 in the dislocation reaction itself. We performed a BAT3 knock-down in 293T cells through stable expression of a short RNA hairpin against BAT3 (Figure 3A).

Despite the strong knock-down seen for BAT3, we observed at best a modest effect on dislocation of Ri332, as assessed by pulse-chase analysis (Figure 3B). This by no means excludes a role for BAT3 in dislocation of Ri332, as redundancy through the existence of multiple chaperone complexes is not unlikely. The observed effect on Ri332 stands in sharp contrast to the effect observed when we tested the role of BAT3 in dislocation of the alpha chain of the T-cell receptor (TCR**α**), which undergoes rapid degradation when expressed in the absence of its usual receptor partner subunits. Knock-down of BAT3 resulted in near complete stabilization of TCR**α** in a pulse-chase experiment (Figure 3C).

Of interest, TCR**α** carries four N-linked glycans, which are rapidly removed by

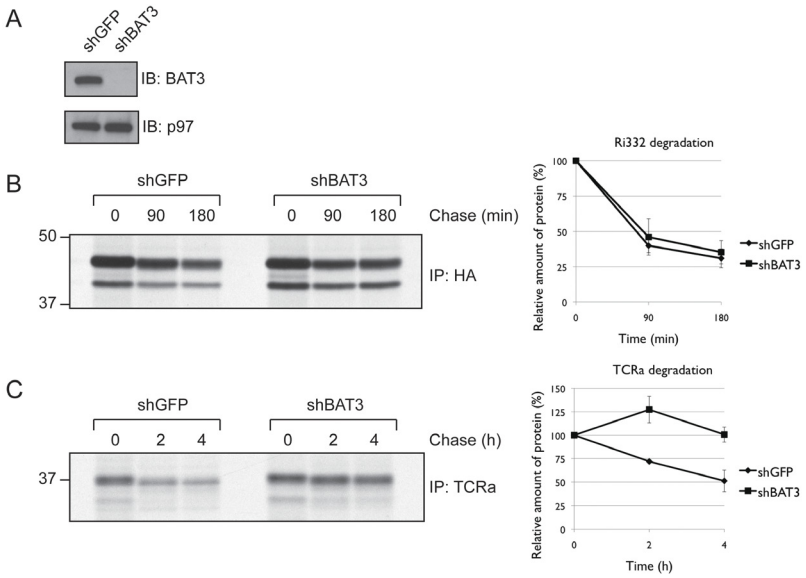

Figure 3. BAT3 is required for dislocation of TCRα.
(A) 293T were stably transduced with short RNA hairpins against either GFP or BAT3. SDS lysates were immunoblotted for either BAT3 or p97. (B) BAT3 knock-down cells (a) were transiently transfected with HA-Ri332 and subjected to pulse-chase analysis. Densitometric quantitation of the relative amount of protein is shown (n=9). (C) As in (B), except that cells were transfected with TCRα (n=3).

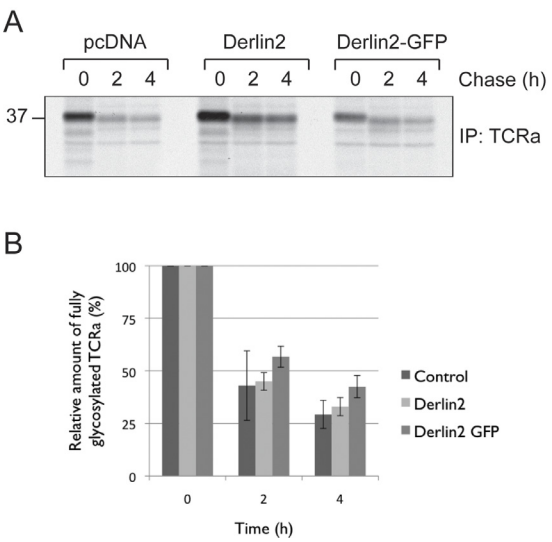

Figure 4. Impaired BAT3 recruitment to Derlin2 slows dislocation.
(A) 293T cells were transiently transfected with TCRα and either pcDNA, Derlin2, or Derlin2-GFP (see figure 1D). TCR**α** degradation was assessed by pulse-chase analysis. (B) Densitometric quantitation of the relative amount of protein is shown (n=4).

cytoplasmic peptide N-glycanase when it is successfully discharged in the cytosol [21]. As TCRa accumulates predominantly as the fully glycosylated version, the absence of BAT3 hampers the active removal of TCRa from the ER membrane.

Disrupted BAT3 binding by Derlin2 slows TCRα degradation

Having established a role for BAT3 in the degradation of TCR**α**, we wondered whether this could be correlated with its recruitment by Derlin2. As overexpression of Derlin2, and more so Derlin2-GFP, frustrated its interaction with BAT3, (Figure 1D) we tested whether this had any consequences for TCR**α** degradation. TCR**α** degradation is reduced in cells that overexpress Derlin2-GFP (Figure 4). The stabilization we observed is modest but in agreement with the continued, but reduced, binding of BAT3 to Derlin2-GFP we discussed above. Members of the Derlin family can form homo- and hetero-dimers, which could overcome, at least in part, the steric hindrance imposed by the bulky GFP molecule used as fusion partner [14].

TCRα is engaged by BAT3

Can we capture directly the interaction between BAT3 and TCR**α**? When degradation is allowed to proceed unperturbed, dislocation is tightly coupled to degradation of the substrate, making this a rather transient interaction. We transiently transfected 293T cells with TCR**α** and labeled them to steady state with [^{35}S] cysteine/methionine (overnight labeling). The lysate was precleared with pre-immune serum, followed by immunoprecipitation for TCR**α** to retrieve any interacting proteins. The immunoprecipitate was then dissolved in 1% SDS at 37 degrees Celsius and subjected to a second round of immunoprecipitation to interrogate the complex for the presence of the indicated proteins.
We could retrieve endogenous BAT3 from the TCR**α** immunoprecipitate, thus visualizing this transient interaction (Figure 5, lane 4). The visualized TCR**α** (lane 1) does not represent the population that can interact with BAT3, as the indicated polypeptide for TCR**α** represents fully glycosylated and thus ER-localized TCR**α**. It is likely that the dislocated population of TCR**α** escapes detection due to low signal levels or as a consequence of the sequential immunoprecipitation. In addition to BAT3, we also retrieved p97 in complex with TCR**α** (lane 5). This hexameric AAA ATPase is thought to provide the mechanical force that extracts proteins from the ER and it has been implicated in the dislocation of TCR**α**, thus validating the retrieval of BAT3 [11].

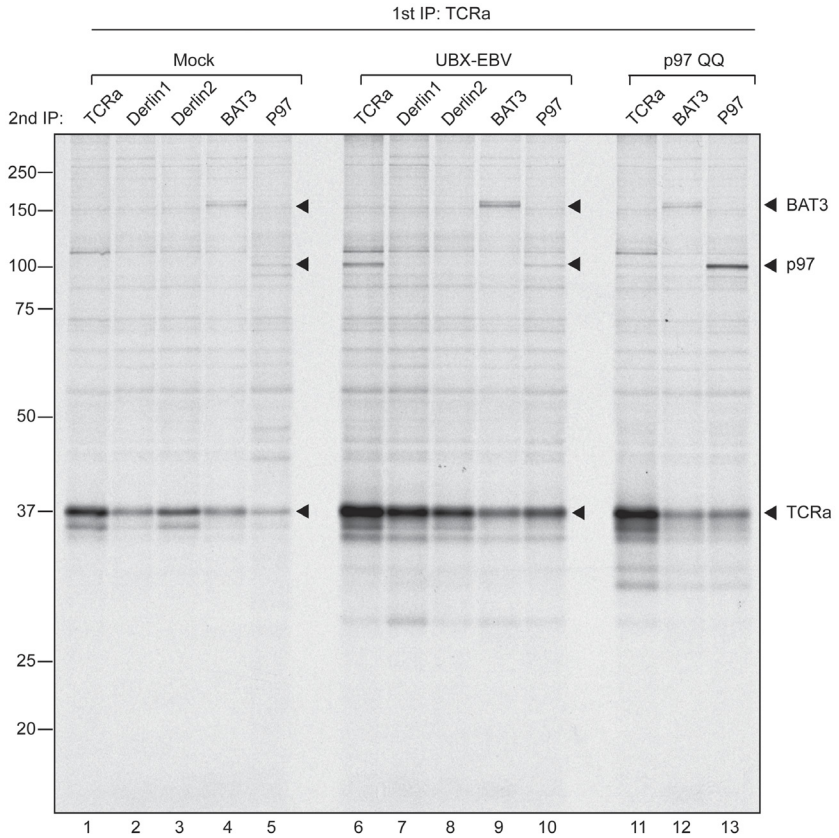

Figure 5. TCRα is engaged by BAT3

293T cells were transiently transfected with TCRα and either empty vector, UBX-EBV, or p97 QQ, and labeled overnight with [35S] methionine/cysteine to achieve steady state labeling. Cells were harvested and subjected to NP40 lysis. The lysates were precleared using pre-immune serum and immobilized protein A. Lysates were adjusted for total levels of incorporated isotope and subjected to immunoprecipitation for TCRα. The captured protein was eluted in 1% SDS at 37°C followed by a second immunoprecipitation for the indicated proteins.

As a control, we performed the same experiment in cells that were co-transfected with TCR**α** and either UBX-EBV or p97 QQ. We showed previously that co-expression of UBX-EBV stabilizes the degradation of TCR**α** and leads to the accumulation of a deglycosylated dislocation intermediate [12]. In line with this observation, we retrieve more TCR**α** overall (lane 6 versus 1) and more BAT3 specifically (lane 9 versus 4). The p97 QQ mutations render inactive the ATPase activity of the protein, but still allow it to engage a substrate [22]. Accordingly, when we co-expressed p97 QQ we retrieved more TCR**α** overall (lane 11 versus 1) and more p97 specifically (lane 13 versus 5). Co-expression of UBX-EBV as well as p97 QQ

results in higher levels of TCR**α**, as either membrane extraction, or delivery to the proteasome is blocked. However, only when TCR**α** is co-expressed with UBX-EBV do we retrieve more endogenous BAT3, ruling out a post-lysis interaction.
We note that two BAT3 species of distinct molecular weight are recovered in association with TCR**α**. Several isoforms of the protein have been annotated, and we retrieve at least two of them in association with a dislocation substrate.

Discussion

Proteins expelled from the ER by dislocation are likely to be at least partially unfolded, although an assessment of their true conformational state remains an obvious challenge. Unless tight coupling exists between dislocation and degradation, these (partly) unfolded polypeptides are exposed to an aqueous environment and are prone to aggregation. The latter applies *a fortiori* when considering membrane proteins such as Class I MHC products, one of the few examples for which there is evidence of a soluble cytoplasmic intermediate with its TM segment present and intact [4]. We show here that the cytoplasmic chaperone BAT3 is recruited to Derlin2 at the ER membrane, can engage ER glycoproteins that are subject to dislocation, and that BAT3 is required for dislocation of TCR**α**.

A disruption of proteasomal degradation not only halts breakdown of ER-derived proteins, but often leads to their accumulation within the ER lumen. This is complemented by the requirement for poly-ubiquitylation to complete the dislocation reaction, giving rise to the idea that dislocation of a substrate is mostly tightly coupled to its degradation. Examples exist where such coupling is undone, for instance the Human Cytomegalovirus proteins US11 and US2, both of which funnel Class I MHC heavy chains into a dislocation pathway, and result in accumulation of the heavy chain in the cytoplasm when proteasomal proteolysis is blocked. We showed that in the presence of the EBV-DUB, ER-derived glycoproteins accumulate in the cytoplasm but are not degraded [12]. Even though these ER proteins accumulate in the cytoplasm, it is unclear how they are maintained in a soluble state once there. The cytoplasm contains folding machinery that prevents protein aggregation. HSC70 and HSP90, and their heat-shock induced counterparts, are examples of chaperones that engage (partly) unfolded polypeptides in the cytoplasm. Even though these chaperones have been linked to ER protein maturation and dislocation (reviewed in [23]), particularly for the example of HSC70 and its involvement in

dislocation of the misfolded cystic fibrosis transmembrane conductance regulator DF508 [24], it remains to be established whether they play a direct role in dislocation and bridge the gap between the chaperone-rich ER lumen and the proteasome.
BAT3 has a role in the degradation of defective polypeptides synthesized at the ribosome, and may shuttle such substrates to the proteasome [25,26]. We now show that BAT3 engages defective ER proteins discharged from the ER, and that BAT3 and its interactors accumulate as a complex when proteasomeal targeting is blocked by expression of the EBV-DUB.

Derlin2 is a small ER membrane protein. Members of the Derlin family have all been implicated in dislocation and may form part of a putative channel (dislocon) that facilitates the passage of misfolded ER proteins to the cytoplasm [14,15,18,19]. We now find that BAT3 interacts with Derlin2 and associates with at least a select set of misfolded proteins. BAT3 is at the nucleus of a protein complex that shields the hydrophobic transmembrane domain of tail-anchored (TA) proteins after ribosomal synthesis and prior to engagement by a dedicated ER-targeting chaperone [17,27]. BAT3 could perform a similar task for unfolded ER proteins at a dislocation channel, especially when such substrates contain a hydrophobic transmembrane stretch. Similarly, BAT3 was found to sequester mis-targeted proteins from the translocon [26].
Upon depletion of BAT3, the dislocation substrate TCR**α** accumulates primarily inside the ER lumen (Figure 3C). As BAT3 can function as a co-chaperone recruiter, the interactions we observe most likely occur in the context of a multi-protein complex. In fact, the BAT3-nucleated complex responsible for capturing TA proteins fresh off the ribosome has recently been implicated in protein dislocation [13].
Even though Derlin2 occurs in a complex with both Derlin1 and SEL1L [14], we retrieve BAT3 exclusively with Derlin2 in our immunoprecipitation experiments (Figure 1B). The choice of detergent may contribute to this selectivity: BAT3 may well associate with other components of the dislocation machinery, or the complex may simply not be sufficiently stable to allow retrieval of all of its constituents.
There are two moments during the dislocation process at which a chaperone like BAT3 could be of importance. The first moment is after complete extraction of the polypeptide by p97, but prior to its degradation. We can capture dislocation intermediates at this stage by expression of the EBV-DUB and observe increased association of TCR**α** with BAT3 under these conditions. In addition, BAT3 associates with the proteasome [25], opening the possibility that it shuttles dislocated proteins

to the proteasome, akin to proteasomal shuttling factors such as RAD23 [28]. The second moment is prior to substrate engagement by p97. P97 can engage a protein ready for extraction through its cofactors UFD1 and NPL4, both of which recruit p97 to poly-ubiquitylated proteins [6,7,8]. However, the active domains of the E2 and E3 enzymes responsible for substrate ubiquitylation face the cytoplasmic side of the ER. Ubiquitin conjugation to the polypeptide chain thus requires the substrate to at least peek out of the ER prior to engagement of p97. This window is then extended, as substrates require de-ubiquitylation prior to their full extraction from the ER so they may pass through the central pore of p97 [20]. It is at this moment that chaperone activity could be required to allow a smooth exit from the ER and prevent a blockade induced by exposed hydrophobic domains.

Materials and methods

Antibodies, Cell Lines, Constructs, and Reagents

Antibodies to Derlin1, Derlin2, SEL1L, p97 and TCR**α** have been described [14,18,21]. Antibodies against the hemagglutinin (HA) epitope tag were purchased from Roche (3F10), antibodies against BAT3 were obtained from Abcam (ab88292).

HEK293T and Hela cells were purchased from American Type Culture Collection. Cells were cultured in Dulbecco's modified Eagle's medium (DMEM), cells transduced with pLKO.1-based vectors were selected and maintained in 1μg/ml puromycin (Invitrogen).

The Derlin2, Derlin2-GFP, HA-Ri332, p97, and TCR**α** constructs used for transfection experiments have all been described [12,14]. Short RNA hairpins against either GFP or BAT3 in pLKO.1 vectors were obtained from Open Biosystems.

In vitro transcription translation, Transient Transfection, and Viral Transduction

In vitro transciption translation essays were performed in Rabbit Reticulocyte Lysate obtained from Promega (TnT T7), as were canine microsomal membranes. Hela cells were transiently transfected using Fugene (Roche), and 293T cells using Trans-IT (Takara Mirus Bio), according to the manufacturer's instructions. Virus production in 293T cells and viral transduction have been described [29].

Immunoprecipitations, Pulse-Chase Experiments, and SDS-PAGE

Cells were lysed in NP40 lysis buffer (0.5% NP40, 10mM Tris-HCl, 150mM NaCl, 5mM $MgCl_2$, pH7.4) supplemented with a complete protease inhibitor cocktail (Roche) and 2.5mM N-Ethylmaleimide. The immunoprecipiation was performed us-

ing 30μl of immobilized rProtein A (IPA 300, Repligen) with the relevant antibodies, or with 12μl anti-HA Affinity Matrix (3F10, Roche), for 3h at 4°C with gentle agitation. The lysates were normalized to relative protein concentration prior to incubation with antibodies.

To achieve steady-state protein labeling, cells were incubated overnight with 500mCi of [^{35}S]methionine/cysteine (Perkin Elmer) in methionine/cysteine-free DMEM supplemented with 10% dialyzed IFS at 37°C.

Pulse-chase experiments were performed as described [30]. In short, prior to pulse labeling, the cells were starved for 45 min in methionine/cysteine-free DMEM at 37°C. Cells were then labeled for 10 min at 37°C with 250mCi of [^{35}S] methionine/cysteine. Incorporated radioactivity was quantified after lysis and TCA precipitation. Target protein was isolated through immunoprecipitation, and immune complexes were eluted by boiling in reducing sample buffer, subjected to SDS-PAGE (10%), and visualized by autoradiography. Densitometric quantification of radioactivity was performed on a PhosphorImager (Fujifilm BAS-2500) using Image Reader BAS-2500 V1.8 software (Fujifilm) and Multi Gauge V2.2 (Fujifilm) software for analysis.

Immunoblotting

For immunoblot analysis, cell lysates were prepared by solubilizing cells in 1% SDS. Protein concentrations of the lysates were determined using the BCA assay (Pierce), and equivalent amounts of total cellular protein were used for immunoblotting.

Confocal Microscopy

Cells were grown on coverslips, fixed in 4% paraformaldehyde, quenched with 20mM glycine, 50mM NH_4Cl, and permeablized in 0.05% Saponin (Sigma) at room temperature. All succeeding steps are performed in the presence of 0.05% Saponin. Fixed and permeablized cells were blocked in 4% BSA and incubated either with anti-HA-Fluorescein (Roche), anti-BAT3, anti-Derlin2 or a combination thereof. Fluorophore-conjugated antibodies were obtained from Molecular Probes (Invitrogen). Images were acquired using a spinning disk confocal microscope, a Nikon 60x magnification, and a 1x numerical aperture oil lens.

References

1. Bagola K, Mehnert M, Jarosch E, Sommer T (2011) Protein dislocation from the ER. Biochim Biophys Acta 1808: 925-936.
2. Ron D, Walter P (2007) Signal integration in the endoplasmic reticulum unfolded

protein response. Nat Rev Mol Cell Biol 8: 519-529.
3. Rapoport TA (2007) Protein translocation across the eukaryotic endoplasmic reticulum and bacterial plasma membranes. Nature 450: 663-669.
4. Wiertz EJ, Jones TR, Sun L, Bogyo M, Geuze HJ, et al. (1996) The human cytomegalovirus US11 gene product dislocates MHC class I heavy chains from the endoplasmic reticulum to the cytosol. Cell 84: 769-779.
5. Wiertz EJ, Tortorella D, Bogyo M, Yu J, Mothes W, et al. (1996) Sec61-mediated transfer of a membrane protein from the endoplasmic reticulum to the proteasome for destruction. Nature 384: 432-438.
6. Ye Y, Meyer HH, Rapoport TA (2001) The AAA ATPase Cdc48/p97 and its partners transport proteins from the ER into the cytosol. Nature 414: 652-656.
7. Jarosch E, Taxis C, Volkwein C, Bordallo J, Finley D, et al. (2002) Protein dislocation from the ER requires polyubiquitination and the AAA-ATPase Cdc48. Nat Cell Biol 4: 134-139.
8. Braun S, Matuschewski K, Rape M, Thoms S, Jentsch S (2002) Role of the ubiquitin-selective CDC48(UFD1/NPL4)chaperone (segregase) in ERAD of OLE1 and other substrates. EMBO J 21: 615-621.
9. Finley D (2009) Recognition and processing of ubiquitin-protein conjugates by the proteasome. Annu Rev Biochem 78: 477-513.
10. Navon A, Goldberg AL (2001) Proteins are unfolded on the surface of the ATPase ring before transport into the proteasome. Mol Cell 8: 1339-1349.
11. DeLaBarre B, Christianson JC, Kopito RR, Brunger AT (2006) Central pore residues mediate the p97/VCP activity required for ERAD. Mol Cell 22: 451-462.
12. Ernst R, Claessen JH, Mueller B, Sanyal S, Spooner E, et al. (2011) Enzymatic blockade of the ubiquitin-proteasome pathway. PLoS Biol 8: e1000605.
13. Wang Q, Liu Y, Soetandyo N, Baek K, Hegde R, et al. (2011) A Ubiquitin Ligase-Associated Chaperone Holdase Maintains Polypeptides in Soluble States for Proteasome Degradation. Mol Cell.
14. Lilley BN, Ploegh HL (2005) Multiprotein complexes that link dislocation, ubiquitination, and extraction of misfolded proteins from the endoplasmic reticulum membrane. Proc Natl Acad Sci U S A 102: 14296-14301.
15. Oda Y, Okada T, Yoshida H, Kaufman RJ, Nagata K, et al. (2006) Derlin-2 and Derlin-3 are regulated by the mammalian unfolded protein response and are required for ER-associated degradation. J Cell Biol 172: 383-393.
16. Manchen ST, Hubberstey AV (2001) Human Scythe contains a functional nuclear localization sequence and remains in the nucleus during staurosporine-

induced apoptosis. Biochem Biophys Res Commun 287: 1075-1082.
17. Mariappan M, Li X, Stefanovic S, Sharma A, Mateja A, et al. (2010) A ribosome-associating factor chaperones tail-anchored membrane proteins. Nature 466: 1120-1124.
18. Lilley BN, Ploegh HL (2004) A membrane protein required for dislocation of misfolded proteins from the ER. Nature 429: 834-840.
19. Ye Y, Shibata Y, Yun C, Ron D, Rapoport TA (2004) A membrane protein complex mediates retro-translocation from the ER lumen into the cytosol. Nature 429: 841-847.
20. Ernst R, Mueller B, Ploegh HL, Schlieker C (2009) The otubain YOD1 is a deubiquitinating enzyme that associates with p97 to facilitate protein dislocation from the ER. Mol Cell 36: 28-38.
21. Huppa JB, Ploegh HL (1997) The alpha chain of the T cell antigen receptor is degraded in the cytosol. Immunity 7: 113-122.
22. Ye Y, Meyer HH, Rapoport TA (2003) Function of the p97-Ufd1-Npl4 complex in retrotranslocation from the ER to the cytosol: dual recognition of nonubiquitinated polypeptide segments and polyubiquitin chains. J Cell Biol 162: 71-84.
23. Buchberger A, Bukau B, Sommer T (2010) Protein quality control in the cytosol and the endoplasmic reticulum: brothers in arms. Mol Cell 40: 238-252.
24. Younger JM, Chen L, Ren HY, Rosser MF, Turnbull EL, et al. (2006) Sequential quality-control checkpoints triage misfolded cystic fibrosis transmembrane conductance regulator. Cell 126: 571-582.
25. Minami R, Hayakawa A, Kagawa H, Yanagi Y, Yokosawa H, et al. (2010) BAG-6 is essential for selective elimination of defective proteasomal substrates. J Cell Biol 190: 637-650.
26. Hessa T, Sharma A, Mariappan M, Eshleman HD, Gutierrez E, et al. (2011) Protein targeting and degradation are coupled for elimination of mislocalized proteins. Nature.
27. Leznicki P, Clancy A, Schwappach B, High S (2010) Bat3 promotes the membrane integration of tail-anchored proteins. J Cell Sci 123: 2170-2178.
28. Vembar SS, Brodsky JL (2008) One step at a time: endoplasmic reticulum-associated degradation. Nat Rev Mol Cell Biol 9: 944-957.
29. Soneoka Y, Cannon PM, Ramsdale EE, Griffiths JC, Romano G, et al. (1995) A transient three-plasmid expression system for the production of high titer retroviral vectors. Nucleic Acids Res 23: 628-633.
30. Claessen JH, Mueller B, Spooner E, Pivorunas VL, Ploegh HL (2010) The

transmembrane segment of a tail-anchored protein determines its degradative fate through dislocation from the endoplasmic reticulum. J Biol Chem 285: 20732-20739.

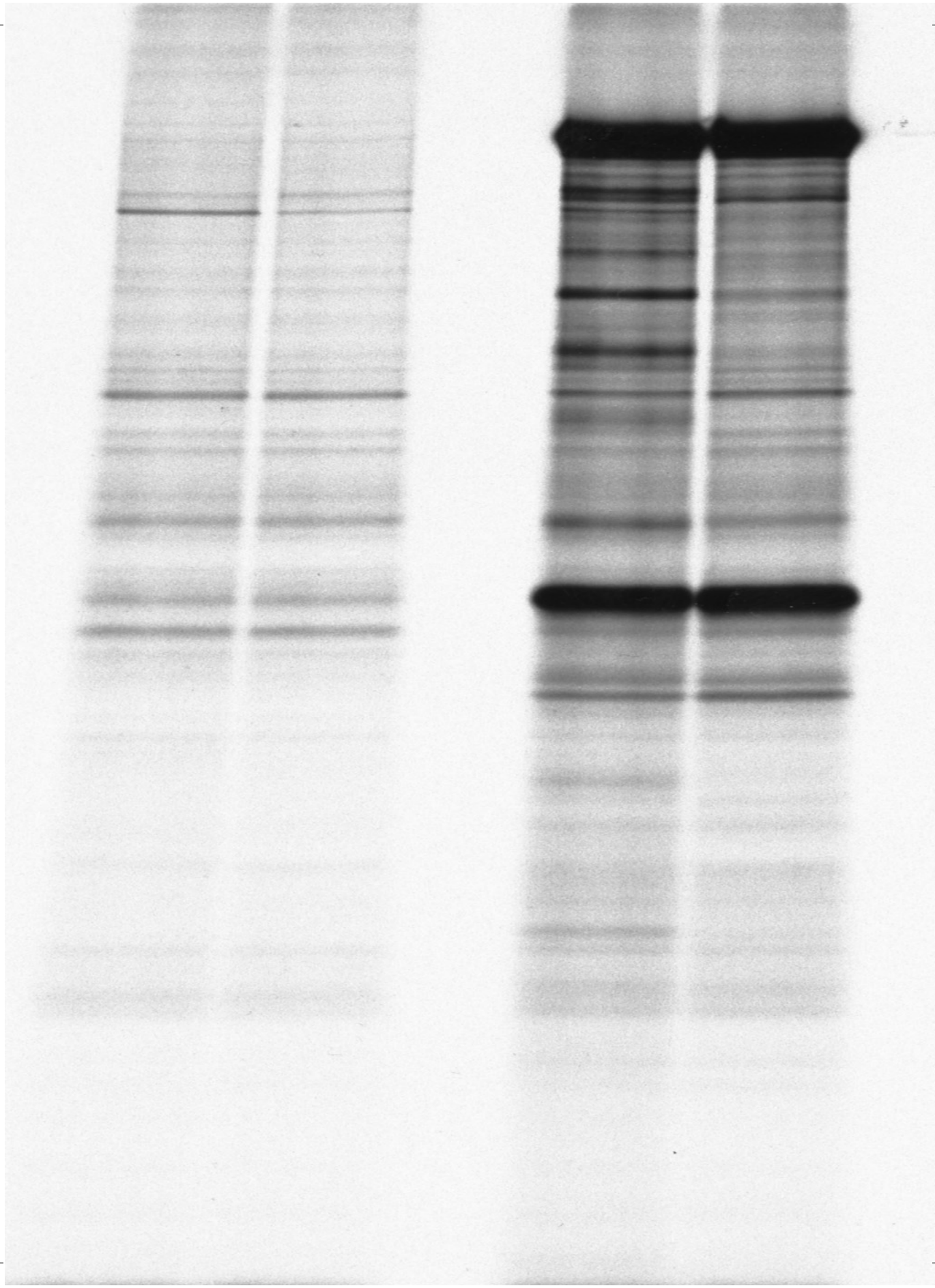

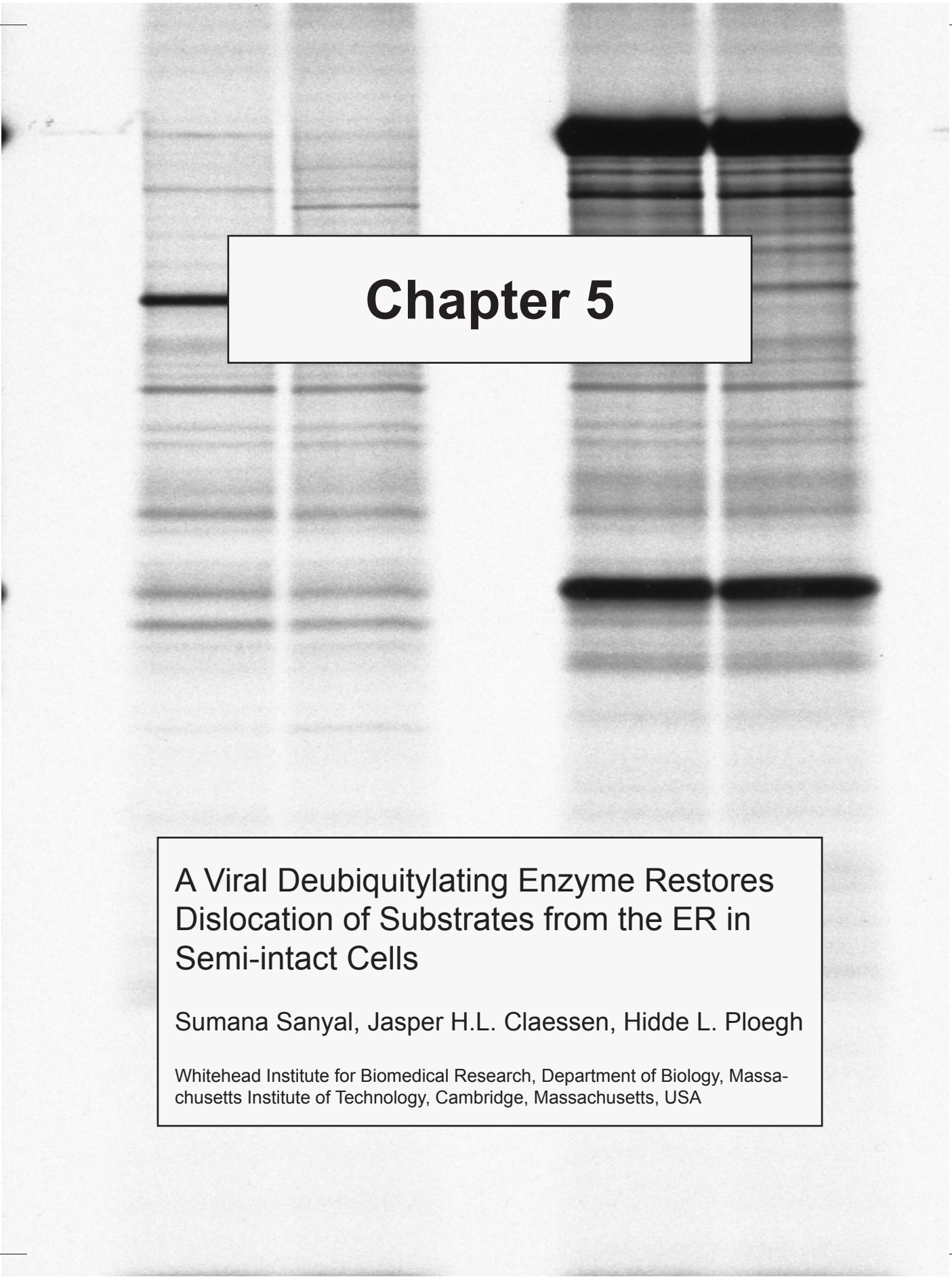

Chapter 5

A Viral Deubiquitylating Enzyme Restores Dislocation of Substrates from the ER in Semi-intact Cells

Sumana Sanyal, Jasper H.L. Claessen, Hidde L. Ploegh

Whitehead Institute for Biomedical Research, Department of Biology, Massachusetts Institute of Technology, Cambridge, Massachusetts, USA

Abstract

Terminally misfolded glycoproteins are ejected from the endoplasmic reticulum (ER) to the cytosol and destroyed by the ubiquitin proteasome system (UPS). A dominant negative version of the deubiquitylating enzyme Yod1 (Yod1C160S) causes accumulation of dislocation substrates in the ER. Failure to remove ubiquitin from the dislocation substrate might therefore stall the reaction at the exit site from the ER. We hypothesized that addition of a promiscuous deubiquitylase (DUB) should overcome this blockade and restore dislocation. We monitored ER-to-cytosol transport of misfolded proteins in cells permeabilized at high cell density by perfringolysin O, a pore-forming cytolysin. This method allows ready access of otherwise impermeant reagents to the intracellular milieu with minimal dilution of cytoplasmic components. We show that addition of the purified Epstein-Barr Virus (EBV) DUB to semi-intact cells indeed initiates dislocation of a stalled substrate intermediate, resulting in stabilization of substrates in the cytosol. Our data provide new mechanistic insight in the dislocation reaction and support a model where failure to deubiquitylate an ER-resident protein occludes the dislocon and causes upstream misfolded intermediates to accumulate.

Introduction

Protein transport across the ER encompasses reactions on both the cytoplasmic and luminal side of the ER membrane. While we understand in considerable detail the structure and modus operandi of components necessary for co-translational transport of nascent polypeptides through the translocon [1], much remains to be learned about the reverse process: protein transport from the ER to the cytoplasm en route to degradation by the ubiquitin-proteasome system (UPS). In eukaryotic cells a fraction of newly synthesized proteins misfolds early during their biogenesis and is degraded. Efficient disposal of defective proteins is essential, since these proteins – even if only partially folded – may compete with their functional counterparts for substrate binding or for complex formation with interaction partners and so exert a dominant-negative effect [2]. Defective secretory and transmembrane proteins likewise present an inherent risk: if released from the cell or exposed at the cell surface, they could interfere with function. Eukaryotic cells therefore must exert stringent quality control over secretory proteins, initiated at their site of synthesis. Terminally misfolded proteins in the ER are recognized and targeted for disposal, mostly in the cytosol. How such proteins traverse the ER membrane to reach the cytosol remains to be established. Several proteins including the Hrd1 E3-ligase [3], Sec61 and members of the Derlin family of proteins have been proposed to form a dislocation channel [4-6] to facilitate export of misfolded substrates across the ER. Alternative non-conventional modes of transport across the ER bilayer have been suggested [7] and challenged [8]. Multiple strategies presumably exist in mammalian cells to facilitate substrate passage into the cytosol, depending on specificity and physical characteristics of the substrates, but currently known pathways mostly converge on degradation by the UPS. How exactly the initial encounter with an appropriate E3 ligase(s) occurs is easily envisioned for an ER-resident protein that spans the membrane and has at least a portion exposed to the cytosolic ubiquitylation machinery, but how a completely luminal degradation substrate engages its cognate Ub ligase(s) is less apparent. Auxiliaries that recognize the misfolded state in the ER lumen presumably direct degradation substrates to the appropriate location [9,10]. A cascade of E1, E2 and E3 activities catalyzes ubiquitylation, a reaction that can be reversed by ubiquitin-specific proteases, of which there are many [11].

The analysis of the mammalian Hrd1-Sel1L ubiquitin E3 ligase complex has uncovered a complex set of functionally important interactors that act downstream of ubiquitylation, amongst which the AAA ATPase p97, and in turn - via p97 - an even

more expansive set of interactors [9,12]. While the role of some proteins in this pathway is clear, the involvement of others is either controversial or lacks experimental support. The confusing and somewhat contradictory data on the involvement of specific proteins reflects the technical challenges - notably the lack of robust in vitro systems - inherent in current approaches to study dislocation.

The ubiquitin-specific protease Yod1 plays a role in clearing the ER of several misfolded substrates [13,14]. Expression of a dominant-negative version of Yod1 (the YodC160S mutant, which lacks catalytic activity) leads to accumulation in the ER of substrates (in their non-ubiquitylated state) that would otherwise have been discharged and destroyed [13]. We hypothesized that a failure to remove ubiquitin from a dislocation substrate en route from the dislocon to the next station in the dislocation pathway would stall the substrate, and so block all further dislocation. We exploited the activity of an Epstein Barr Virus-derived ubiquitin-specific protease domain, excised from its normal sequence context and expressed as the isolated active domain – EBV-DUB – to interfere with ubiquitin-dependent events in protein quality control [15]. To overcome the block imposed by Yod1C160S, we proposed that expression of EBV-DUB protease would remove Ub from substrates targeted for degradation and stabilize them either at the ER membrane or in the cytosol [15]. Expression of EBV-DUB indeed caused an enzymatic blockade of the UPS and resulted in accumulation in the cytosol of intermediates and in the lumen of the ER that would otherwise have been destroyed. The ubiquitylation events that determine extraction from the ER are thus separable from ubiquitylation reactions that target a substrate for proteasomal degradation (Figure 1).
Occlusion of the dislocon by ubiquitylated intermediates and concomitant trapping of other substrates in the ER could account for the effects of expression of dominant negative Yod1, but formal proof for the suggestion is lacking. Alternatively, both the expression of dominant negative Yod1, of EBV-DUB, or the combination of the two might set in motion a program of gene expression that fundamentally alters the molecular composition of the ER and the dislocation machinery. With the above unsolved questions in mind, we have developed an in vitro assay to test the proposed model that stipulates two cycles of ubiquitylation and deubiquitylation to arrive at recognition, extraction and disposal of an ER luminal misfolded protein [9].

Here we test the role of deubiquitylation in this model using an in vitro dislocation assay performed in semi-intact cells. The configuration of this assay not only al-

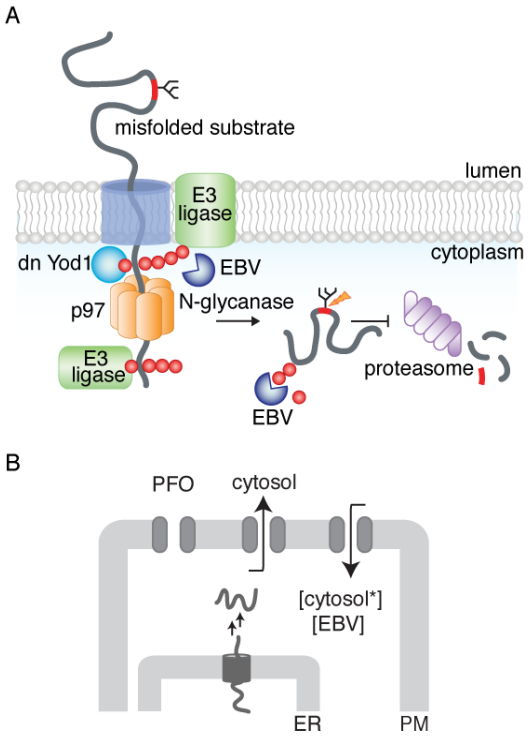

Figure 1. Intracellular protein degradation by the ubiquitin proteasome system
(A) Model for misfolded protein transport from the ER to the cytosol. A terminally misfolded glycoprotein is recognized by luminal chaperones and targeted to a putative channel in the membrane. The partially unfolded substrate is dislocated across the ER bilayer where ubiquitylation occurs through membrane bound ubiquitin ligases, facilitating recruitment of p97. Deubiquitylation by Yod1 facilitates substrate transport through the hexameric AAA-ATPase to reach the cytosol where a second round of ubiquitylation presumably occurs. As depicted in figure, expression of a dominant negative Yod1 (Yod1C160S) arrests polyubiquitylated substrates at the ER membrane. Cytosolic N-glycanase removes the glycan moiety from the substrate, prior to proteasomal degradation. In the presence of soluble EBV-DUB, polyubiquitin chains are removed from the substrate either at the ER membrane or in the cytosol and stabilized. (B) In vitro assay to monitor protein dislocation from the ER to the cytosol in semi-intact cells. Cells with their plasma membrane selectively permeabilized are incubated with concentrated cytosol (cytosol*) and EBV. If deubiquitylation is required for dislocation, addition of EBV to cells with substrates arrested in the ER should resume dislocation from the ER to the cytosol.

lows us to avoid dilution of cytoplasmic components, it also enables manipulation, within certain limits, of the composition of the cytoplasmic environment through osmotic delivery of small molecules and proteins, including active and inactive versions of enzymes such as EBV-DUB or trypsin, as well as ATP and GTP analogs. In order to establish unambiguously the effect of EBV-DUB on cells that express the catalytically inactive Yod1, we created semi-intact cells through treatment with perfringolysin O (PFO), a cholesterol-binding pore-forming toxin. We delivered purified EBV to the cytoplasm of these semi-intact cells by administration of a transient

hypotonic shock, and so directly explored the role of deubiquitylation in the transport of misfolded proteins. Delivery of exogenous EBV-DUB to semi-intact cells loaded with a stalled dislocation substrate released such intermediates from the ER and jump-started delivery to the cytoplasm. Our results provide a new mechanistic insight and direct proof of a key feature of the proposed mechanism of dislocation. Since delivery of exogenous cytosol supports substrate dislocation in semi-intact cells, it should be possible to identify specific cytosolic components that are essential to this process.

Results

PFO mediated selective permeabilization of the plasma membrane

ER protein quality control entails recognition of terminally misfolded proteins through interaction of chaperones, lectins and co-factors [9,10]. Substrates are then targeted to the dislocon, a putative channel of unknown composition, presumably as partially unfolded intermediates. These intermediates undergo a round of ubiquitylation by the Hrd1 E3 ligase complex (or another appropriate E3 ligase complex) for recruitment of downstream dislocation components (p97-Npl4-Ufd1) and subsequent de-ubiquitylation for passage through the p97 hexameric complex [9]. Expression of a dominant negative variant of Yod1 (Yod1C160S), a deubiquitylating enzyme, arrests misfolded substrates in the ER lumen [13] implying that at least a fraction of the accumulated substrate intermediates at the ER membrane must be ubiquitylated. We propose that – once in the cytosol – substrates must undergo a second round of ubiquitylation to engage the proteasome complex. N-glycanase acts on glycoprotein substrates to remove attached N-linked glycan moieties, a reaction apparently dispensable for degradation [19], but experimentally quite informative because of the tell-tale reaction products that are diagnostic for dislocation. Deglycosylated, polyubiquitylated substrates are then targeted to the proteasome and degraded (Figure 1).
Experimental analyses of dislocation have been confounded by the intrinsic properties of the ER membrane, which is easily disrupted by the commonly used homogenization techniques or upon detergent solubilization. Measurements of protein transport from the ER requires a more intact ER structure than is provided by standard homogenization protocols. To this end we devised a PFO-based method [20] of preparing semi-intact cells to monitor protein dislocation, modified by performing the permeabilization step in a minimal volume at high cell density

(Figure 1B). We hypothesized that supplying purified EBV-DUB in the presence of concentrated cytosol to semi-intact cells that harbor a block in dislocation due to Yod1C160S should overcome this barrier and release substrates from the ER to cytosol. The method of creating semi-intact cells through mechanical shearing [21-23] or treatment with Streptolysin O [20,21,23,23] is well-documented and has been successfully used in the past to reconstitute protein transport through the secretory pathway. PFO is a member of the cholesterol-binding family of bacterial

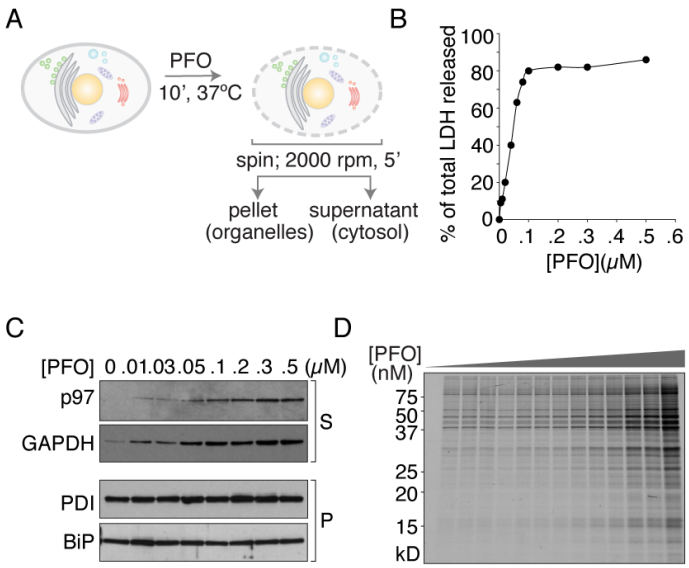

Figure 2. Characterization of PFO-mediated cell-permeabilization

(A) Schematic of Perfringolysin O mediated semi-intact cell preparation. Adherent cells in culture are trypsinized to bring into suspension and treated with 100 nM PFO on ice. Excess unbound PFO is removed by diluting to 1.0 ml, centrifuged (500 x g, 5 min, 4ºC) and incubated at 37ºC after resuspension in 50 µl (0.5X HBSS -/+ exogenous cytosol and EBV) to induce pore formation. After indicated time intervals reaction mixture is centrifuged (500 x g, 5 min, 4ºC) to separate supernatant and pellet fractions, which consist of the cytosol and organelles respectively. (B) Supernatant fractions collected from PFO-treated cells were tested for release of cytosolic LDH activity with increasing concentrations of PFO. (C) The supernatant and pellet fractions were probed for cytosolic and ER luminal marker proteins by immunoblotting to verify proper separation. GAPDH and p97 were measured in the cytosolic fraction; BiP and PDI were used as ER luminal markers and measured in the pellet fractions. As shown, with increasing concentrations of PFO used for permeabilization, the amount of GAPDH and p97 released increases, suggestive of a higher number of pores formed at the plasma membrane. BiP and PDI in the pellet fractions remain constant under all conditions, indicating that the ER integrity is maintained at the PFO concentrations used. (D) [35S]cysteine/methionine labeled cells were subjected to permeabilization with varying PFO concentrations (0, 5, 10, 20, 25, 30, 40, 50, 75, 100, 200, 300, 400 and 500 nM). The supernatants collected were visualized by autoradiography to measure size distribution of materials released from cells as a function of PFO concentration. All experiments were performed atleast twice.

toxins. After binding to the plasma membrane, PFO monomers diffuse laterally in the plane of the bilayer and interact as homotypic aggregates that form large transmembrane pores (diameter ~25 nm [20,21,23,24]. Although PFO binds to the plasma membrane at 0 ºC, perforation requires exposure of PFO-treated cells to 37 ºC. To assay dislocation, we exploit this pore-forming property of PFO (Figure 2A). Confluent HEK293T cells (~1 x 10^7) are harvested by brief trypsinization, washed once with Hank's buffer (HBSS), resuspended in 50 µl of HBSS and maintained on ice. 50 µl of 0.2 µM PFO (in HBSS) is added to the cell suspension and incubated on ice for 5 min to allow binding of the toxin to cholesterol at the plasma membrane without perforating the cells. Excess unbound PFO is then removed by diluting to 1 ml and centrifugation (500 x g for 5 min at 4ºC), followed by incubation of the cell suspension in a minimal volume of 50 µl at 37 ºC for 10 min to initiate pore formation. Supernatant and pellet fractions are then separated by mild centrifugation for 5 min at 500xg. The supernatant fraction contains cytosolic proteins as shown by the dose-dependent increase in released LDH activity (Figure 2B). In addition, the amount of cytosolic GAPDH and p97, enzymes of cytosolic disposition, appear in the supernatant with increasing concentrations of PFO as observed by immunoblotting (Figure 2C). The levels of ER-luminal soluble proteins PDI and BiP remain unchanged in the pellet fraction over this concentration range of PFO, indicating that integrity of the ER membrane is retained. Analysis by SDS-PAGE of the supernatant fraction obtained at different PFO concentrations shows a size distribution of released [^{35}S]cysteine/methionine materials that is independent of PFO concentration, whereas the amount of materials released increases as the PFO concentration is raised (Figure 2D). This observation suggests that the number of pores, but not their size, is a function of PFO concentration. The rate of pore formation is rapid: a time-course of the release of cytosolic contents upon treatment with 0.1 µM PFO reaches a plateau within ~10 minutes and the size of the pores formed is sufficient to allow passage of proteins as large as ~200 kDa (Figure 2D). Cells treated with PFO remain functional in many respects, evident from protein trafficking events along the secretory pathway in semi-intact cells, as measured by glycan maturation of Vesicular Stomatitis Virus glycoprotein (VSV-G). Kinetics of VSV-G trafficking from the ER to the Golgi in semi-intact cells supplemented with ATP and cytosol was monitored by its acquisition of complex-type N-linked glycans, as assessed by digestion of VSV-G with Endoglycosidase H. Samples of VSV-G recovered from PFO-treated and intact cells were identical in this regard. As described below, glycan maturation was blocked in semi-intact cells upon inclusion of non-hydrolysable NTP analogs GTPgS and ATPgS, which are without effect in

intact cells, demonstrating access to the cytosol of cell-impermeant compounds to perforation by PFO. Similarly, in influenza-infected cells we monitored maturation of Neuraminidase (NANase), a type-II membrane glycoprotein and hemagglutinin, and observed no differences in the rates of complex N-linked glycan acquisition for intact and PFO-treated semi-intact cells (unpublished observations).

Substrate dislocation measured in semi-intact cells: appearance of a trypsin sensitive deglycosylated intermediate of RI_{332}

We tested our assay strategy (see schematic in Figure 1B) in HEK293T cells expressing either Yod1C160S or EBV-DUB, starting with a set of substrates commonly used as model misfolded proteins, including both soluble and membrane proteins. As reporters, we used a truncated version of ribophorin (RI_{332}; soluble), T-cell receptor alpha subunit (TCRa; type-I membrane protein) and Class I MHC molecules (type-I membrane protein) in U373 cells that express the US11 immunoevasin from Human Cytomegalovirus (HCMV) as reporters [18].
RI_{332} is a glycoprotein, the majority of which carries a single N-linked glycan, with a minor fraction never receiving its glycan (non-glycosylated) in the ER [15, 25]. Once exported from the ER to the cytosol, the N-linked glycan is removed by cytosolic N-glycanase, resulting in a shift in electrophoretic mobility distinct from that of the non-glycosylated form of RI_{332}. To measure dislocation in semi-intact cells, we treated HEK293T cells that express RI_{332} with 0.1µM PFO and incubated them with concentrated cytosol supplemented with ATP at 37ºC. At the indicated time intervals we separated the pellet and supernatant fractions to probe for RI_{332} by immunoprecipitation. In cells expressing only RI_{332} we observed time-dependent proteasomal degradation (Figure 3A, lanes 3, 4) of RI_{332}, tightly coupled to its export from the ER. Therefore RI_{332} is not detected in the supernatant (cytosolic) fractions in the absence of proteasome inhibitors. In cells transfected with Yod1C160S, all RI_{332} remains in the ER lumen due to blocked dislocation [13,13], and hence we find RI_{332} in the pellet fraction in its glycosylated form (lanes 5-8). In contrast, co-transfection with EBV-DUB stabilizes RI_{332} in either one of two stages [15]: a fraction of RI_{332} is arrested in the ER membrane due to removal of ubiquitin required for substrate engagement by p97-Ufd1-Npl4. The fraction dislocated into the cytosol is deglycosylated, but not degraded, because the cytosolic fraction of RI_{332} lacks the polyubiquitin tag essential for proteasomal degradation [15,15]. Indeed, deglycosylated RI_{332} appears in the cytosol at 90 mins (lanes 9-12). The accumulation of the deglycosylated intermediate is similar to what we observe when proteasomal activ

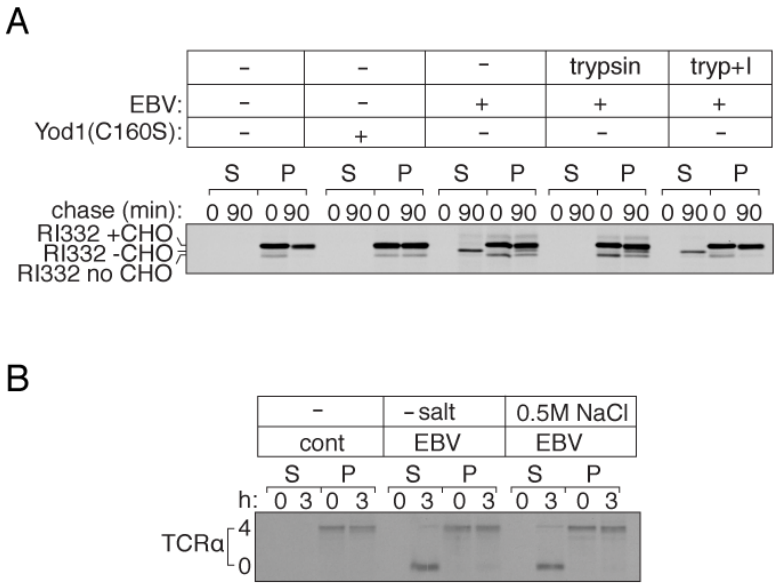

Figure 3. Misfolded protein dislocation measured in semi-intact cells.
(A) HEK293T cells were transiently transfected with RI332 and either Yod1 (C160S) or EBV. Cells were pulse labeled for 10 min with [35S]cysteine/methionine, permeabilized using PFO and chased for 90 min in Hank's buffer supplemented with 40 µg cytosol prepared separately and 1 mM ATP. At 0 and 90 min timepoints, semi-intact cells were centrifuged at 500xg for 5 min at 4ºC to separate supernatant and pellet fractions, RI332 was immunoprecipitated from all fractions and resolved by autoradiography. In the absence of Yod1(C160S) or EBV, RI332 is degraded in semi-intact cells with kinetics similar to that observed in intact cells (lanes 1-4). In the presence of Yod1(C160S) RI332 is arrested at the ER membrane (lanes 5-8). In the presence of EBV protease, polyubiquitin chains are preemptively removed and RI332 is arrested either at the ER membrane or in the cytosol. At the higher time point, deglycosylated RI332 appears in the cytosolic fraction indicating dislocation of the substrate from the ER to the cytosol and stabilization (lanes 9-12). Semi-intact cells transfected with EBV and RI332 were incubated in the presence of either trypsin alone (lanes 13-16) or with trypsin pre-treated with trypsin inhibitor (17-20), for 10 min at 37ºC. De-glycosylated RI332 is proteolysed in the presence of added trypsin, verifying its cytosolic orientation whereas it remains protected when proteolytic activity of trypsin is blocked by pre-treating with an inhibitor. Images are representative of experiments performed atleast twice. (B) TCRα is dislocated to the cytosol and degraded at the proteasome in semi-intact cells. HEK293T cells transfected with TCRα were permeabilized with PFO to separate supernatant and pellet. Fully glycosylated TCRα appeared in the pellet fraction whereas deglycosylated TCRα appeared in the supernatant, indicating dislocation from the ER to the cytosol. Extraction of deglycosylated TCRα into the cytosol remains unaffected in the presence or absence of 0.5M NaCl.

ity is impaired by chemical inhibitors such as Zl_3VS [16,16,26,26].
Is the fraction of deglycosylated RI_{332} indeed cytosolically oriented? If PFO treatment compromises plasma membrane integrity without permeabilizing the ER, deglycosylated cytosolic RI_{332} should be trypsin-sensitive, whereas fully-glycosylated, luminally-oriented RI_{332} should remain protected. We prepared semi-intact cells and added purified trypsin via a mild hypotonic shock (vide infra) to measure protease sensitivity of RI_{332}. As observed with microsome preparations [15,15], added trypsin destroyed the deglycosylated version of RI_{332} without attacking the fully glycosylated form (lanes 13-16); trypsin added after pre-treatment with a trypsin inhibitor did not proteolyse deglycosylated RI_{332}, as expected (lanes 17-20).
Similarly, the T cell receptor alpha subunit (TCRa) – a membrane bound glycoprotein – is retained in the ER and destroyed when expressed in the absence of its subunits required for proper assembly, which involves dislocation, progressive deglycosylation and proteasomal proteolysis [16,16]. Using PFO as a tool to fractionate cytosol from subcellular organelles, we could capture deglycosylated TCRa in the supernatant fraction when transfected with EBV-DUB (Figure 3B). In HEK293T cells that express TCRa and EBV-DUB, deglycosylated TCRa appeared in the cytosol after 3 hours of chase (both in the presence and absence of high salt), as evident from its partitioning (lanes 5-12) into the supernatant upon PFO-mediated fractionation. This observation is in contrast to deglycosylated RI_{332}, which shows a greater tendency of associating with the membrane and requires addition 0.5M NaCl for most efficient extraction into the supernatant fraction.

Dislocation of misfolded proteins is restored in permeabilized cells through exogenous addition of purified EBV-DUB

In cells that express Yod1C160S, fully glycosylated RI_{332} accumulates in the ER lumen because dislocation is blocked [15,15]. We hypothesize that this arrest is due to the inability of ubiquitylated RI_{332} to be extracted and instead causes an obstruction in the dislocon. Can addition of purified exogenous EBV-DUB to these semi-intact cells jump-start dislocation of RI_{332} through removal of Ub from the RI_{332} intermediate stalled at the ER? We used PFO to permeabilize HEK293T cells that co-express RI_{332} and Yod1C160S, and did so in the presence of purified EBV-DUB, delivered to the cytoplasm by means of a transient mild hypotonic shock. Residual cytosol was removed from these semi-intact cells by washing with buffer. To resume dislocation, the reaction mixture was supplemented with concentrated HEK293T cytosol (40µg total protein) and ATP (1 mM). Incubation of PFO-perfo-

rated cells with EBV-DUB in the absence of added cytosol fails to restore dislocation of RI_{332} from the ER: no product appears in the supernatant fractions (figure 4A lanes 1-12). Addition of 10 - 40 µg (total protein) of cytosol (5 mg/ml) together with EBV-DUB allows dislocation of RI_{332} to resume. Cytosolic components are therefore essential to facilitate the process. Our data suggest the following: In the presence of Yod1C160S, a very minor fraction – beyond the limit of detection by our biochemical methods – of membrane-bound RI_{332} retains its ubiquitylated status, blocking any further association of luminally oriented RI_{332} with the E3 ubiquitin ligase. As a consequence, most RI_{332} remains confined to the lumen of the ER in its glycosylated form. The lack of detectable ubiquitylated RI_{332} in the autoradiograms is suggestive of a very minor fraction of ubiquitylated substrate responsible for stalling further dislocation; we know of no deubiquitylating enzymes that reside within the ER lumen that could reverse ubiquitylation. Upon addition of exogenous EBV-DUB, this fraction is deubiquitylated and reaches the cytoplasm, allowing continued dislocation of the luminally positioned substrate. Appearance of a significantly larger fraction of deglycosylated RI_{332} – easily visualized by autoradiography – suggests that the rate of ubiquitylation by the E3 ligase is comparable to that of deubiquitylation by EBV-DUB, allowing continuous passage of RI_{332} from the ER lumen to the cytosol. This experiment demonstrates the feasibility of jump-starting, in a synchronized manner, the dislocation reaction.

Transport of misfolded proteins from the ER to the cytosol requires ATP, as inferred from the involvement of p97, a AAA-ATPase. To examine more directly the NTP requirement in the process of dislocation of RI_{332} in PFO-perforated cells, we added either ATP, GTP or their non-hydrolyzable analogs. Addition of ATP allowed dislocation of RI_{332} to proceed, whereas the inclusion of ATPgS blocked it (Figure 4B; lanes 9-16). Presence of either GTP or GTPgS did not affect dislocation (Figure 4B; lanes 17-24). In contrast to the process of dislocation, transport along the secretory pathway in semi-intact cells remained GTP-sensitive. As a positive control for the ability of GTPgS to block a trafficking step in PFO-perforated cells, we monitored transport of VSV-G from the ER to the Golgi in semi-intact cells, based on acquisition of complex glycan modifications (Figure 4C). As read-out we followed the conversion of N-linked oligosaccharides on VSV-G from their high mannose Endo-H sensitive precursors to terminally glycosylated, mature Golgi forms, resistant to Endo-H digestion. We compared kinetics of VSV-G trafficking in intact cells with that in PFO-permeabilized semi-intact cells (Figure 4C). Transport of VSV-G through the Golgi was greatly diminished in semi-intact cells in the absence of cytosol, evident from its sensitivity to Endo-H digestion (unpublished). When

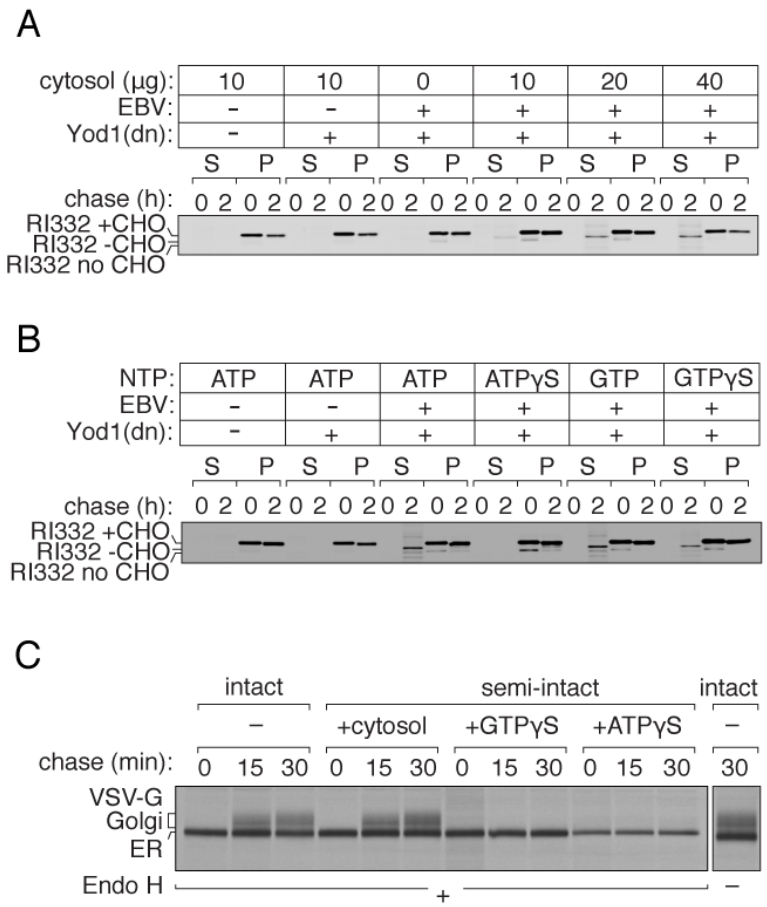

Figure 4. Dislocation of substrates is restored in semi-intact cells through exogenous addition of EBV-DUB

(A) Cytosol dependence of substrate dislocation after EBV addition. HEK293T cells were transfected with RI332 and Yod1(C160S). Control cells were transfected with pcDNA. Cells were pulse labeled with [35S]cysteine/methionine, permeabilized and incubated with 10 µg EBV and varying amounts of cytosol (0, 10, 20 or 40 µg) in Hank's buffer at 37 ºC. At 0 and 90 mins, aliquots were withdrawn, supernatant and pellet fractions separated by centrifugation and probed by SDS-PAGE and autoradiography. (B) HEK293T cells transfected with RI332 were radiolabeled, permeabilized and incubated with EBV and cytosol supplemented with ATP (1 mM), ATPγS (1mM), GTP (1mM) or GTPγS (1mM). Supernatant and pellet fractions were probed for dislocated RI332. (C) In PFO-permeabilized HEK293T cells the secretory pathway remains functional and sensitive to GTPγS. HEK293T cells transfected with VSV-G were pulsed with [35S]cysteine/methionine, PFO-permeabilized and chased with cytosol for 0, 15 and 30 min in the presence of concentrated cytosol (lanes 4-6), or cytosol supplemented with either GTPγS (7-9) or ATPγS (10-12). At every time point VSV-G was recovered from lysates by immunoprecipitation on chicken VSV-G antibody, digested with Endoglycosidase H and resolved by SDS-PAGE. Trafficking of VSV-G in intact cells was monitored in parallel (lanes 1-3).

compared to intact cells, we achieved near-complete recovery of VSV-G maturation in semi-intact cells when supplemented with concentrated cytosol. We observed inhibition of transport of VSV-G in semi-intact cells when cytosol was supplemented with GTPgS. Transport through the secretory pathway thus requires GTP hydrolysis [27,27,28,28], whereas dislocation of misfolded proteins does not.

Efficiency of EBV add-back increases with decreasing buffer osmolarity and increase in EBV-DUB concentration

Dislocation of RI_{332} in semi-intact cells upon addition of purified EBV-DUB increases with the amount of cytosol added (Figure 4A). To optimize conditions and improve delivery of macromolecules to semi-intact cells, we tested increasing concentrations of EBV-DUB and decreasing osmolarity of the permeabilization buffer. We reduced ionic strength to achieve a greater osmotic differential and so improve delivery of EBV-DUB to semi-intact cells. As anticipated, by increasing the amount of purified EBV-DUB supplied, we observed a dose-dependent increase in the amount of dislocated intermediate (Figure 5A, 5B). Similarly, by reducing osmolarity from 1X to 0.2X Hank's buffer equivalent to modulate delivery of EBV-DUB, we observed an increase in the amount of deglycosylated intermediate that appeared in the cytosolic fraction (Figure 5C, 5D).

Exogenous addition of EBV-DUB stabilizes class-I MHC and TCRa in semi-intact cells

To extend our findings to substrates beyond RI_{332}, we monitored export and degradation of T-cell receptor alpha chain (TCRa) in HEK293T cells (Figure 6A). TCRa is a glycoprotein in which four N-glycosylation sequons are used; when expressed in HEK293T cells, TCRa is degraded by the UPS [16,16,29]. Cells co-expressing TCRa and Yod1C160S were pulse-labeled with [^{35}S]cysteine/methionine, permeabilized with PFO and exposed to exogenously added EBV-DUB in the presence and absence of additional cytosol. In the presence of added EBV-DUB and cytosol, deglycosylated TCRa appeared in the supernatant fraction at the 3 hour time point, indicating that transport had resumed with concomitant stabilization of dislocated TCRa. We observed appearance of a minor fraction of deglycosylated TCRa in the absence of added ATP and cytosol, possibly due to residual cytosol, despite permeabilization. Supplementing the reaction mixture with concentrated cytosol and ATP significantly improved recovery of cytosolic deglycosylated TCRa, as also

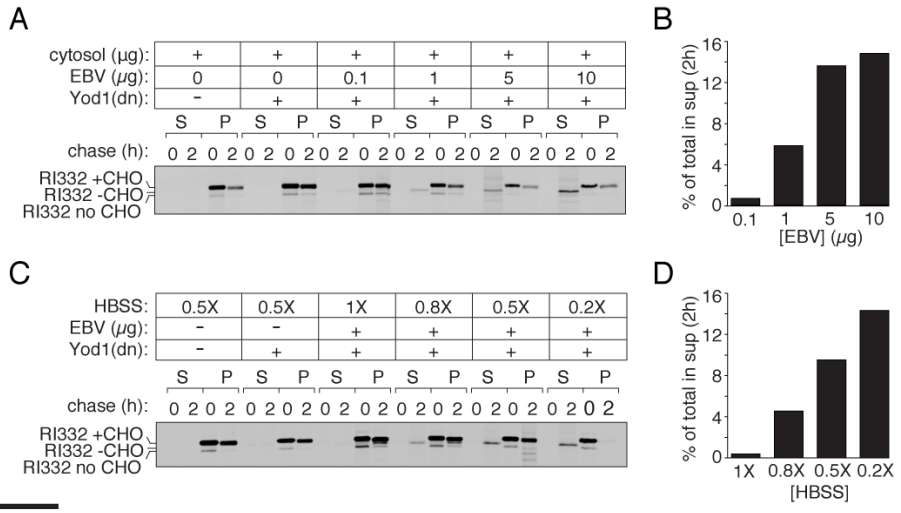

Figure 5. Characterization of purified EBV delivery to semi-intact cells.
(A) Dose-dependent EBV delivery to semi-intact cells. HEK293T cells were transfected with RI332 and Yod1 (C160S) to stall dislocation in the ER. Semi-intact cells prepared with PFO were incubated with 40 µg of cytosol, 1 mM ATP and varying amounts of EBV to monitor dose-dependence of RI332 export from the ER. In parallel, one set of control cells received only RI332. Another set of control cells received RI332 and Yod1(C160S) and were incubated with a mock reaction mixture without EBV present. (B) Quantitation of the autoradiogram shown in (A). Graphs represent the amount of radioactivity in the supernatant fractions at 2 hours as a fraction of total radioactivity in the supernatant and pellet fractions. (C) Dependence of EBV delivery to semi-intact cells on buffer osmolarity. HEK293T cells transfected with RI332 and Yod1 were permeabilized using PFO. Semi-intact cells were incubated in 10 µg of purified EBV, 1 mM ATP and 40 µg of cytosol in Hank's buffer of 1X, 0.8X, 0.5X or 0.2X ionic strength respectively, to provide a greater hypotonic shock for better EBV delivery to semi-intact cells. (D) Quantitation of the autoradiogram shown in (C). All experiments were performed atleast twice.

seen for RI_{332}.

In astrocytoma cells that express HCMV US11, Class I MHC molecules are rapidly degraded by the UPS [18,30]. PFO-permeabilized US11-expressing cells supported rapid degradation of Class I molecules when supplemented with ATP and cytosol (Figure 6B; lanes 1-6). To test the effect of EBV-DUB on MHC Class I degradation, we created PFO-mediated semi-intact cells to supply purified EBV-DUB. US11-expressing astrocytomas proved difficult to transiently transfect with Yod1C160S due to poor transfection efficiency. However, addition of EBV-DUB to these semi-intact cells almost completely arrested fully glycosylated MHC-I in the ER, with the appearance of a minor fraction of deglycosylated MHC-I in the cytosolic fractions at the 20 and 40 min time-points (Figure 6B; lanes 7-12). Ubiquitylation of Class-I molecules must therefore be a rate-limiting step in this case, contrary to what we observe for RI_{332}. We surmise that addition of EBV-DUB rapidly removes polyubiquitin chains from MHC Class I, at a rate faster than re-ubiquitylation and subsequent recruitment of the dislocation components. The net result is that

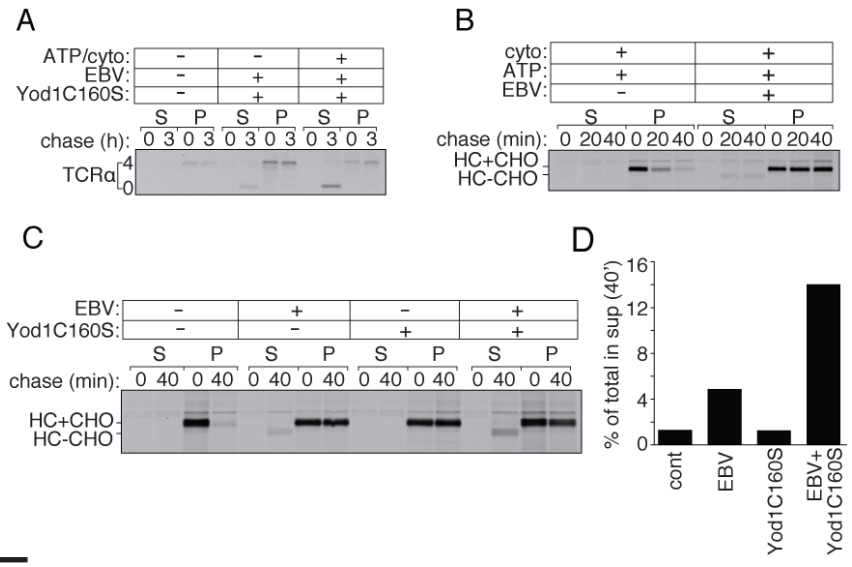

Figure 6. TCRα and class I MHC dislocation measured in semi-intact cells
(A) HEK293T cells transfected with TCRα and Yod1 (C160S) were pulsed with [35S]cysteine/methionine, permeabilized using PFO and incubated with purified EBV supplemented with 40 µg cytosol and 1mM ATP. (B) Astrocytoma cells stably transfected with HCMV US11 were pulsed with [35S]cysteine/methionine, permeabilized using PFO and incubated with 40 µg cytosol and 1mM ATP for 0, 20 and 40 min in the absence or presence of purified EBV. (C) US-11 expressing astrocytomas were stably transfected with either wtYod1 or Yod1C160S. Cells were radiolabeled, followed by PFO-permeabilization to supply concentrated cytosol in the presence of absence of purified EBV for 0 and 40 min. (D) Quantitation of the autoradiogram shown in (C). Graphs represent the amount of radioactivity in the supernatant fractions at 40 mins as a fraction of total radioactivity present in the supernatant and pellet fractions. Images are representative of experiments performed twice.

the reaction stalls. In cells that co-express US11 and Yod1C160S, Class I MHC products would be positioned such that further addition of EBV-DUB would allow a greater fraction of the substrate to arrive in the cytosol and be deubiquitylated and deglycosylated. To test our hypothesis, we generated a cell line that stably expresses US11 with either Yod1C160S or Yod1WT, as confirmed by immunoblotting. These cells were pulse-labeled with [^{35}S]cysteine/methionine, followed by PFO-treatment to form semi-intact cells. EBV-DUB was supplied to these semi-intact cells and incubated with concentrated cytosol for 0 and 40 min (Figure 6C). At each time point, cells were separated into supernatant and pellet fractions. In the presence of Yod1WT with no EBV-DUB added, Class I MHC is degraded rapidly as expected. When these cells express Yod1C160S, Class I MHC remains stable in its glycosylated form in the ER (lanes 5-8). While semi-intact cells supplied with EBV-DUB show a near complete stabilization of Class I in the ER, with a minor fraction appearing in the cytosol, addition of EBV-DUB to cells that stably express Yod1C160S leads to a greater fraction of Class I in the cytosol in its deglycosylated

form (Figure 6D). This observation supports our hypothesis that the presence of Yod1C160S positions the substrate in its ubiquitylated state at the ER, such that the downstream dislocation components are in place for extraction to the cytosol to occur. Consequently, addition of EBV-DUB to these cells results in a larger fraction of the substrate to appear in the cytosol. These data are strongly suggestive of distinct modes of E3 ubiquitin ligase involvement in the pathway of RI_{332} and MHC-I dislocation.

Dislocation substrates are polyubiquitylated in the presence of Yod1C160S

We blocked dislocation of misfolded substrates in the ER by expression of Yod1C160S, causing accumulation of glycosylated RI_{332}. As proposed in the model, we hypothesize that this stabilization is due to stalled dislocation, owing to occlu-

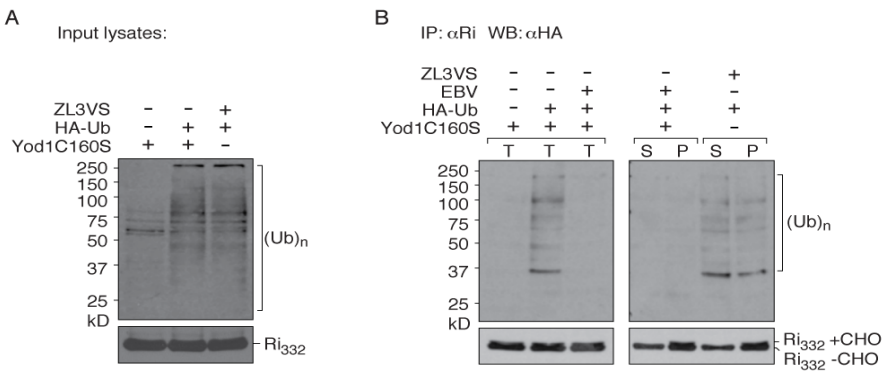

Figure 7. Polyubiquitylation of a dislocation substrate prior to degradation
HEK293T cells were transfected with RI332, Yod1C160S and empty vector or HA-Ub. Cells were permeabilized with 100 nM PFO and incubated with purified EBV in 0.5X HBSS. After 60 min incubation, samples were either directly solubilized in buffer containing 0.5% NP-40 supplemented with 5 mg/ml NEM or supernatant and pellet fractions were first separated by centrifugation followed by dilution/lysis. RI332 was immunoprecipitated on Protein A beads coupled to anti-RI antibodies, eluates resolved by SDS-PAGE and polyubiquitylated material visualized by anti-HA. In parallel, cells transfected with RI332 and HA-Ub were treated with 20 µM ZL3VS to inhibit the proteasome. Cells were permeabilized using PFO and separated into cytosolic and pellet components. RI332 was immunoprecipitated from both fractions, eluates were resolved by SDS-PAGE and visualized using anti-HA antibodies. (A) Lysates from cells expressing RI332, empty vector or HA-Ub, -/+ Yod1C160S and -/+ ZL3VS were directly immunoblotted and probed with anti-HA for ubiquitin levels and anti-RI for RI332 levels. (B) Left panel: Semi-intact cells expressing Yod1C160S, RI332 and empty vector/HA-Ub were incubated with -/+ 1 µg purified EBV. After 60 min, reaction was terminated by lysis in 0.5% NP-40 lysis buffer and immunoprecipitated with anti-RI antibodies. The eluates were visualized by immunoblotting with anti-HA antibodies. T: total. Right panel: After 60 min incubation with EBV or ZL3VS, cells were first separated into cytosol and pellet fractions, immunoprecipitated with anti-RI antibodies and eluates were visualized by immunoblotting with anti-HA antibodies. Immunoisolated material was also probed with anti-RI antibodies for RI332 levels. S: supernatant (cytosol), P: pellet. Images are representative of experiments performed three times.

sion of ubiquitylated RI_{332} from the central pore of p97, or of any other endogenous substrate that might require dislocation via this pathway. Purified EBV-DUB supplied to semi-intact cells overcomes this blockade and restores dislocation. Detecting ubiquitylated substrate intermediates in autoradiograms has been challenging – possibly due to low levels and inherent instability of such intermediates. In an alternative approach, we transiently transfected HEK293T cells with untagged RI_{332}, Yod1C160S and either empty control plasmid or HA-Ub (Figure 7). We permeabilized cells with PFO and supplied purified EBV-DUB to allow release of stalled RI_{332} from the ER. After incubating with EBV-DUB for 60 min, samples were solubilized in NP-40 lysis buffer in the presence of 5 mg/ml NEM to block endogenous DUB activities during lysis and immunoprecipitated RI_{332} with anti-ribophorin antibodies. Eluted samples were then resolved on SDS-PAGE and immunoblotted with anti-HA antibodies. In cells that express Yod1C160S and HA-Ub, a smear of polyubiquitylated RI_{332} was detected in the immunoprecipitated sample. When exogenous EBV was added back to these permeabilized cells, ubiquitylated intermediates disappeared, indicating substrate de-ubiquitylation. Upon separating the cytosol and the pellet fractions, deglycosylated RI_{332} appeared in the cytosol and glycosylated RI_{332} remained in the pellet fraction. In parallel, in cells expressing wtYod1 treated with ZL3VS to block proteasomal activity, polyubiquitylated RI332 appeared in both the cytosolic and pellet fractions. These data, in conjunction with pulse-chase assays, support our proposed model that dislocation substrates remain ubiquitylated in the presence of Yod1C160S, causing them to accumulate at the ER membrane. Yod1C160S prevents dislocation not only of the substrates introduced by transfection, but presumably also of other, endogenous proteins destined for dislocation. While we can demonstrate the presence of ubiquitylated RI_{332} in cells that express Yod1C160S, it is unlikely to be the only ubiquitylated substrate that could contribute to occlusion of the dislocation machinery. Regardless, inclusion of EBV-DUB removes Ub from RI_{332}, a reaction that coincides with the initiation of dislocation.

Discussion

Using a number of reporters with distinct physical properties (RI_{332}, TCRa, MHC-I), we show that dislocation in semi-intact cells requires ATP and cytosol, confirming and extending our earlier data for MHC-I in digitonin permeabilized cells [30]. Unlike protein trafficking through the secretory pathway, dislocation of substrates from the ER was insensitive to the inclusion of GTPgS. We had proposed earlier that deubiquitylation of substrates designated for proteasomal degradation is a neces-

sary step for dislocation from the ER. If correct, two rounds of ubiquitylation would be required for dislocation and degradation of RI_{332},: an initial round at the ER membrane to engage the p97 complex, followed by deubiquitylation, and a second round of ubiquitylation in the cytosol to tag substrates for proteasomal degradation. Ubiquitylation at the ER membrane appears to be essential more for recognition by downstream effectors rather than for providing a handle for generating a mechanical force for substrate passage through the p97 complex [31]. Data presented here with multiple substrates confirm this model of protein dislocation.

We provide a key mechanistic insight in the dislocation reaction that clears misfolded proteins from the ER. We find that expression of Yod1C160S, a dominant negative version of an ER-associated deubiquitylase, impedes dislocation through the accumulation of a ubiquitylated intermediate. Through delivery of a heterologous deubiquitylase in a semi-intact cell preparation, we can relieve this inhibition and jump-start the dislocation reaction. The level to which the stalled intermediate accumulates is such that we cannot detect biochemically the presence of the ubiquitylated species, yet the consequences of providing an exogenous active deubiquitylase, EBV-DUB, is compelling evidence that even these small amounts of the ubiquitylated intermediate must be sufficient to occlude the dislocon and halt the transfer of proteins across the membrane.
Intracellular transport of proteins in a cell-free system requires that events observed in vitro faithfully recapitulate the process occurring in vivo. Although methods based on subcellular fractionation or detergent-solubilized crude extracts have provided important information regarding intracellular protein trafficking, limitations include the disruption of essential cellular architecture in the course of homogenization or cell lysis. Semi-intact cells, from which segments of the plasma membrane have been selectively removed, retain the necessary subcellular integrity essential for intracellular transport to proceed. Such systems allow access of otherwise cell-impermeant macromolecules to the cytoplasmic side and so enable mechanistic analyses related to a pathway.

Here we use PFO – a cholesterol-dependent bacterial pore-forming toxin – to perforate the plasma membrane under mild physiological conditions and monitor protein dislocation from their initial ER localization to the cytosol. The PFO-based assay provides a level of precision and sensitivity that we have been unable to match in microsome preparations or other available strategies. The assay reports on intracellular transport of proteins with minimal damage to subcellular organelles.

We observed efficient protein trafficking along the secretory pathway as monitored through VSV-G and HA transport when compared to intact cells. Furthermore, we could readily monitor dislocation of glycoproteins from the ER to the cytosol, and obtained clean separation of ER-resident (glycosylated) and cytoplasmic (deglycosylated) substrates. We had comparatively limited success in measuring dislocation of Class I MHC products in US11/US2-expressing cells [32], and for this reason developed the PFO-based alternative to the microsome-based system. Digitonin-based semi-intact cell systems in our hands also perform less robustly than the PFO system described here. Treatment with PFO is largely directed and confined to the plasma membrane, conferring little to no perturbation of the integrity of the ER membrane. Given the involvement of a variety of membrane-integral and membrane-tethered proteins that must connect to cytoplasmic components to carry out the entire dislocation and degradation pathway [22], minimal disruption of cellular architecture appears to be a prerequisite to observe these reactions in semi-intact cells.

Materials and Methods

Antibodies, Cell Lines, Constructs

Antibodies against HA-epitope were purchased from Roche (3F-10). Polyclonal anti-PDI serum (rabbit) was generated with bacterially expressed human PDI, anti-BiP serum (rabbit) was against human BiP. Antibodies against GAPDH and p97 were purchased from Abcam. TCRa antibody has been described before [15,16]. ATPgS and GTPgS were purchased from Sigma. HEK293T cells were purchased from American Type Culture Collection and cultured. US11 cell lines have been described [12,13]. The construct containing EBV-DUB has been described before [15,17]. For purification, the gene encoding EBV-DUB was modified to include a histidine tag, cloned into an expression vector and overexpressed and purified from BL-21 competent E. coli. Deletion constructs of ribophorin (RI_{332}) and the dominant negative mutant construct of YOD1 have been described elsewhere [13]. HA-agarose beads were purchased from Roche Applied Science and Protein A-agarose beads were from RepliGen Bioprocessing.

Transient Transfections and Viral Transductions

HEK293T cells were transiently transfected using Fugene6 (Roche Diagnostics) according to the manufacturer's instructions. Cell transduced with pLHCX-based vectors (Clonetech) were selected and maintained in 125 µg/ml of hygromycin B

(Roche Applied Science).

Overexpression and Purification of His_6-PFO(C459A)

The gene encoding perfringolysin O (PFO) from Clostridium perfringens was modified to replace the only cysteine with alanine (C459A) and include and NH_2-terminal hexahistidine tag [14,17]. This construct was subsequently cloned into the pRSETB expression vector (Invitrogen) and kindly provided to us by A. Johnson (Texas A&M, College Station, TX). After transformation into BL21 E. coli competent cells, over-expression and purification was carried out using routine Ni-NTA affinity purification. The hexa-histidine tag and the single amino acid substitution does not significantly affect the cholesterol binding activity of PFO as described [17].

Pulse-Chase Analysis, Immunoprecipitation, SDS-PAGE: Intact Cells

Pulse chase experiments were performed as previously described [14,18]. Briefly, ~1 x 10^7 cells were detached by trypsinization and starved for 45 min in methionine/cysteine free Dulbecco's modified Eagle's medium at 37ºC prior to pulse labeling. Cells were labeled for 10 min at 37ºC with 10mCi/ml [^{35}S]methionine/cysteine (expressed protein mix; PerkinElmer) and chased for indicated time intervals. At appropriate time intervals aliquots were withdrawn and treated with 0.1 μM PFO as described below. Immunoprecipitations were performed for atleast 3h at 4ºC with gentle agitation. Samples were eluted by boiling in reducing sample buffer, subjected to SDS-PAGE and visualized by autoradiography.

PFO-Mediated Permeabilization of Intact Cells

~1 x 10^7 cells were detached from 10 cm dishes by brief trypsinization, washed once with Hank's balanced salt solution (HBSS) and resuspended in 50 μl (HBSS) on ice. 50 μM 200 nM PFO was added to cells in suspension to obtain a final concentration of 100 nM and maintained on ice for 5 min. Excess PFO (unbound to the plasma membrane) was removed by diluting with 1ml HBSS and centrifugation (5 min; 500 x g). Cell pellets were resuspended in 50 μl HBSS and incubated at 37ºC for 10 min. Following permeabilization, cells were centrifuged at 500 x g for 5 min to collect supernatants. Pellets obtained were washed once with 1 ml HBSS and resuspended in 50 μl HBSS containing 1% SDS. Separation of the cytosol and the organelle fractions were verified by immunoblotting for GAPDH, p97 (as cytosolic markers), BiP and PDI (as soluble ER luminal markers).

Add-back Assays in PFO-Permeabilized Cells

Cells transfected with either RI_{332} or TCRa were grown to 80-90% confluency and metabolically labeled with [^{35}S]cysteine/methionine at 37ºC in suspension. To create semi-intact cells for add-back of purified EBV, cells were treated with 0.1 μM PFO (in HBSS) on ice as described above. Excess PFO was removed by diluting in

HBSS and centrifugation. For measuring substrate dislocation in semi-intact cells the reaction mixture consisted of ~0.5 x 10^7 PFO treated cells, 1 mM ATP, 40 µg of concentrated cytosol and 10 µg purified EBV resuspended in 50 µl of 0.5X HBSS, and incubated at 37ºC for appropriate time intervals. At each time point, withdrawn cell suspension was centrifuged at 500 x g for 5 min to separate the pellet and supernatant fractions. The pellet was lysed in NP-40 containing 0.1% SDS. The supernatants were diluted to 1 ml in NP-40 lysis buffer containing 0.1% SDS. Substrates were recovered from supernatant and pellet fractions by immunoprecipitation, resolved by SDS-PAGE and visualized by autoradiography.

Preparation of Cytosol From HEK293T Cells

To prepare concentrated cytosol, HEK293T cells were grown in 15 cm dishes to confluency and harvested by brief trypsinization. Harvested cells were resuspended in 100µl of Hank's buffer and treated with 100 nM PFO on ice. Excess, unbound PFO was removed by diluting with excess Hank's buffer, centrifuging (500 x g) and resuspended in 20 µl of Hank's buffer to introduce minimal dilution of cytosolic components. The cell suspension was then incubated at 37ºC for 10 min to induce pore formation by PFO. The supernatant (~100 µl) was collected after a 10000 x g spin, measured for protein concentration and immunoblotted for cytosolic and soluble ER luminal marker proteins. Cytosol concentration typically varied between 10-20 mg/ml. Concentrated cytosol was aliquoted into 50 µl volume, flash frozen in liquid nitrogen and stored at -80 ºC for later use.

References

1. Park E, Rapoport TA (2011) Mechanisms of Sec61/SecY-Mediated Protein Translocation Across Membranes. Annu Rev Biophys. doi:10.1146/annurev-biophys-050511-102312.
2. Braakman I, Bulleid NJ (2011) Protein folding and modification in the mammalian endoplasmic reticulum. Annu Rev Biochem 80: 71–99. doi:10.1146/annurev-biochem-062209-093836.
3. Carvalho P, Stanley AM, Rapoport TA (2010) Retrotranslocation of a misfolded luminal ER protein by the ubiquitin-ligase Hrd1p. Cell 143: 579–591. doi:10.1016/j.cell.2010.10.028.
4. Scott DC, Schekman R (2008) Role of Sec61p in the ER-associated degradation of short-lived transmembrane proteins. J Cell Biol 181: 1095–1105. doi:10.1083/jcb.200804053.

5. Ye Y, Shibata Y, Yun C, Ron D, Rapoport TA (2004) A membrane protein complex mediates retro-translocation from the ER lumen into the cytosol. Nature 429: 841–847. doi:10.1038/nature02656.
6. Lilley BN, Ploegh HL (2004) A membrane protein required for dislocation of misfolded proteins from the ER. Nature 429: 834–840. doi:10.1038/nature02592.
7. Ploegh HL (2007) A lipid-based model for the creation of an escape hatch from the endoplasmic reticulum. Nature 448: 435–438. doi:10.1038/nature06004.
8. Olzmann JA, Kopito RR (2011) Lipid Droplet Formation Is Dispensable for Endoplasmic Reticulum-associated Degradation. Journal of Biological Chemistry 286: 27872–27874. doi:10.1074/jbc.C111.266452.
9. Claessen JHL, Kundrat L, Ploegh HL (2012) Protein quality control in the ER: balancing the ubiquitin checkbook. Trends Cell Biol 22: 22–32. doi:10.1016/j.tcb.2011.09.010.
10. Smith MH, Ploegh HL, Weissman JS (2011) Road to Ruin: Targeting Proteins for Degradation in the Endoplasmic Reticulum. Science 334: 1086–1090. doi:10.1126/science.1209235.
11. Reyes-Turcu FE, Ventii KH, Wilkinson KD (2009) Regulation and Cellular Roles of Ubiquitin-Specific Deubiquitinating Enzymes. Annu Rev Biochem 78: 363–397. doi:10.1146/annurev.biochem.78.082307.091526.
12. Mueller B, Klemm EJ, Spooner E, Claessen JH, Ploegh HL (2008) SEL1L nucleates a protein complex required for dislocation of misfolded glycoproteins. Proceedings of the National Academy of Sciences 105: 12325–12330. doi:10.1073/pnas.0805371105.
13. Ernst R, Mueller B, Ploegh HL, Schlieker C (2009) The otubain YOD1 is a deubiquitinating enzyme that associates with p97 to facilitate protein dislocation from the ER. Mol Cell 36: 28–38. doi:10.1016/j.molcel.2009.09.016.
14. Claessen JHL, Mueller B, Spooner E, Pivorunas VL, Ploegh HL (2010) The transmembrane segment of a tail-anchored protein determines its degradative fate through dislocation from the endoplasmic reticulum. J Biol Chem 285: 20732–20739. doi:10.1074/jbc.M110.120766.
15. Ernst R, Claessen JHL, Mueller B, Sanyal S, Spooner E, et al. (2011) Enzymatic blockade of the ubiquitin-proteasome pathway. PLoS Biol 8: e1000605. doi:10.1371/journal.pbio.1000605.
16. Huppa JB, Ploegh HL (1997) The alpha chain of the T cell antigen receptor is degraded in the cytosol. Immunity 7: 113–122.

17. Flanagan JJ, Tweten RK, Johnson AE, Heuck AP (2009) Cholesterol exposure at the membrane surface is necessary and sufficient to trigger perfringolysin O binding. Biochemistry 48: 3977–3987. doi:10.1021/bi9002309.
18. Wiertz EJ, Jones TR, Sun L, Bogyo M, Geuze HJ, et al. (1996) The human cytomegalovirus US11 gene product dislocates MHC class I heavy chains from the endoplasmic reticulum to the cytosol. Cell 84: 769–779.
19. Misaghi S, Pacold ME, Blom D, Ploegh HL, Korbel GA (2004) Using a small molecule inhibitor of peptide: N-glycanase to probe its role in glycoprotein turnover. Chem Biol 11: 1677–1687. doi:10.1016/j.chembiol.2004.11.010.
20. Shatursky O, Heuck AP, Shepard LA, Rossjohn J, Parker MW, et al. (1999) The mechanism of membrane insertion for a cholesterol-dependent cytolysin: a novel paradigm for pore-forming toxins. Cell 99: 293–299.
21. Walev I, Bhakdi S, Hofmann F, Djonder N, Valeva A, et al. (2001) Delivery of proteins into living cells by reversible membrane permeabilization with streptolysin-O. Proc Natl Acad Sci USA 98: 3185.
22. Beckers CJ, Keller DS, Balch WE (1987) Semi-intact cells permeable to macromolecules: use in reconstitution of protein transport from the endo plasmic reticulum to the Golgi complex. Cell 50: 523–534.
23. Ikonen E, Tagaya M, Ullrich O, Montecucco C, Simons K (1995) Different requirements for NSF, SNAP, and Rab proteins in apical and basolateral transport in MDCK cells. Cell 81: 571–580.
24. Nelson LD, Chiantia S, London E (2010) Perfringolysin O association with ordered lipid domains: implications for transmembrane protein raft affinity. Biophys J 99: 3255–3263. doi:10.1016/j.bpj.2010.09.028.
25. de Virgilio M, Weninger H, Ivessa NE (1998) Ubiquitination is required for the retro-translocation of a short-lived luminal endoplasmic reticulum glyco protein to the cytosol for degradation by the proteasome. J Biol Chem 273: 9734–9743.
26. Mueller B, Lilley BN, Ploegh HL (2006) SEL1L, the homologue of yeast Hrd3p, is involved in protein dislocation from the mammalian ER. Journal of Cell Biology 175: 261–270. doi:10.1083/jcb.200605196.
27. Balch WE (1990) Small GTP-binding proteins in vesicular transport. Trends Biochem Sci 15: 473–477.
28. Symons M, Rusk N (2003) Control of vesicular trafficking by Rho GTPases. Current Biology 13: R409–R418.
29. Yu H, Kaung G, Kobayashi S, Kopito RR (1997) Cytosolic degradation of T-cell

receptor alpha chains by the proteasome. J Biol Chem 272: 20800–20804.
30. Shamu CE, Story CM, Rapoport TA, Ploegh HL (1999) The pathway of US11-dependent degradation of MHC class I heavy chains involves a ubiquitin-conjugated intermediate. J Cell Biol 147: 45–58.
31. Ye Y, Meyer HH, Rapoport TA (2003) Function of the p97-Ufd1-Npl4 complex in retrotranslocation from the ER to the cytosol: dual recognition of nonubiquitinated polypeptide segments and polyubiquitin chains. Journal of Cell Biology 162: 71–84. doi:10.1083/jcb.200302169.
32. Furman MH, Ploegh HL, Tortorella D (2002) Membrane-specific, host-derived factors are required for US2- and US11-mediated degradation of major histocompatibility complex class I molecules. J Biol Chem 277: 3258–3267. doi:10.1074/jbc.M109765200.

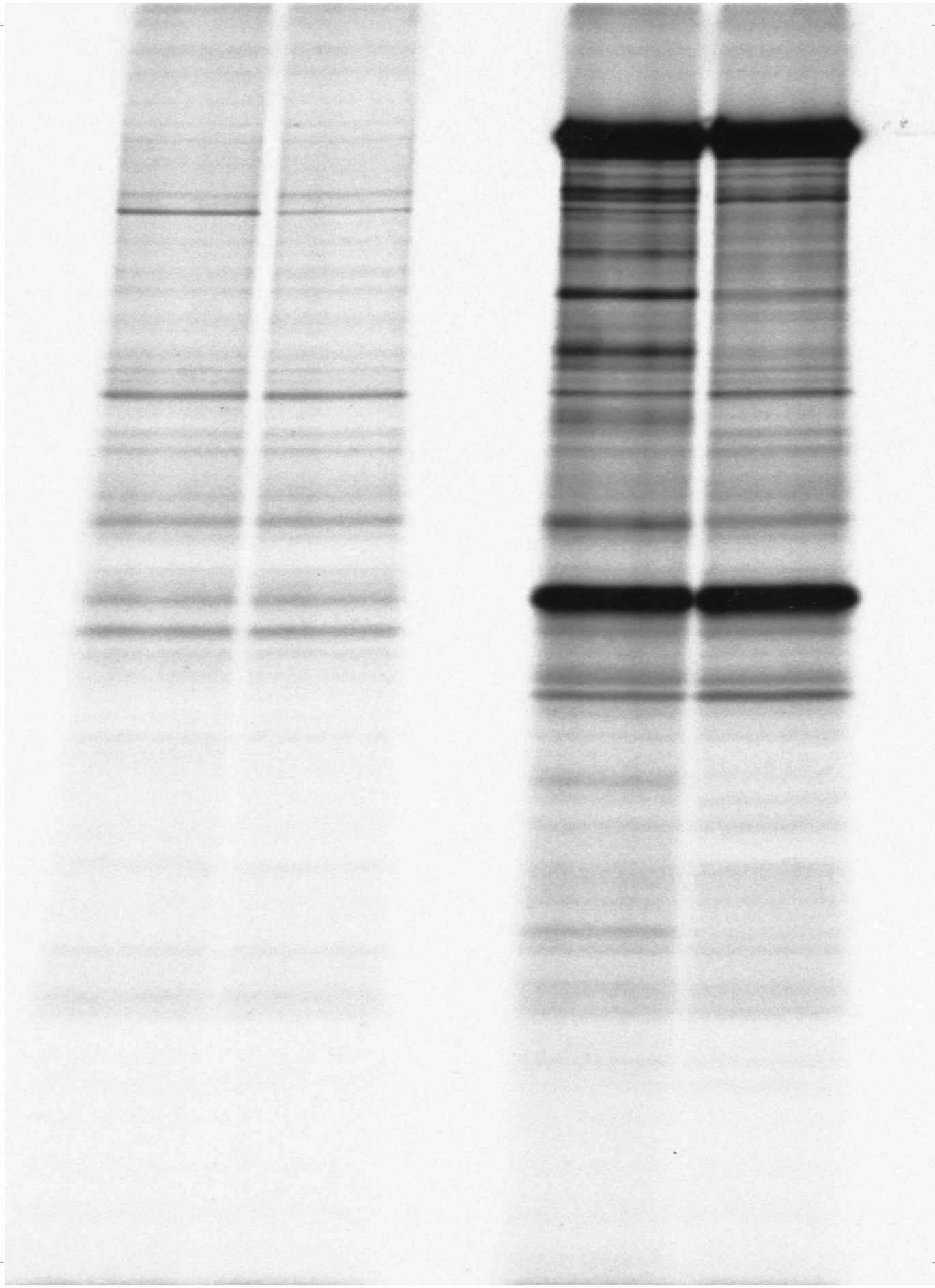

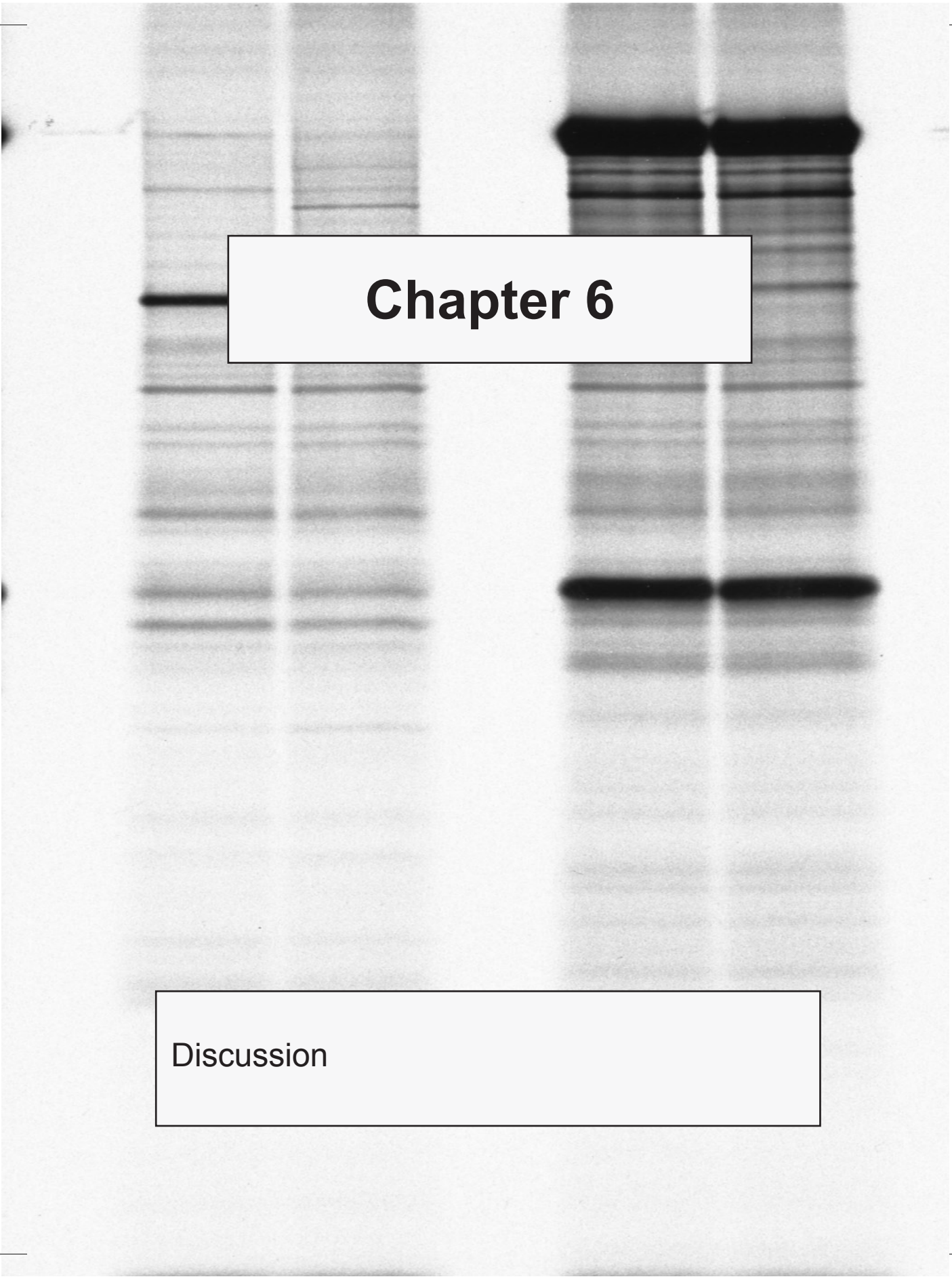

Chapter 6

Discussion

Fidelity in protein synthesis is an evolutionary requirement to ensure consistent production of functional proteins, be it as part of a multiprotein complex or as individual polypeptides. Even simple mistakes can alter binding specificity of an enzyme, change the signaling domain of a receptor or mislocalize a housekeeping protein, to name but a few examples. As mistakes in protein synthesis do not always find their roots in interpretation of the genetic code, there are no suspected benefits of diversity at this stage, and any misfits of protein synthesis are quickly and selectively degraded to prevent problems further down the road, a process known as protein quality control.

Protein quality control is not limited to one specific moment in protein synthesis, or to any single compartment where the protein may reside. Proteins destined for the secretory pathway undergo quality control from the cradle to the grave. We know of control mechanisms that inspect proteins as they are synthesized at the ribosome [1], and that inspect the proper insertion or translocation into the endoplasmic reticulum (ER) [2]. Inside the ER, newly synthesized proteins are modified by processes such as glycosylation and disulfide bond formation, in order to acquire their three-dimensional structure, and to find binding partners when appropriate. This is referred to as protein folding and assembly (as discussed in the introductory chapter). Despite the implied stringency in quality control in the ER, some misfolded proteins (as they are now called) can still and do escape, and travel further down the endomembrane pathway. The mutant protein CFTRΔF508 serves as an example [3]. Those proteins that escape ER quality control can be cleared by the same mechanisms that are in place to sequester proteins that have sustained damage in the endocytic pathway, be it en route to or having arrived at their final destination, and be destroyed in the lysosomes.

Quality control is easily imagined as a concept, but it is more difficult to translate it into molecular terms. How is a defective polypeptide recognized? What constitutes a misfolded protein? And when is an error considered terminal? This last point is well illustrated by the enigmatic re-entry of ER proteins into the Calnexin/Calreticulin folding cycle, facilitated by UGT1 until they pass quality control. UGT1 re-glucosylates the terminal mannose residue on a N-glycan group, whereas loss of exactly this glucose is considered to be a hallmark of terminally misfolded proteins [4].
It is difficult to predict which perturbations, or ‘mistakes’, are tolerated by a protein. This is nicely illustrated in chapter 2, where four changes in the transmembrane domain (TMD) of UBC6e, a tail-anchored membrane protein, result in four different

phenotypes. First, deletion of the TMD prevents membrane anchoring, and results in mislocalization of the mutant protein. Even though this disallows interaction with the HRD1-SEL1L complex, this truncation does not affect the half-life of the protein. Next, replacement of the TMD with that of three different proteins resulted in an additional three distinct behaviors. Replacement of the TMD of Ubc6e with that of CD4 resulted in a mutant protein that behaved as wild-type UBC6e. In contrast, replacement with the TMD of either Cytochrome B5 or UBC6, gave rise to proteins that are successfully inserted into the ER membrane, but are rapidly degraded albeit with different kinetics [5].

In seeking an explanation in the kinetics of protein-protein interactions to account for quality control in the ER, consider the following. The tight natural fold of a protein buries hydrophobic domains or polar residues that could initiate unwanted partnerships with other proteins. A surplus of folding chaperones would buffer such unwanted interactions by engaging any exposed domains. This is nicely illustrated by proteins that are part of multiprotein complexes such as the alpha chain of the T-Cell Receptor (TCRa), which carries two charged residues in its TMD. These amino acids aid in assembly of the full T-Cell Receptor, but induce its degradation when expressed without its receptor co-factors [6]. The question remains of how the quality control machinery distinguishes newly synthesized proteins or those still in the process of folding, from those terminal cases that need to be destroyed.

How terminally misfolded glycoproteins are removed from the ER and targeted for destruction by the ubiquitin-proteasome system was the subject of the work presented here. Whereas little is known about the exact nature of quality control, much has been discovered about the proteins that execute it. Extensive genetic work in yeast and careful proteomics studies in mammalian cell systems have resulted in a more complete model of protein quality control in the ER. For simplicity's sake, I divide this process into three individual steps.
First, a protein is recognized as misfolded and delivered to the ER membrane for extraction. During this process, the unfolded polypeptide remains in close association with chaperones that ensure its solubility in the crowded ER lumen. These proteins can be roughly divided into two groups. First, proteins of the lectin family, which interact with N-linked glycans on the misfolded protein (eg. OS9, EDEMs, XTP3), and are thought to deliver the protein to a site of exit [4]. As mannose residues are progressively trimmed from the N-linked glycans on misfolded proteins, a case has been made for de-mannosylation as an indicator of protein quality control

[4]. It is by no means an absolute requirement, as proteins devoid of N-linked glycans still undergo quality control in the ER. The second group of proteins consists of chaperones thought to keep the misfolded protein soluble (BiP) and protein disulfide modifiers (PDIs, ERdj5, thioredoxins) that reduce disulfide bonds in the misfolded protein to ease its transfer across the ER membrane [4].
The second step in quality control in the ER constitutes the transfer of the misfolded polypeptide from the ER to the cytosol. No well-defined channel has been discovered known to perform this task, thought to be the polar opposite of protein translocation into the ER, but the protein complexes that surround E3 ligases involved in quality control have been proposed to drive this protein dislocation (as discussed in the introduction) [7].
Finally, once in the cytosol, the misfolded protein is targeted to the proteasome. As ubiquitylation drives both extraction as well as proteasomal targeting of the substrate, these steps are often thought to be coupled. However, we have shown that these reactions must be seen separately, as dislocation can be uncoupled from degradation, as demonstrated in Chapter 3 and 5 [8]. Once again, the unfolded polypeptide is found in association with chaperones to prevent its aggregation, now in the crowded cytosol (Chapter 4) [9].

A pressing question is the identity of the proteinaceous channel, referred to as the dislocon, that transfers misfolded ER proteins to the cytosol (see also the introduction). Protein complexes nucleated by E3 ligase molecules have been proposed as gatekeepers in this process [7]. Two mechanistic hurdles characterize this model. First, if protein dislocation is indeed accomplished through such a channel, misfolded proteins must be extracted one at a time, making it a rate-limiting step in dislocation, and thus quality control in the ER. Such a system would be adequate to maintain base-level ER homeostasis, but it is difficult to wed this model with the onslaught of misfolded proteins produced after treatment with drugs such as DTT or tunicamycin, both of which (are assumed to) induce abundant misfolding of ER proteins. A second limitation is not one of numbers but one of size. In order to maintain the integrity of the ER membrane barrier, and thus of the ER luminal environment, the diameter of the pore through which proteins are funneled can be only of limited size, as demonstrated for the translocon [10]. This implies complete unfolding and de-aggregation of misfolded proteins prior to extraction, steps for which relevant machinery has not yet been identified. It is worth pointing out that the dislocation machinery of the ER is also though to facilitate transfer of a number of bacterial toxins (such as Cholera toxin [11]and Pseudomonas Exotoxin A [12])

and viral particles (eg Simian Virus 40 [13]; polyoma virus), further expanding the size limit imposed on the dislocon. Such agents will serve as useful tools to investigate how the ER disposes of bulky structures, be it exogenous agents (toxins, viruses) or endogenous protein aggregates. It seems appropriate that a different mechanism is in place to handle the disposal of such bulk cargo.

The difficulty in assigning concrete mechanistic steps in the dislocation reaction is best illustrated by the interaction of the misfolded protein with the AAA ATPase p97. This hexameric protein is often referred to as the motor that drives dislocation [14]. Despite extensive structural work, including several high-resolution electron microscopy-based reconstructions and crystal structures, the question of how p97 engages its substrates remains unresolved [15].

Molecular snapshots of dislocation could describe discrete mechanistic steps involved in protein dislocation from the ER. Application of a factor that halts or impairs dislocation offers the chance to dissect the molecular machinery involved at a particular mechanistic step. Expression of the active EBV DUB, as described in chapter 3, creates a snapshot that offers two key new insights. First, a de-ubiquitylating activity is required to complete protein dislocation from the ER [8]. Second, dislocated ER proteins associate with cytosolic chaperones (BAT3), essential for their extraction (Chapter 4) [9]. The development of these and similar new tools will help to further dissect mechanistic steps that drive dislocation.
Development of a robust in vitro system to study protein dislocation enables further mechanistic analysis. As demonstrated in chapter 5, such studies can also be undertaken in permeabilzed cell systems.

Protein quality control in the ER is most commonly studied in tissue culture cells with no special notice to tissue specificity, due to the ease with which these cells can be manipulated. Some work has been done in professional secretory cells, such as differentiated B lymphocytes, but this has mostly focused on the role of the unfolded protein response in the dramatic expansion of ER capacity. Detailed mapping of the relevant quality control mechanisms in a tissue specific manner could be a helpful guide to choose the relevant experimental setup. In addition, recent research indicated that several proteins involved in ER quality control are linked to different phases of the cell cycle (UFD1) [16] and meisosis [17]. This deserves further attention.

References

1. Yewdell JW (2011) DRiPs solidify: progress in understanding endogenous MHC class I antigen processing. Trends Immunol 32: 548-558.
2. Hessa T, Sharma A, Mariappan M, Eshleman HD, Gutierrez E, et al. (2011) Protein targeting and degradation are coupled for elimination of mislocalized proteins. Nature.
3. Ward CL, Kopito RR (1994) Intracellular turnover of cystic fibrosis transmembrane conductance regulator. Inefficient processing and rapid degradation of wild-type and mutant proteins. J Biol Chem 269: 25710-25718.
4. Smith MH, Ploegh HL, Weissman JS (2011) Road to ruin: targeting proteins for degradation in the endoplasmic reticulum. Science 334: 1086-1090.
5. Claessen JH, Mueller B, Spooner E, Pivorunas VL, Ploegh HL (2010) The transmembrane segment of a tail-anchored protein determines its degradative fate through dislocation from the endoplasmic reticulum. J Biol Chem 285: 20732-20739.
6. Bonifacino JS, Cosson P, Klausner RD (1990) Colocalized transmembrane determinants for ER degradation and subunit assembly explain the intracellular fate of TCR chains. Cell 63: 503-513.
7. Claessen JH, Kundrat L, Ploegh HL (2012) Protein quality control in the ER: balancing the ubiquitin checkbook. Trends Cell Biol 22: 22-32.
8. Ernst R, Claessen JH, Mueller B, Sanyal S, Spooner E, et al. (2011) Enzymatic blockade of the ubiquitin-proteasome pathway. PLoS Biol 8: e1000605.
9. Claessen JH, Ploegh HL (2011) BAT3 Guides Misfolded Glycoproteins Out of the Endoplasmic Reticulum. PLoS One 6: e28542.
10. Park E, Rapoport TA (2011) Preserving the membrane barrier for small molecules during bacterial protein translocation. Nature 473: 239-242.
11. Guimaraes CP, Carette JE, Varadarajan M, Antos J, Popp MW, et al. (2011) Identification of host cell factors required for intoxication through use of modified cholera toxin. J Cell Biol 195: 751-764.
12. Moreau D, Kumar P, Wang SC, Chaumet A, Chew SY, et al. (2011) Genome-wide RNAi screens identify genes required for Ricin and PE intoxications. Dev Cell 21: 231-244.
13. Geiger R, Andritschke D, Friebe S, Herzog F, Luisoni S, et al. (2011) BAP31 and BiP are essential for dislocation of SV40 from the endoplasmic reticulum to the cytosol. Nat Cell Biol 13: 1305-1314.
14. Stolz A, Hilt W, Buchberger A, Wolf DH (2011) Cdc48: a power machine in pro-

tein degradation. Trends Biochem Sci.
15. Halawani D, Latterich M (2006) p97: The cell's molecular purgatory? Mol Cell 22: 713-717.
16. Chen M, Gutierrez GJ, Ronai ZA (2011) Ubiquitin-recognition protein Ufd1 couples the endoplasmic reticulum (ER) stress response to cell cycle control. Proc Natl Acad Sci U S A 108: 9119-9124.
17. Brar GA, Yassour M, Friedman N, Regev A, Ingolia NT, et al. (2011) High-Resolution View of the Yeast Meiotic Program Revealed by Ribosome Profiling. Science.

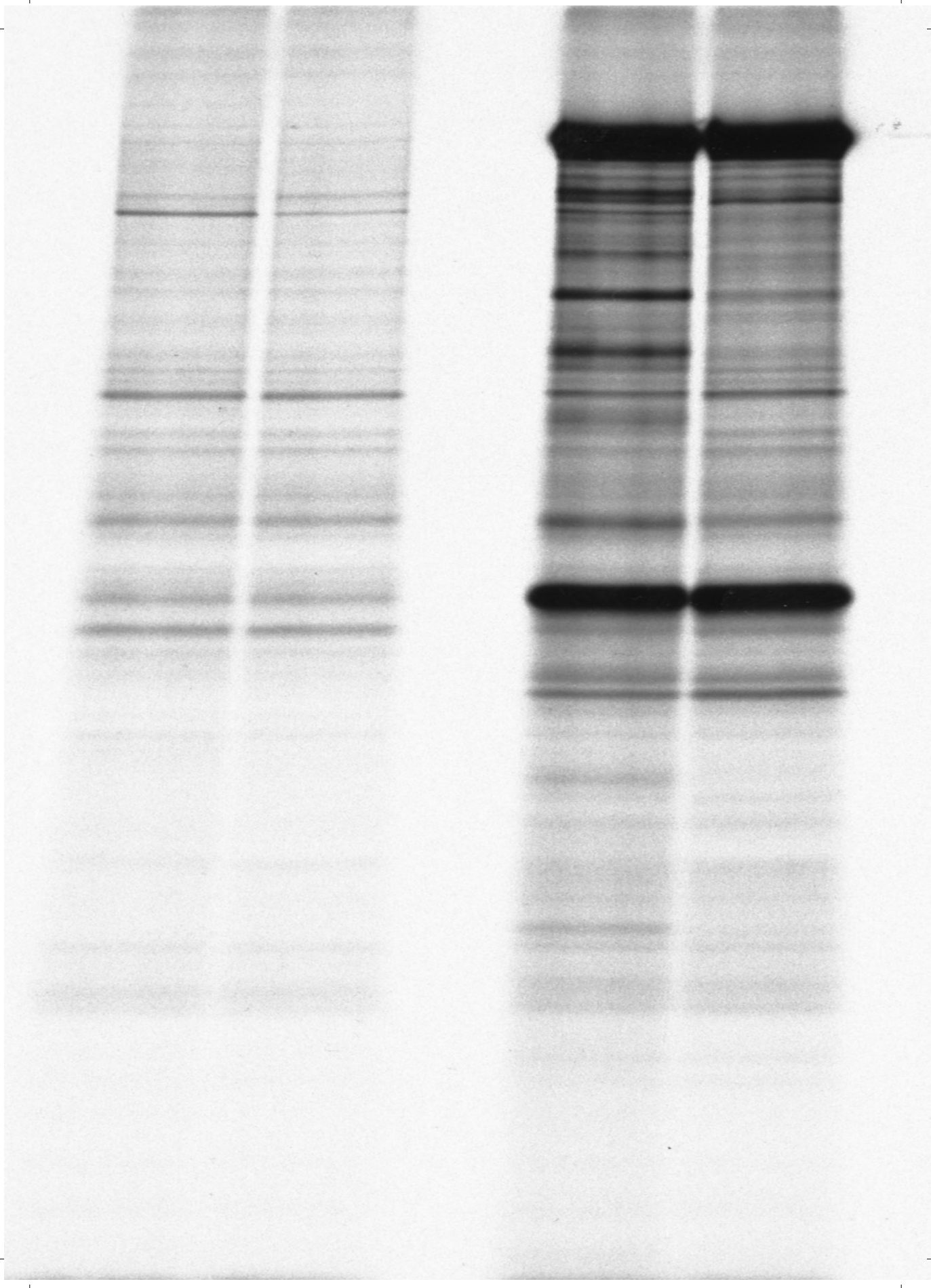

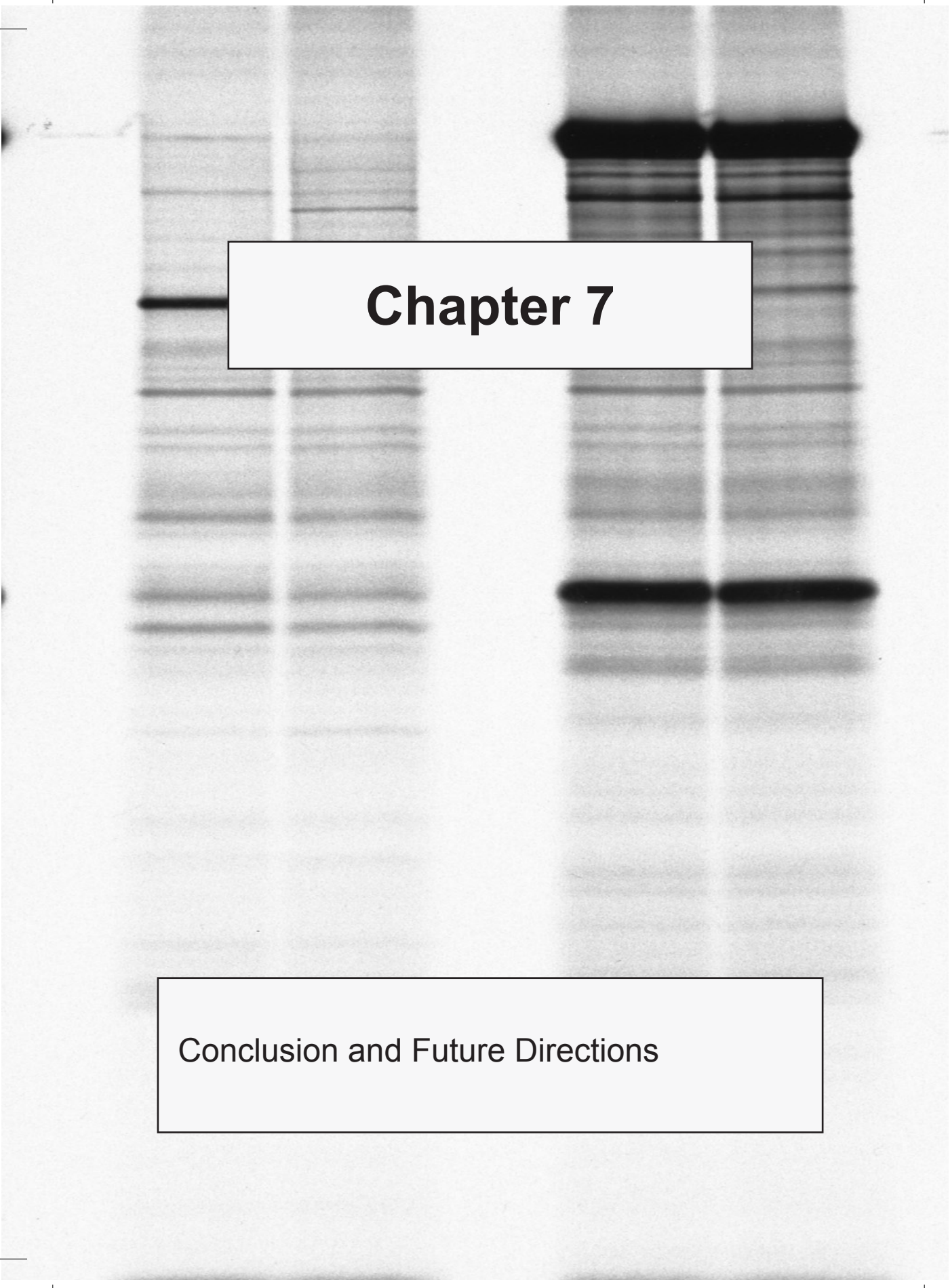

Chapter 7

Conclusion and Future Directions

Conclusion

Protein quality control in the ER selects dysfunctional proteins and targets them for destruction by the ubiquitin proteasome system before they can escape to the secretory pathway. Despite the identification of many proteins involved, the exact mechanisms of key steps in the process remain to be more accurately defined. In this thesis, I present work that sheds light on the role of the ubiquitin machinery in ER dislocation. I show that the working of a membrane-anchored E2 enzyme critically depends on its interaction with the dislocation complex within the plane of the ER membrane. Once ubiquitylated, the misfolded protein recruits the p97 protein complex to initiate extraction from the ER. This step critically depends on a de-ubiquitylating activity present at the p97 complex itself. Finally, to allow a smooth exit, misfolded ER proteins associate with cytosolic chaperones.

Future Directions

Transfer of an individual misfolded ER protein across the ER membrane criticially depends on its ubiquitylation. To understand the mechanism of this reaction, a number of questions await answering. First, it will be important to assess the folding state of the protein as it transfers across the membrane barrier, as this will give a clue as to the size restraints that are imposed on the hypothesized pore. If proteins are indeed dislocated in a fully unfolded state, then the appropriate machinery to ensure such unfolding awaits identification. Secondly, even though a growing number of E3 ligases have been identified to play a role in dislocation, the number of identified E2 conjugating enzymes is limited. It will be important to understand which E2-E3 pairs are formed to facilitate dislocation, and to assess the promiscuity of this pairing to gage redundancy in this system. With this information in hand, it will be key to determine the exact nature of the ubiquitin modification that drives the dislocation reaction. Is there are specific type of ubiquitin linkage required? Is there a requirement for mono-, multi-, or poly-ubiquitylation of the substrate? Finally, with the involvement of DUBs to complete the dislocation reaction, there is a chance to modify the type of ubiquitin modification. We currently don't know whether re-ubiquitylation occurs to achieve proteasomal targeting, though this would be in line with our current understanding of the UPS. If so, does re-ubiquitylation require and E3 or an E4-type activity? And is the ubiquitin chain modified in type and/or linkage? A clear understanding of dislocation will depend on the detailed knowledge of the nature of the ubiquitin chains as they are constructed or trimmed.

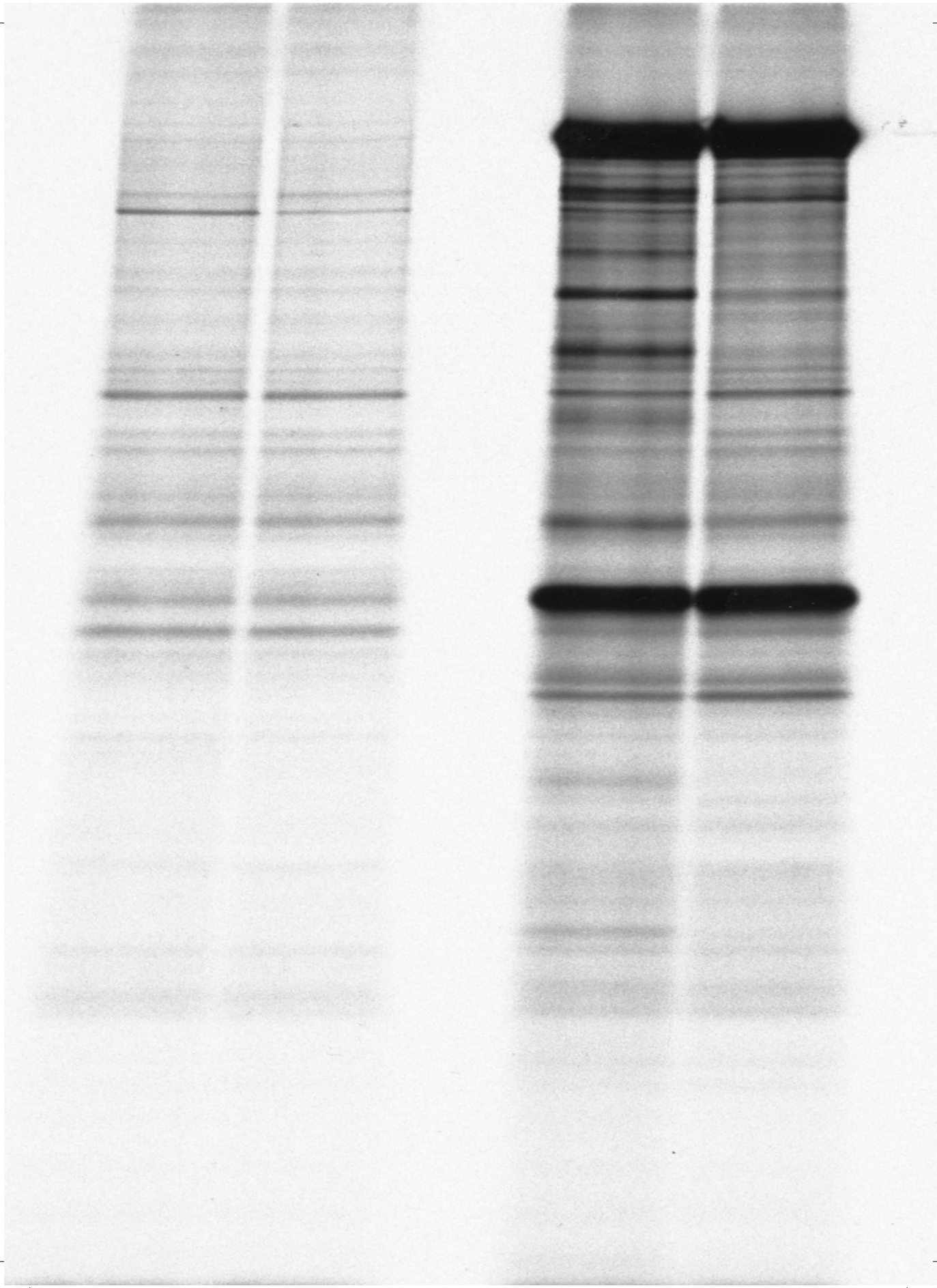

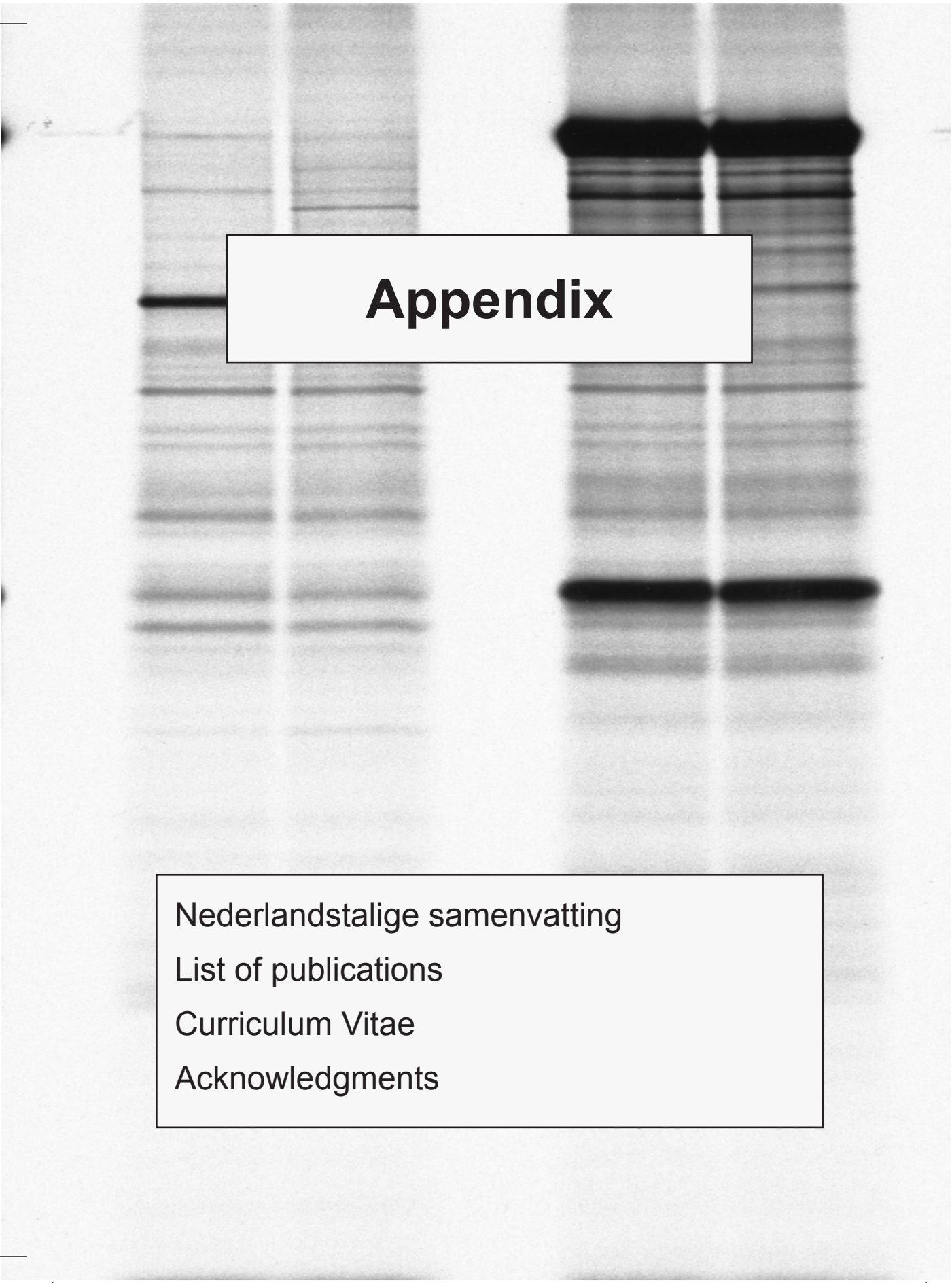

Appendix

Nederlandstalige samenvatting

List of publications

Curriculum Vitae

Acknowledgments

Nederlandstalige Samenvatting

Een belangrijk kenmerk van de eukaryotische cel is de aanwezigheid van lipide membranen. Het plasma membraan vormt een barrière tussen de cel en zijn omgeving en binnen de cel bestaan verschillende compartimenten die via een membraan gescheiden zijn van het cytosol. Intracellulaire compartimenten bieden de mogelijkheid gespecialiseerde functies te scheiden in daar toe uitgeruste organellen.

Alle eiwitten in de cel worden gesynthetiseerd door ribosomen in het cytosol. Hoe deze eiwitten vervolgens in het endomembraan systeem terechtkomen, verankerd in het membraan of als oplosbaar eiwit, is een belangrijk vraagstuk. We weten nu dat een nieuw gesynthetiseerd eiwit op weg naar een organel het membraan passeert als ongestructureerd polipeptide keten, een proces dat 'translocatie' wordt genoemd. Voor transport van het cytosol naar het endoplasmisch reticulum (ER), vindt translocatie plaats door een membraanporie gevormd door het Sec61 eiwit complex. Aangezien deze porie slechts groot genoeg is om doorgang te verlenen aan een ongestructureerd polipeptide weten we dat het eiwit zijn driedimensionale structuur aanneemt na aankomst in het ER. Het proces van eiwitvouwing en het aannemen van de correcte driedimensionale structuur is een essentiële stap in eiwitmaturatie. Een correcte eiwitstructuur draagt bij aan de stabiliteit van een eiwit, zorgt voor selectieve interactie met substraat of partner eiwitten en kan de lokalisatie van het eiwit beïnvloeden. De kwaliteit van eiwitten die dit proces ondergaan wordt gewaarborgd door een systeem van kwaliteitscontrole in het ER. Een nog onbekend mechanisme scheidt correct gevouwen eiwitten van niet-correct gevouwen eiwitten. Eiwitten met een correcte structuur worden getransporteerd naar de plek van bestemming, terwijl eiwitten met onherstelbare fouten moeten worden afgebroken. Deze kwaliteitscontrole beschermt de cel tegen ongewenste eiwitinteracties en een opeenhoping van niet-functionele eiwitten. De afbraak van niet-functionele eiwitten die zich in het ER bevinden, wordt uitgevoerd door het proteasoom in het cytosol. Voor transport naar het cytosol moeten de eiwitten dus opnieuw door de membraanbarrière van het ER worden gesluisd, een proces dat 'dislocatie' wordt genoemd.

Tijdens of na aankomst in het cytosol worden de eiwitten gemodificeerd met ubiquitine en getransporteerd naar het proteasoom om te worden afgebroken. Ubiquitine is een klein eiwit dat als signaal aan een substraat eiwit gekoppeld kan worden. De dislocatie reactie, de rol van ubiquitine en van eiwitten betrokken bij ubiquitine modificatie is het onderwerp van dit proefschrift.

Hoofdstuk 1 dient als introductie voor dit proefschrift. Hier beschrijf ik de huidige kennis over eiwitkwaliteitscontrole in het ER in detail, met een nadruk op de dislocatiereactie en de rol van het ubiquitine-proteasoom systeem.

In hoofdstuk 2 ga ik in op de rol van het eiwit UBC6e in de dislocatie reactie. UBC6e is een E2 enzym dat een belangrijke rol speel in het markeren van eiwitten voor afbraak door het proteasoom. We laten hier zien dat UBC6e de topologie heeft van een 'staartverankerd' membraan eiwit. Staartverankerde membraan eiwitten worden na translatie met de C-terminus in het ER membraan verankerd, een reactie die afhankelijk is van het chaperonne eiwit ASNA1. Vervolgens laten we via vervangingsmutanten zien dat het transmembraan domein van UBC6e een belangrijke rol speelt in zijn interactie met ASNA1. Dit geldt voor translocatie, en vervolgens voor zijn rol in de dislocatie reactie. Aangezien sommige van de geteste mutanten instabiel zijn, konden we aantonen dat ook eiwitten uit de 'staartverankerde' membraan eiwitklasse worden afgebroken door het ubiquitine-proteasoom systeem.

In hoofdstuk 3 beschrijf ik een nieuwe methode om eiwitafbraak door het proteasoom uit te schakelen. Eiwitten worden na modificatie met ubiquitine, meestal in de vorm van poly-ubiquitine, door het proteasoom herkend en vervolgens afgebroken. Expressie van een promiscue en erg actief de-ubiquitylerings enzym (DUB), namelijk het katalytische domein van het Epstein-Barr viraal eiwit BPLF1, zorgt dat dit signaal vroegtijdig wordt verwijderd. Dit heeft als gevolg dat eiwitten niet meer door het proteasoom worden herkend, en dus niet meer worden afgebroken. In de aanwezigheid van de EBV-DUB worden niet-correct gevouwen eiwitten echter nog wel verwijderd uit het ER. Wij hebben aangetoond dat deze reactie kritisch afhankelijk is van een de-ubiquitylerings activiteit en zien nu ER eiwit ophopen in het cytosol. Aggregatie van deze ongestructureerde eiwitten wordt voorkomen door associatie met cytosolische chaperonnes, waaronder BAT3.

Hoofdstuk 4 beschrijft de rol van de cytosolische chaperonne BAT3 in de dislocatie reactie. Met behulp van biochemie en licht microscopie tonen wij aan dat BAT3 en dislocatie-machinerie zich op de dezelfde locatie bevinden bij het ER membraan. Een reductie in BAT3 expressie via siRNA heeft een negatief effect op de dislocatie van misgevouwen eiwitten. Dit resultaat laat zien dat BAT3 een belangrijke rol speelt tijdens dislocatie. Ik kan vervolgens laten zien dat een misgevouwen ER

eiwit en BAT3 in een complex aanwezig zijn in het cytosol en dat dit afhankelijk is van een goed verlopende dislocatie reactie.

In Hoofdstuk 5 bespreek ik tenslotte een nieuwe methode om dislocatie te bestuderen. Deze methode maakt gebruik van een toxine dat poriën in de membraan maakt. Geperforeerde cellen kunnen reagentia opnemen die normaalgesproken de barrière van het cel membraan niet kunnen passeren. Met behulp van deze methodiek laten we zien dat tijdens dislocatie ATP wordt verbruikt en geen GTP. Ook tonen deze experimenten definitief aan dat dislocatie een de-ubiquitylerings stap vereist. Wanneer we een dislocatieblokkade opwerpen door intracellulaire expressie van een inactieve DUB, kan deze worden overwonnen door het introduceren van een exogene DUB.

In dit proefschrift laat ik zien dat het ubiquitine-systeem een belangrijke rol speelt in de dislocatie van verkeerd gevouwen ER eiwitten. Zowel eiwit modificatie met ubiquitine, als ook het verwijderen ervan zijn kritische stappen in dislocatie.

Publications

Feng, Y, Sokol, E, Proia, T, **Claessen, JHL**, Ploegh,HL, Wang, Q, Gupta, PB. Invasive, drug-resistant, stem-like cancer cells are highly secretory and sensitized to ER stress. (Submitted)

Sanyal, S, **Claessen, JHL**, and Ploegh, HL. Exogenous addition of ubiquitin-specific protease restores dislocation of a stalled intermediate in semi-intact cells. J Biol Chem. 2012, May 22; advance online publication
(Chapter 5)

Claessen, JHL, Kundrat, L, Ploegh, HL, Protein quality control in the ER: balancing the ubiquitin checkbook. Trends Cell Biol. 2011, 22(1) pp. 22 - 32
(Chapter 1)

Claessen, JHL, and Ploegh, HL, BAT3 guides misfolded glycoproteins out of the endoplasmic reticulum., PLoS One, Dec 8
(Chapter 4)

Ernst, R*, **Claessen, JHL***, Mueller, B, Sanyal, S, Spooner, E, van der Veen, AG, Kirak, O, Schlieker, CD, Weihofen, WA, Ploegh, HL, Enzymatic blockade of the ubiquitin-proteasome pathway. PLoS Biol. 2011, Mar;8(3)
(*= Equal first author)
(Chapter 3)

Claessen, JHL, Mueller, B, Spooner, E, Pivorunas, VL, Ploegh, HL, The transmembrane segment of a tail-anchored protein determines its degradative fate through dislocation from the endoplasmic reticulum. J Biol Chem. 2010, Jul 2;285(27)
(Chapter 2)

Mueller, B, Klemm, EJ, Spooner, E, **Claessen, JHL**, Ploegh, HL, SEL1L nucleates a protein complex required for dislocation of misfolded glycoproteins. Proc Natl Acad Sci USA. 2008, Aug 26;105(34):12325-30

Curriculum Vitae

Jasper Henri Laurens Claessen was born on May 21, 1984, in Hardenberg, and attended the local gymnasium, Vechtdal College. After graduating in 2002, he began his studies at the University College Utrecht, and it was here that he was drawn to the biological sciences. After three years, including a semester at Deakin University, Melbourne, Australia, he graduated with his BSc Cum Laude in 2005. He continued his studies at Utrecht University, where he gained his first research experience studying protein trafficking with Prof. dr. Judith Klumperman at the Department of Cell Biology. For his Master thesis work, he joined the lab of Prof. Dr. Hidde Ploegh at the Whitehead Institute, Massachusetts Institute of Technology, Cambridge, USA. Intrigued by the pathways that control quality and quantity control of protein synthesis in the endomembrane system, he returned to Hidde Ploegh's laboratory for his PhD research after obtaining his MSc in 2008. For the last four years, he studied the protein quality control mechanism in the endoplasmic reticulum, with a focus on the involved ubiquitin-machinery. His work was supported by a fellowship from the Boehringer Ingelheim Fonds. The defense of his doctoral thesis, entitled 'Protein Quality Control in the ER: Balancing the Ubiquitin Chequebook', will take place on July 5th, 2012. In the fall of this year, he will start a postdoctoral fellowship with Dr. Sean Munro at the MRC Laboratory of Molecular Biology in Cambridge, UK.

Acknowledgments

Although it is my name alone that is featured on the cover of this book, the work presented here was shaped by a group of outstanding people. A PhD ‘experience’ can sometimes, as the Dutch expression goes, feel like being the lone cyclist, riding against the wind. However, through my various triumphs and failures, I was fortunate to always find myself in the presence of people who encouraged me, with advice and help, or offered some much needed distraction.

I always gained an enormous amount of energy from coming to work in an environment as challenging, stimulating, and rewarding as our lab. I will surely miss being a part of it. Whether it was late at night, or over the weekend, it was hard to find one-self alone in the Ploegh lab. And even in those wee hours, people were eager to help each other solve problems, rather than rushing to leave. It was an ideal place to take my first steps as a scientist and I hope that the excitement of asking questions, and finding ways to answer them, will stay with me for the rest of my life.

Foremost I would like to thank Hidde Ploegh for supervising my work. The lab’s collaborative and stimulating environment is completely of your making, and I thank you for letting me be a part of that. You have been an inspiring example of how to think about science- always encouraging me to consider the next step, and if possible, even a few more steps ahead. Also, I want to thank you for the freedom you gave me to pursue my own interests. The feeling that anything I wanted to do was possible has been an enormous luxury. I am confidant to take the next step in my career with the tools that you have given me.

I especially want to thank Britta Mueller and Christian Schlieker. Working with you during my time as a visiting Masters student inspired me to come back for my PhD here. You quickly transitioned from role models to friends, and science has never been as fun as when the two of you were here. Luckily we still share our love for food, drink and fun, and I hope we will continue to see much of each other in the future.

My special gratitude also goes to Jadyn Damon, who has been my loyal ‘baymate’ during my time here. Thank you for answering all my stupid questions about biology and keeping that ignorance a private affair. Thank you for not getting upset about me stealing supplies from your bench, or with my rants and swearing in

Dutch when I had yet again ruined another experiment. Best of luck in this last leg of your PhD and I hope we can meet over drinks soon and address each other as ‘doctor.’

I also want to thank Robert Ernst and Sumana Sanyal, with whom I worked on the projects described in chapter 3 and 5. It was a pleasure working with the both of you. You both share a sharp mind and great experimental ‘hands’. I am glad that we have these beautiful stories to show for our shared efforts.

I can’t forget Karin Strijbis, my coffee buddy for the last three years. As soon as you moved to our room we became been close friends. I will miss your get-it-done mentality, and all our chats about really just anything. Thank you for all your honest comments and all the fun we had together.

Lots of thanks also to Lenka Kundrat for constructing that monstrosity of a table in the review we published together. I am also excited to finish the work I started with Martin Witte and David Rosmarin. It was great fun to work together instead of just ‘talking shop’, and I look forward to enjoying the fruits of our labor. I will also miss sharing beers and dinners with Paul Koenig, all the best with the last part of your Ph.D. I should also not forget Eric Spooner- I told you I would start bothering you with large mass-spec experiments in my last year, and so I did. Thank you for all the work you did for me.

A special word of thanks for Robert Miller, the backbone and soul of the lab. You made the place run like a well-oiled machine while I was here. But most I will remember our shared appetite for a well-earned drink, and our adventures at the Patriots, shooting pool, and of course the Scooperbowl.

The list will soon grow too long, so I’d like to thank all present and past members of the Ploegh lab for all the fun times, the support, and for being the fantastic group of people that make up this special place. I have nothing but well wishes for all of you.

I want to especially thank the Boehringer Ingelheim Fonds for supporting my research. Much more than just financial support, you have made a vital contribution to my PhD education. Both through organizing special meetings for all the fellows to exchange scientific ideas and experiences, but also by allowing me to attend a number of important scientific conferences where I could present and discuss

my work with preeminent members of the field. I am proud to be a member of the Boehringer family.

Finally, on a more personal note, I want to thank my parents and brother for all the encouragement over the last few years, and the years that brought me to this point. You have always supported me in all the decisions I have made in my life, wherever they took me, and I am very excited to celebrate my PhD with you- once I graduate.

At last, I want to thank Juliette for making my life so much richer and more fun. Thank you putting up with my passion for late night experiments and working through the weekend- and for dragging me away from work to go and explore the globe with you. My world has never been bigger.